THE
PHYSICAL REVIEW
A Journal of Experimental and Theoretical Physics
VOL. 44, No. 4 AUGUST 15, 1933 SECOND SERIES

The Secondary and Tertiary Particles Produced by Cosmic Rays

J. H. SAWYER, JR., *Rice Institute, Houston, Texas*
(Received June 30, 1933)

A search, by means of Geiger counters, was made for scattered cosmic rays in the region around a large iron block but no scattering could be detected. Experiments were tried with one counter just above a metal plate and two counters, placed side by side below it. It was found that the metal plate increased the number of triple coincidences between the three counters. The increase in the number of triple coincidences rose to a maximum and then diminished to zero as the thickness of the metal plate was increased. This effect was observed with plates of lead, tin and aluminum. It was greatest with lead and very small with aluminum. The results can be explained by supposing that secondary particles from the air above the apparatus produce tertiary particles in the metal plate which pass through the lower counters. The absorption coefficient of the air secondaries in lead was found to be 0.5 and that of the lead tertiaries to be 2.58.

THE purpose of this work was to make a study by means of Geiger-Müller counters of the scattering of the cosmic radiation and the production of secondary particles.

Evidence of scattering of cosmic-ray particles was first obtained by Rossi.[1] Johnson and Street[2] next measured the number of secondaries produced in a scattering experiment making use of a lead scatterer. The work of Schindler[3] on the absorption coefficients and the "uebergangs-effekte" with various materials also shows the production of secondaries. His data have been further examined by Johnson,[4] who obtains both absorption and production coefficients of the secondary corpuscular radiation.

Later, very definite evidence for the presence of scattered particles accompanying the cosmic radiation has been established by work with the cloud expansion chamber. This was first done by Skobelzyn[5] and followed by Mott-Smith and Locher,[6] Anderson,[7] and Blackett.[8] Each of these have found secondary rays issuing from the walls and pistons of their chambers, also from plates placed in the chamber. Recently, Rossi[9] has worked with the Geiger-counter method on the production of secondaries and has examined them in a number of different ways.

In the first experiments a search was made for scattered particles with two counters one above the other. These define a vertical beam of cosmic rays, and a third counter was placed outside of this beam so that no single particle could pass through all three counters unless it was deviated or scattered after passing through the upper two.

[1] B. Rossi, Phys. Zeits. **33**, 304 (1932); Rend. Lincei **15**, 734 (1932).
[2] T. H. Johnson, and J. C. Street, Phys. Rev. **40**, 638 (1932).
[3] H. Schindler, Zeits. f. Physik **72**, 625 (1931).
[4] T. H. Johnson, Phys. Rev. **41**, 545 (1932).
[5] D. Skobelzyn, Zeits. f. Physik **54**, 686 (1929).
[6] L. M. Mott-Smith, and G. L. Locher, Phys. Rev. **38**, 1399 (1931).
[7] C. D. Anderson, Phys. Rev. **41**, 405 (1932).
[8] P. M. S. Blackett, and G. P. S. Occhialini, Proc. Roy. Soc. **A139**, 699 (1933).
[9] B. Rossi, Zeits. f. Physik **82**, 643 (1933).

The three Geiger counters which were used in all the experiments were of the usual copper-sealed-in-glass type with a length of 20 cm and a diameter of 4.8 cm. The coincidences were amplified and selected with a vacuum tube arrangement similar to that which has been described by T. H. Johnson and were then automatically recorded.

The apparatus used is shown in Fig. 1. The scattering material is a large iron block 30.5 cm high, 15 cm wide, and 40 cm long. The top two

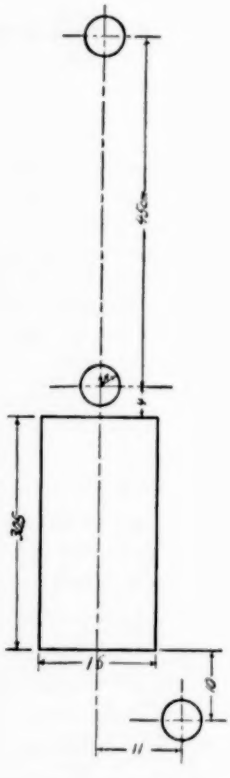

FIG. 1. First arrangement of counters. Dimensions in centimeters.

counters were placed so that the beam defined by them passed entirely through the iron block. The third counter was placed just outside this beam as shown in the figure. Alternating runs of 12 hours each were made with the iron block in the path and removed. Any increase in the triple coincidence counting rate must then be due to the iron scattering the rays. However, a slight decrease with the iron present was found. The results are given in Table I.

TABLE I.

	Total count	Interval (hours)	Rate, counts/hr.	Difference, counts/hr.
Absorber in	80	138	0.579±0.044	0.22±0.069
Absorber out	99	124.5	0.799±0.054	

A test was also made with the third counter close to one side of the iron block and 15 cm from its top. With this arrangement the scattering must necessarily occur at a somewhat larger angle. As in the first experiment, the introduction of the iron produced a small decrease in the number of triple coincidences. The results are given in Table II.

TABLE II.

	Total count	Interval (hours)	Rate, counts/hr.	Difference, counts/hr.
Absorber in	155	47.0	3.30±0.177	−0.39±0.268
Absorber out	151	41.1	3.69±0.201	

These results show that there is no appreciable scattering of the cosmic rays after traversing a block of iron 30 cm thick and also that the number of secondary rays emerging from the block was too small to be detected.

Since the probable error is 0.069 per hour (Table I) a change of 0.14 per hour might have been detected. The upper two counters define a beam of cosmic rays of about 30 particles per hour so that 1.4 scattered or secondary particle per 300 incident particles might have been detected.

The decrease of about 0.2 per hour observed is no doubt due to the absorption by the iron of the rays passing through the lower counter which thus reduces the chance count.

According to Heisenberg's theory[10] for electrons having an energy large compared to the binding energy of the electrons in the atom, the number z_1 of secondaries of energy $\geqslant \epsilon_1$ is given by

$$z_1 = 0.30z(R \cdot s/\epsilon_1)mc^2 \log (\epsilon_0/\epsilon_1).$$

Here, z is the number of primary particles falling on unit area in unit time, R is the effective range of electrons of energy ϵ_1, s is the density of the

[10] W. Heisenberg, Ann. d. Physik **13**, 430 (1932).

material and mc^2 is the rest energy of an electron. Now, if we consider the first experiment, the path in the iron of a secondary produced at the middle of the block will be approximately 15 cm. The relation connecting this path with the energy has been given by Bohr,

$$R_s=(\epsilon/mc^2)^2[(z_a+z_k)/sz_a^2]$$

where R_s is the path, ϵ the energy, z_a the atomic number, and z_k the number of electrons in the nucleus. To a rough approximation, we find then for the path of 15 cm, the energy necessary is

$$\epsilon=1000\ mc^2.$$

Since the probable error is 0.07 per hour (Table I), a change of 0.14 per hour might have been detected. The upper two counters define a beam of the cosmic-ray shower in which are 30 particles per hour. Hence, the resolving power of the apparatus may be said to be 0.14/30 or 0.005. On substitution of the above values in Heisenberg's relation, we find

$$z_1/z=0.3(15\times 7.8/1000)\ \log 10,$$

assuming $\epsilon_0=10{,}000\ mc^2$.

This fraction must be scattered over an area of approximately 500 square centimeters. Hence, we see that the fraction which would be scattered into the counter of area 96 square centimeters would be approximately 0.016. However, the actual decrease found when the iron was present caused by the change in chance count due to the absorption of particles passing through counters 2 and 3, was of sufficient magnitude to cancel this and give a net decrease.

Experiments were next tried with one counter above a lead plate and two below it as shown in Fig. 2. The two lower counters were placed side by side symmetrically about the vertical plane through the upper counter.

With this arrangement triple coincidences can be produced by a particle passing through two of the counters and producing a secondary particle in the lead which passes through the third counter or by a particle passing through the upper counter and producing two secondaries in the lead plate which pass through the two lower counters one through each.

It was found that the lead plate increased the

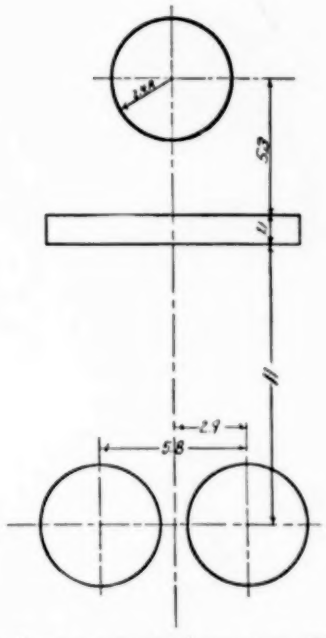

FIG. 2. Second arrangement of counters. Dimensions in centimeters.

number of coincidences observed and that the increase depended on the thickness of the plate. The results obtained are given in Table III and are shown graphically in Fig. 3.

TABLE III.

Thickness (cm)	Total count	Interval hours	Rate counts/hr.
0	58	20.0	2.84±0.25
.47	68	9.8	6.9 ± .56
.63	67	8.6	8.1 ± .64
1.1	75	10.0	7.5 ± .58
1.58	68	9.75	6.85± .56
2.22	145	25.75	5.6 ± .28
3.2	92	19.75	4.73± .32
3.97	55	15.0	3.7 ± .31
5.08	54	14.5	3.1 ± .31
6.8	95	31.32	3.03± .21

If the triple coincidences were due to secondaries produced in the lead by the primary cosmic-ray particles, we should expect to get a curve like the dotted line in Fig. 3. The secondaries would gradually build up with increasing thickness of lead until equilibrium with the primaries was reached as shown by the dotted line, which would then fall off slowly with the absorption of the primaries.

The observed curve can be explained, on the assumption that the particles which produce the

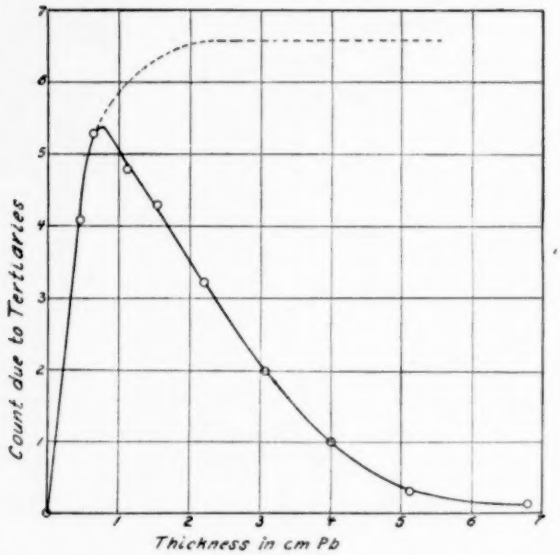

FIG. 3. Counts due to tertiaries as a function of thickness of lead plate.

effect are tertiary particles, generated in the lead by light element secondaries produced in the regions above the scatterer. In this case the rise in the curve is due to the building up of the number of tertiaries to the equilibrium value. Then, the decrease with increasing thickness is due to the absorption in the lead of the air secondaries.

The fact that an effect due to the tertiaries produced by the lead secondaries in the larger thicknesses is not detected can be explained by a consideration of their energies. The absorption coefficient of lead secondaries in lead has been calculated by Johnson, and found to be 0.98. This in comparison with the value calculated for air secondaries, namely 0.5, shows the lead secondaries have considerably less energy. It follows from this that the tertiaries formed by the absorption of lead secondaries must have very small energies. Hence, their absorption coefficient in lead must be large, greater than the 2.58 calculated for air tertiaries, i.e., lead tertiaries ejected by air secondaries. Then it follows that only a very thin layer at the bottom of the lead block is effective in ejecting tertiaries due to lead secondaries into the lower counters. The tertiaries formed in this layer are too few to be detected.

The distribution of the particles over horizontal surfaces is uniform; so we need only consider variations over vertical distances. Now, absorption of the air secondaries in the lead obeys an exponential law with the absorption coefficient, μ_s. This absorption coefficient is also the proportionality factor for the production of tertiaries with respect to the number of secondaries absorbed, since each secondary is absorbed by emitting tertiaries of some form. So we have the total number of lead tertiaries emerging from the bottom of a block of thickness l due to the air secondaries absorbed in a layer of thickness dx at a distance x from the bottom given by

$$dn_t = K\mu_s e^{-\mu_s(l-x)} e^{-\mu_t x} dx,$$

assuming for the tertiaries exponential absorption with coefficient, μ_t. K is here a factor proportional to the number of air secondaries falling on unit area in unit time.

On integration we obtain

$$n_t = e^{-\mu_s l} K\mu_s \int_0^x e^{x(\mu_s-\mu_t)} dx$$

$$= e^{-\mu_s l} K\mu_s [1 - e^{-x(\mu_t-\mu_s)}/(\mu_t-\mu_s)],$$

which on substitution of l for x gives us the total number of tertiaries emerging from the lead

$$\overline{n_t} = K\mu_s e^{-\mu_s l}[1 - e^{-l(\mu_t-\mu_s}/(\mu_t-\mu_s)].$$

This equation contains two absorption coefficients, μ_s and μ_t, which can be determined from the observed data. By trial and error method it was found that the absorption coefficients required are

$$\mu_s = 0.50, \quad \mu_t = 2.58.$$

Table IV gives the calculated and observed values. From these it is evident that the theory agrees with the experimental values within the experimental errors.

TABLE IV.

Thickness of Pb (cm)	No. tertiaries calculated	Thickness of Pb (cm)	No. tertiaries observed
0.3	3.4	0.47	4.1±0.25
.5	4.15	.63	5.2± .56
1.0	5.0	1.1	4.8± .58
2.0	3.3	2.2	3.2± .28
3.0	2.05	3.0	2.0± .32
4.0	1.17	3.97	1.0± .31
5.0	0.75	5.08	0.3± .31
6.0	.4		
7.0	.22	6.8	.1± .21

It is interesting to note that the value of μ_s, 0.50 agrees exactly with that found by Johnson from an entirely different type of experiment.

A similar series of experiments was made with aluminum instead of lead. A relatively small increase in the triple coincidence rate was found. The results are shown in Table V.

TABLE V.

Thickness of Al (cm)	Total count	Interval hours	Rate counts/hr.
0	257	53	4.85±0.20
.84	111	23	4.8 ± .31
1.68	123	23	5.35± .32
3.36	117	23	5.1 ± .31
5.04	152	33.8	4.5 ± .25

Another similar set of experiments was then done with tin as the scatterer. Results are given in Table VI.

The results with lead, tin and aluminum show that the effect varies with the atomic number. This agrees with Heisenberg's theory of absorption, according to which with heavier atoms most of the absorption is due to production of secondary particles. With lighter atoms, the absorption is largely due to "bremsung" or more distant collisions, not ejecting electrons from the material.

TABLE VI.

Thickness of Sn (cm)	Total count	Interval hours	Rate counts/hr.
0	72	20.15	3.6±0.28
.64	134	22.75	5.8± .34
1.28	138	20.75	6.6± .38
1.92	147	20.6	7.3± .39
2.54	97	13.5	7.0± .73
3.81	129	20.75	6.2± .36
5.08	352	69.0	5.1± .18

I wish to express my sincere gratitude to Professor H. A. Wilson and to Dr. L. M. Mott-Smith for their interest and valuable suggestions.

New High-Altitude Study of Cosmic-Ray Bands and a New Determination of Their Total Energy Content

I. S. BOWEN, R. A. MILLIKAN AND H. V. NEHER, *California Institute of Technology*

(Received June 19, 1933)

(1) The Millikan-Cameron cosmic-ray curve extending for 80 equivalent meters of water below the top of the atmosphere up to 7.5 m has here been extended by accurate measurements in the critical region from 7.5 m up to 3.34 m (29,200 ft.) of water beneath the top in latitude 34, and up to 4.5 m (22,000 ft.) in the equatorial belt. *The comparison of the two curves permits of the separation of the magnetically deflectable particles from the primary non-deflectable cosmic rays.* (2) The rays thus separated reveal with much definiteness a banded structure of not less than three rather widely separated components, and by virtue of the high altitudes reached fix with considerable certainty the absorption coefficient of the least penetrating band. This single band is responsible for 90 percent of the cosmic-ray ionization of the atmosphere. The absorption coefficients of the more penetrating bands of indefinite number (not less than two) cannot be sharply determined, but their general character is indicated herein, as well as the limitations of this method of their determination. (3) These measurements combined with Bowen and Millikan's stratosphere observations, which agree well with the present measurements in the region in which they overlap, make possible the plotting of *a complete cosmic-ray intensity curve extending from the lowest depths to the top of the atmosphere.* (4) The graphical integration of this curve shows that the total energy reaching the earth in the form of cosmic rays is about one-half that coming to the earth in the form of heat and light from the stars. This makes the cosmic-ray energy in the universe from 30 to 300 times that of all other radiant energies combined.

THE EXTENSION OF ACCURATE COSMIC-RAY MEASUREMENTS UP TO 29,000 FT. ALTITUDES

MILLIKAN and Cameron's[1] accurate measurements extended from 80 meters of water below the top of the atmosphere up to the top of Pike's Peak, which corresponds inside their lead shielding to 7.5 meters of water below the top. However, for the most significant study of the softest and most powerfully ionizing component contained in the cosmic rays, measurements at altitudes above those obtainable on any mountain peaks are essential. We have therefore been particularly interested for several years past in developing methods of pushing accuracy of readings to the highest points at which airplanes can remain aloft at constant altitude long enough to obtain dependable and duplicable intensity measurements.

Our best flights have recently (April and June, 1933) been made at March Field near Riverside, California through the generous assistance of the Army Air Corps, the pilot flying at a constant altitude at different levels up to 29,200 feet long enough at each level to enable the electroscope to be discharged over its complete range three separate times. Fig. 1 shows the record of the flight when time is plotted as abscissa and rate of discharge as ordinate, the crosses at each level showing the sort of duplicability of the different readings at a given level. This graph also brings to light clearly the enormous rate of rise in ionization as the higher altitudes are reached; the total ionization being more than doubled in going from 22,000 feet (4.49 meters of water) to 29,000 feet (3.34 meters of water), although this corresponds to a change in the barometer of but 3.5 inches of mercury or about a tenth of an atmosphere.

Fig. 2 shows the same data with ionization plotted against depth in meters of water beneath the top of the atmosphere. The way the points fall on a smooth curve shows clearly the consistency yielded by these recording electroscopes as here used. The natural interpretation of these curves is that a soft component of the incoming rays, one which is so soft as to be scarcely perceptible at sea level, is responsible for most of the ionization at altitudes at which the pressure is less than say 6 meters of water (altitude 14,000 feet).

But in order more carefully to interpret such readings as are here found new considerations

[1] Millikan and Cameron, Phys. Rev. **37**, 235 (1931).

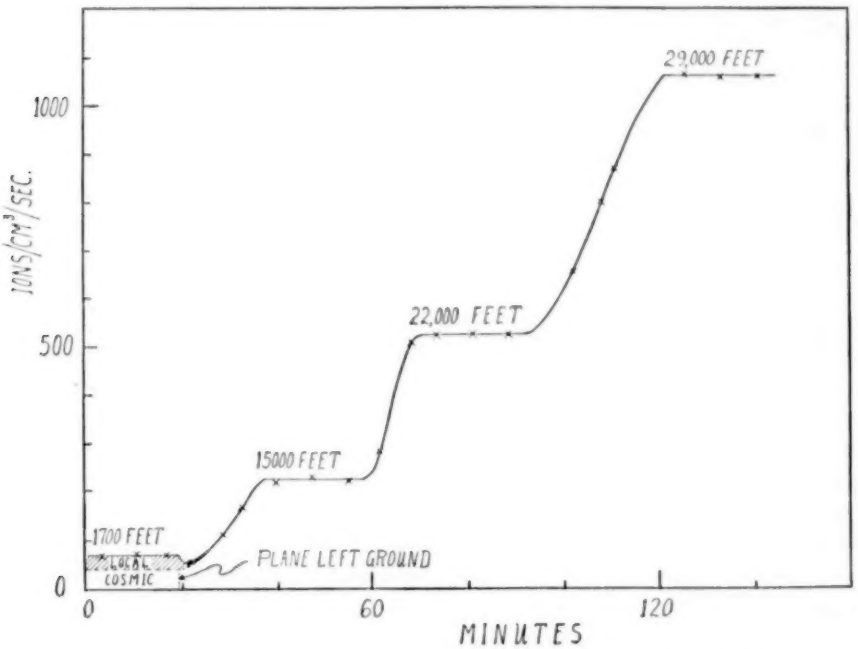

FIG. 1. Record of the rates of ionization in the airplane flight at March Field.

arising from recent studies of the geographical distribution of the rays are significant. The simplest interpretation of the slight equatorial dip in the sea level intensity first announced by Clay,[2] found also by the group of observers working with A. H. Compton[3] and quite recently appearing to the extent of about 7 percent in our own trips[4] back and forth between Mollendo, Peru and New York and Los Angeles is, as already outlined by one of us,[4] that while about 93 percent of the rays reaching sea level are of a sort to be wholly uninfluenced by the earth's magnetic field, the remaining 7 percent of the ionization observed at sea level within our 10 cm lead shield is due to rays magnetically deflectable by that field. If this hypothesis is correct, the ionization that we have found above March Field (lat. 34°N) would be a mixture of that due to magnetically undeflectable rays, and that due to a deflectable component, i.e., it would be a mixture of the ionization produced in the atmosphere by the photons (or neutrons) absorbed therein and that produced by rays which enter the earth's magnetic field (which is supposed to extend for thousands of miles above the earth) as

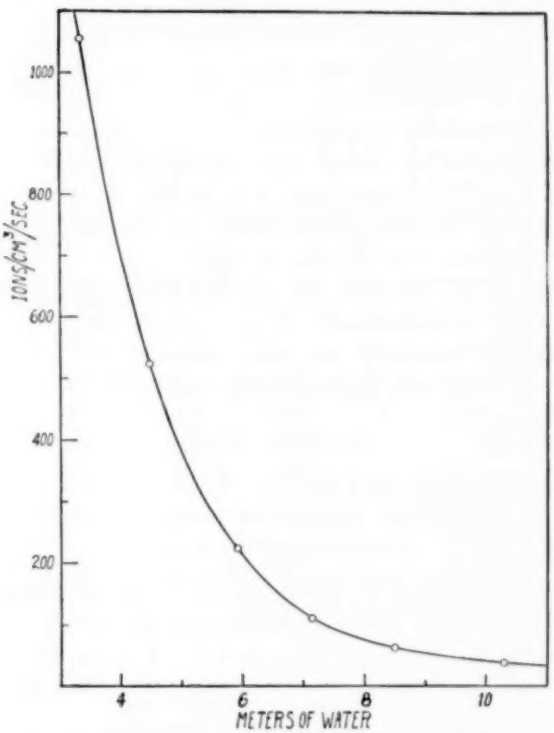

FIG. 2. Cosmic-ray intensities plotted as a function of depth in meters of water below the top of the atmosphere. Observations taken in airplane flight at March Field.

[2] J. Clay, Proc. Roy. Acad. (Amsterdam) **30**, 1115 (1927); **31**, 1091 (1928); **33**, 711 (1930); Naturwiss. **20**, 687 (1932).

[3] A. H. Compton, Phys. Rev. **43**, 387 (1933).

[4] R. A. Millikan, Phys. Rev. **43**, 666 (1933).

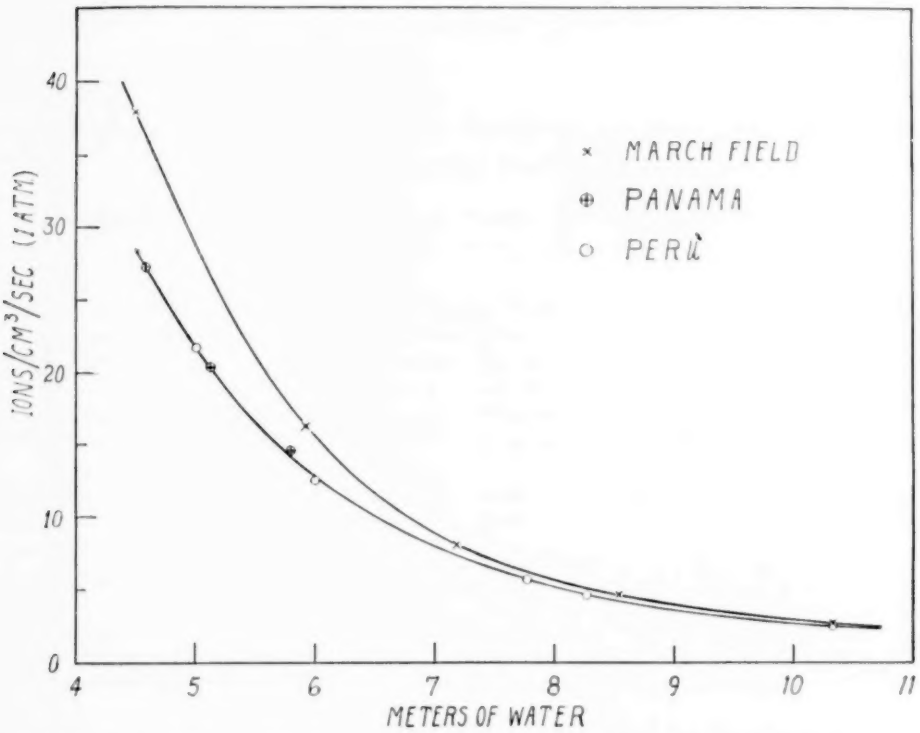

FIG. 3. Comparison of cosmic-ray measurements taken on airplane flights at March Field, Panama and Peru.

charged particles, whether primary or secondary is not here important. *But since in the equatorial belt no deflectable rays of such energies as those actually found by Anderson,*[5] *Kunze*[6] *and ourselves*[4] *to exist in the cosmic rays can possibly penetrate the earth's magnetic field so as to get into that portion of the atmosphere under observation,* it is quite clear that in order to observe in a region in which all the rays are of the kind which are wholly uninfluenced by a magnetic field it is merely necessary to make, somewhere in the equatorial belt, flights similar to the March Field flights.

II. The Separation of Magnetically Deflectable Particles from the Incoming Cosmic Rays

Accordingly in January, 1933, we arranged through the generous assistance of the U. S. Army Air Corps to have one of our new vibration-free recording electroscopes taken in a high altitude flight between Christobal, Panama and Balboa (lat. 8° 43′ N). The plane actually flew for 45 minutes at each of the altitudes 16,000 feet (5.75 m of water), 19,000 (5.08 m) and 22,000 (4.50 m). A similar flight was also made by Neher in a commercial plane between Arequipa, Peru (Lat. 17 S) and Lima, Peru, (Lat. 12 S). The results of these three flights are all plotted in Fig. 3 and show with much conclusiveness that *there is no latitude effect whatever between Panama and Arequipa.* Since the electroscopes actually used were yielding at 22,000 feet 379 ions per cc per sec. this lack of a latitude effect over this stretch is here brought to light with a very considerable accuracy.

Since, then, this equatorial ionization is necessarily due to rays which are not only magnetically undeflectable themselves but have been entirely freed from all charged particle components of all sorts it is of much interest to determine what kind of cosmic-ray bands, *as defined by their absorption coefficients alone,* make up the incoming beam. Millikan and Cameron carried their analysis of this sort from a depth of 80 meters be-

[5] C. D. Anderson, Phys. Rev. **41**, 405 (1932).

[6] Paul Kunze, Zeits. f. Physik **79**, 203 (1932); **80**, 559 (1933).

low the top of the atmosphere up to 7.5 meters, but according to the foregoing observations and points of view their analysis was somewhat vitiated by the presence at sea level (10.33 m of water) of the 7 percent of ionization due to incoming particles. Also the difference between curves 2 and 3 shows that at 22,000 feet (4.5 m) the effect of this particle component has risen to some 39 percent. The rapid decrease of this hypothetical effect of particles in going from 4.5 m to 10.33 m shows, then, that not far below sea level this particle component must in any case drop out entirely. This means that the analysis of the underwater curve, so far as concerns the portion that is lower down than say 15 m below the top of the atmosphere, will be the same as that already published by Millikan and Cameron, but from that point up to 4.5 m, the highest altitude reached in the equatorial flights, it will be peculiarly interesting to know what sort of absorption coefficients are able to reproduce the readings. The results are shown in Tables I, II, and III.

III. The Banded Structure of the Cosmic Rays

In computing the Tables I to III we have used the following procedure. The Millikan-Cameron data make it possible to avoid entirely all errors due to transition effects such as make it necessary for Professor Regener[7] to treat his air and water curves separately. For these Millikan-Cameron under-water data were taken in lakes at altitudes so high that there is a considerable stretch of under-water data which overlaps the airplane data, so that we combine these two sets of observations into one continuous curve, all taken in latitude about 34 N, and extending from the highest point reached in the airplane flight, *viz.*, 3.34 m below the top of the atmosphere, down to 80 m below the top, which is the lowest point reached in the under-water work.

To obtain the corresponding curve in the equatorial belt, in the absence of actual under-water readings near the equator we have simply extended the airplane equatorial curve until it touches the foregoing complete curve obtained in latitude 34, this point of tangency being actually found, to well within the limits of observational uncertainty, at about 15 m below the top. At a later time we hope to obtain direct measurements in the equatorial belt upon this little stretch of the curve connecting air readings and under-water readings, but the foregoing procedure cannot involve errors of appreciable magnitude for the present purposes.

In order, however, to extend the curve still farther down we have fitted Regener's observations at 80 meters to the Millikan-Cameron curve at that point and thus added to the foregoing equatorial observations between 4.5 m and 80 m a tail obtained from Regener's readings from 80 m to 240 m and have obtained thus a complete curve corresponding to observations on the equatorial belt between 4.5 m and 240 m. In order to get the best possible fit we have made slight adjustments in the instrumental zeros reported both by Millikan and Cameron and by Regener, but such adjustments are within the observational uncertainties which appear in the recorded data of both sets of observers. Incidentally, when these very minute rates of ionization are being measured these zero uncertainties introduce a large percentage of error into the resulting limiting absorption coefficient, so that the differences reported in this coefficient by the different observers have no real significance. It is in the foregoing way, then, that the numbers found in the observed column of Table I have been obtained, these numbers representing the number of ions formed per cc per sec. in an electroscope in which the pressure is 1 atmosphere of air. According to our own analysis, as well as that of Professor Epstein, who has had the opportunity to study our data, *it is in no way possible to build up this curve without the assumption of at least three cosmic-ray bands of widely different penetrating power.* This simply fortifies the conclusion reached by Millikan and Cameron from their former less extended data.

Table I shows how this observed curve is built up from the three absorption coefficients $\mu = 0.5$ per m of water, $\mu = 0.07$, and $\mu = 0.015$. The last two of these are very close to those used by Millikan and Cameron in their first attempt to synthesize their under-water curve,[8] their chosen

[7] E. Regener, Phys. Zeits. **34**, 306 (1933).

[8] Millikan and Cameron, Phys. Rev. **32**, 548, 9 (1928).

TABLE I. *Comparison of observed cosmic-ray intensities with those calculated under the assumption that the cosmic rays are made up of three bands with absorption coefficients $\mu=0.5$, 0.07 and 0.015 per m of water.*

h (meters of water)	0.8 $G(0.015)$	6.7 $G(0.07)$	795 $G(0.50)$	Total	Observed	Obs.-Cal.
4.5	0.63	3.06	21.73	25.42	24.62	−0.80
5.0	.62	2.86	15.76	19.24	19.25	+ .01
6.0	.59	2.52	8.46	11.57	11.53	− .04
8.0	.55	1.98	2.54	5.07	4.65	− .42
10	.51	1.57	0.79	2.87	2.52	− .35
15	.436	0.928	.047	1.411	1.414	+ .003
20	.375	.561	.003	0.939	0.939	.000
25	.326	.350		.676	.664	− .012
30	.285	.223		.508	.505	− .003
40	.221	.091		.312	.308	− .004
50	.174	.039		.213	.220	+ .007
60	.138	.017		.155	.166	+ .011
70	.111	.007		.118	.123	+ .005
80	.089	.003		.092	.088	− .004
90	.0721	.0015		.0736	.0680	− .0056
120	.0390	.0001		.0391	.0389	− .0002
160	.0180			.0180	.0188	+ .0008
180	.0124			.0124	.0128	+ .0004
200	.0085			.0085	.0080	− .0005
240	.0041			.0041	.0041	.0000

values being then $\mu=0.08$, $\mu=0.04$, and $\mu=0.02$, though for the foregoing reasons they were then careful to state that "there is no very great importance to be attached to this synthetic curve." Their observations had not then gone to high enough altitudes to get the softest coefficient with any certainty, the value they then used being $\mu=0.3$. In their 1931 paper[9] they had gone high enough to find that this value of the softest coefficient was definitely too small, and they then used for it $\mu=0.8$, while for the harder components they used $\mu=0.20$, $\mu=0.10$, and $\mu=0.03$. It is of course the softest coefficient which the present experiments are calculated to fix with greater certainty. The same uncertainty as to the other components exists as heretofore.

In this present synthesis we have simply added, with the aid of the Gold tables, three ionizations each obtained from

$$I=I_0\int_0^{\pi/2} e^{-\mu h/\cos\theta}\sin\theta d\theta = I_0\int_1^{\infty}\frac{e^{-\mu hx}}{x^2}dx = I_0 G_\mu,$$

the numerical factor at the top of each column being the I_0 (number of ions per cc per sec. at the top of the atmosphere in an electroscope filled with air at 1 atmosphere) of this formula, and the letter G_μ standing for the above-mentioned Gold function. We would emphasize, however, as one of us has repeatedly done before, that though there is no unique solution to such an absorption curve, *all possible solutions give absorption bands or regions bearing a close general resemblance to the foregoing solution.*

To illustrate the extreme types of possible divergence of solutions, we present in Tables II and III two other modes of building up the observed curve, both of which fit the observational data quite as well as does the mode shown in Table I. Table II corresponds to four bands of absorption coefficients, $\mu=0.55$, $\mu=0.12$, $\mu=0.03$, and $\mu=0.0075$, but the following four will fit the observations just as will $\mu=0.55$, $\mu=0.12$, $\mu=0.06$, $\mu=0.015$; but in that case the corre-

TABLE II. *Comparison of observed intensities of cosmic rays with those calculated under the assumption that cosmic rays are composed of four bands of absorption coefficients $\mu=0.55$, 0.12, 0.03, and 0.0075 per m of water.*

h (meters of water)	0.2 $G(0.0075)$	1.9 $G(0.03)$	11.5 $G(0.12)$	1000 $G(0.55)$	Total	Observed	Obs.-Cal.
4.5	0.17	1.26	3.51	20.48	25.42	24.62	−0.80
5.0	.17	1.22	3.18	14.49	19.06	19.25	+ .19
6.0	.17	1.14	2.62	7.40	11.33	11.53	+ .20
8.0	.16	1.00	1.81	2.01	4.98	4.65	− .33
10	.15	0.89	1.28	0.56	2.88	2.52	− .36
15	.140	.677	0.561	.026	1.404	1.420	+ .016
20	.128	.525	.259	.001	0.913	0.945	+ .032
25	.118	.413	.122		.653	.670	+ .017
30	.109	.328	.059		.496	.511	+ .015
40	.094	.211	.014		.319	.314	− .005
50	.082	.139	.004		.225	.226	+ .001
60	.071	.093	.001		.165	.172	+ .007
70	.063	.063			.126	.129	+ .003
80	.055	.043			.098	.094	− .004
90	.0490	.0295			.0785	.0738	− .0047
120	.0345	.0098			.0443	.0447	+ .0004
160	.0222	.0024			.0246	.0246	.0000
180	.0180	.0012			.0192	.0186	− .0006
200	.0146	.0006			.0152	.0138	− .0114
240	.0098	.0001			.0099	.0099	.0000

TABLE III. *Comparison of observed intensities of cosmic rays with those calculated under the assumption that the cosmic rays consist of a band with absorption coefficient $\mu=0.55$ together with a continuous spectrum. The intensity in the continuous spectrum is distributed with respect to absorption coefficient according to the following expression. $I=K\int_{0.00667}^{\infty}(\mu-0.00667)^{1/6}G_\mu d\mu$.*

h (meters of water)	I	940 $G(0.55)$	Total	Observed	Obs.-Cal.
4.5	6.30	19.30	25.60	24.62	−0.98
5.0	5.54	13.61	19.15	19.25	+ .10
6.0	4.41	6.96	11.37	11.53	+ .14
8.0	3.07	1.89	4.96	4.65	− .31
10	2.32	0.53	2.85	2.52	− .33
15	1.352	.024	1.376	1.416	+ .040
20	0.914	.001	0.915	0.941	+ .026
25	.666		.666	.666	.000
30	.510		.510	.507	− .003
40	.326		.326	.310	− .016
50	.225		.225	.222	− .003
60	.164		.164	.168	+ .004
70	.124		.124	.125	+ .001
80	.096		.096	.090	− .006
90	.0756		.0756	.0698	− .0058
120	.0403		.0403	.0407	+ .0004
160	.0198		.0198	.0206	+ .0008
180	.0143		.0143	.0146	+ .0003
200	.0105		.0105	.0098	− .0007
240	.0059		.0059	.0059	.0000

[9] Millikan and Cameron, Phys. Rev. **37**, 246 (1931).

sponding I_0s must assume the sequence of values 775., 5., 4.4, 0.8. In general in any four band analysis the two most penetrating of the components have little significance beyond indicating that there is an exceedingly small number of very penetrating rays mixed with the cosmic-ray beam and that the coefficient of this penetrating tail must then have a value not far from $\mu = 0.02$. In Table III the three most penetrating bands of Table II have been combined into the continuous distribution function indicated at the head of the first column. In each of these tables the instrumental zeros of both Millikan and Cameron's and Regener's experiments have been slightly adjusted, but always within the estimated limits of observational uncertainty, so as to obtain the best fit between the "total" and the observed columns.

This whole analysis has been inserted merely to show how large, or better how small, a divergence of types of solution is possible, and the most striking result is that previously emphasized repeatedly by one of us, even with less extensive data, namely, that *more than 90 percent of the ionization of the atmosphere is due to the softest cosmic-ray band, which stands out by itself quite alone and reasonably monochromatic.*

The maximum variation in the absorption coefficient of this band, as here directly observed, is between say $\mu = 0.5$ and $\mu = 0.6$. *That one single coefficient will take care of the whole ionization between so wide limits within which that ionization is so intense and varies over so wide a range, is one of the most striking and significant features of the cosmic rays brought to light by these studies.*

It is of some interest that $\mu = 0.79$ is the coefficient computed from the Klein-Nishina formula for 27 million volt rays, the energy released in the building of helium out of hydrogen. This formula, however, can in our judgment no longer be regarded as having any validity in the cosmic-ray field. If this band arises from atomic building processes at all its energy relations obtained in other ways point to the synthesis, either of helium or of oxygen out of hydrogen as its cause, but confining ourselves here to its absorption-properties alone one of the striking facts of this present experimental situation is that *this softest and most powerful cosmic-ray component appears to possess a coefficient which is from three to five times that of its nearest neighbor* to which any appreciable intensity can be assigned.

In a somewhat similar attempt at an analysis of the depth-ionization curve Regener[7] has used a function, developed by Kulenkampff,[10] which attempts to correct for the ionization produced by secondary photons. In the derivation of this function, however, Kulenkampff made the as-

[10] V. H. Kulenkampff, Phys. Zeits. **30**, 561 (1929).

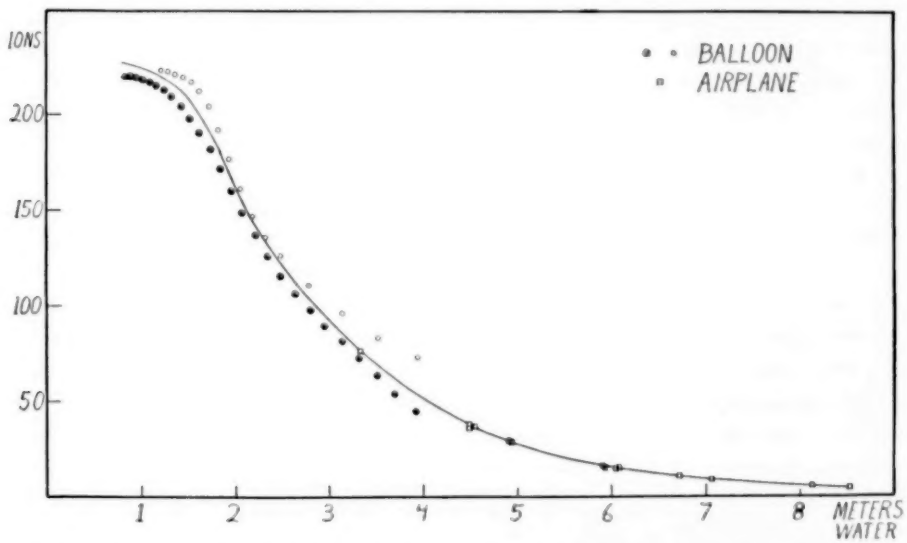

FIG. 4. Complete curve showing variation of cosmic-ray intensities with altitude as given by combining airplane observations and those made with free balloons.

sumption that in Compton scattering 70 percent of the energy of the primary quantum is retained by the scattered secondary photon, 49 percent by the tertiary, etc. A simple calculation on the basis of the Klein-Nishina formula, however, shows that for cosmic rays the secondary photon on the average receives only 20 percent, the tertiary 4 percent, etc. Furthermore, recent cloud chamber experiments by Dr. C. D. Anderson indicate that a large part of cosmic-ray absorption is photoelectric absorption in which no secondary photons are formed. This means, then, that the secondary photons contribute at most only a very few percent of the total ionization. Also, as most of the secondary photons are very much softer than the primaries, equilibrium between them has been practically attained at all observed points. Consequently we have continued to use the simple Gold function in building up the above depth ionization curves.

IV. Comparison of Cosmic-Ray Energy and Star-Light Energy

Having thus obtained with much greater accuracy than heretofore the complete cosmic-ray curve up to an altitude of 29,000 ft., we are now in position to extend it to within 0.6 meter of the top with the aid of the observations made last summer[11] at Dallas, Texas. The result is shown in Fig. 4, and the way the accurate airplane observations fit the balloon-points where the two curves overlap lends additional support to the general correctness of these balloon observations. The integral over this curve *from the top of the atmosphere*, to which it can be easily extrapolated, gives the result that a total of 6.25×10^{7} ions are formed per sec. per sq. cm of the earth's surface. If we assume that each ion requires 32 electron-volts of energy for its formation this corresponds to a total energy of 3.2×10^{-3} erg per sq. cm per sec. falling on the earth in the form of cosmic rays. This may be compared with 6.91×10^{-3} erg sq. cm per sec. received from star light[12] at our position in the Galaxy, or to from 2×10^{-5} erg to 2×10^{-4} erg for a position in intergalactic space. In other words, according to these most recent and most dependable of our integrated cosmic-ray measurements *the energy falling on the earth in this form is about half of the total radiant energy received from the stars, while the cosmic-ray energy of the universe is from 30 to 300 times greater than all other radiant energies combined.*

[11] Bowen and Millikan, Phys. Rev. **43**, 695 (1933).

[12] See accompanying paper by Dr. Korff of this laboratory, p. 300.

Relations Among Fluctuations of the Cosmic-Ray Ionization, of the Terrestrial Magnetic Field, of the Atmospheric Potential Gradient, and of the Absolute Humidity

JAMES W. BROXON, GEORGE T. MERIDETH AND LOUIS STRAIT, *University of Colorado*

(Received June 6, 1933)

In a recent paper the writers reported observations of the cosmic-ray ionization at four-hour intervals during a period of fifteen consecutive days. No regular diurnal variation was observed. The usual dependence of the ionization upon barometric pressure was observed, but no direct dependence upon atmospheric potential gradient, atmospheric temperature or absolute humidity was apparent. Dr. E. O. Hulburt suggested to the writers that there might be some correlation between fluctuations of the cosmic-ray ionization and terrestrial magnetic activity. Defining the cosmic-ray ionization "character" as the product of the average for a particular day by the difference between the maximum and minimum ionization values for that day, the writers found a considerable correspondence between the ionization "character" curve and the curve representing the magnetic character of days during the period of the observations. Further similarities with the corresponding "character" curves for the atmospheric potential gradient and the absolute humidity were brought out. Certain important consequences are pointed out.

IN a recent paper on *Fluctuations of Cosmic-Ray Ionization*,[1] the writers reported observations of the cosmic-ray ionization in a heavily shielded high-pressure chamber made at four-hour intervals during a period of fifteen consecutive days, April 6–20, 1932, with especially controlled laboratory conditions. In addition to the cosmic-ray ionization observations, records of the outdoor air temperature, the relative humidity, the barometric pressure, and the atmospheric potential gradient were obtained during the same period. When the cosmic-ray ionization values were plotted in turn against the barometric pressure, outdoor temperature, absolute humidity, and potential gradient, a first order relation was observed only in the case of the barometric pressure. The observed dependence of the ionization upon the barometric pressure was in good accord with the observations of other experimenters. No regular diurnal variation of the cosmic-ray ionization was observed, the probable error of the observations, calculated on the basis of deviations of individual values from the average, amounting to 0.21 percent of the mean.

Upon the appearance of that paper, Dr. E. O. Hulburt wrote us, calling our attention to the fact that magnetic disturbances often amount to four times as much as the regular diurnal magnetic variations. He further pointed out that if Gunn's[2] suggestion is correct in that diurnal magnetic variations might account for the diurnal variations in cosmic-ray observations by some experimenters, just as the terrestrial magnetic field might account for the dependence upon latitude noted by Compton,[3] Clay,[4] and others, then there might conceivably be a relation between the fluctuations of our ionization values and the larger magnetic disturbances, even though we had observed no regular diurnal variation. He further very kindly included values of the average magnetic character from 49 stations distributed over the earth (from Charactère Magnétique) and the magnetic character at Tucson (from Science Service Cosmic Data) during the period of our cosmic-ray observations.

Since the magnetic character was given for Greenwich days, our observations were regrouped on that basis. Since 5:00 P.M. Mountain Standard Time corresponds to midnight at Greenwich, we grouped our 5:30 P.M. and 9:30

[1] J. W. Broxon, G. T. Merideth and L. Strait, Phys. Rev. **43**, 687 (1933).

[2] R. Gunn, Phys. Rev. **41**, 683 (1932).

[3] A. H. Compton, Phys. Rev. **41**, 111 (1932).

[4] J. Clay, K. Akad, Amsterdam Proc. **33**, 711 (1930); only abstract read.

P.M. readings of April 6 with the 1:30 A.M., 5:30 A.M., 9:30 A.M., and 1:30 P.M. readings of April 7 to represent April 7 on the basis of G.C.T. This left only four readings representing April 6. All values for days referred to in this paper have been selected in this manner.

In an attempt to determine a function of the cosmic-ray ionization observations analogous to the magnetic character of days, the average of the values (generally six) for a particular day was multiplied by the difference between the greatest and the least of the values for that day. This product will be referred to as the cosmic-ray ionization "character" of the day.

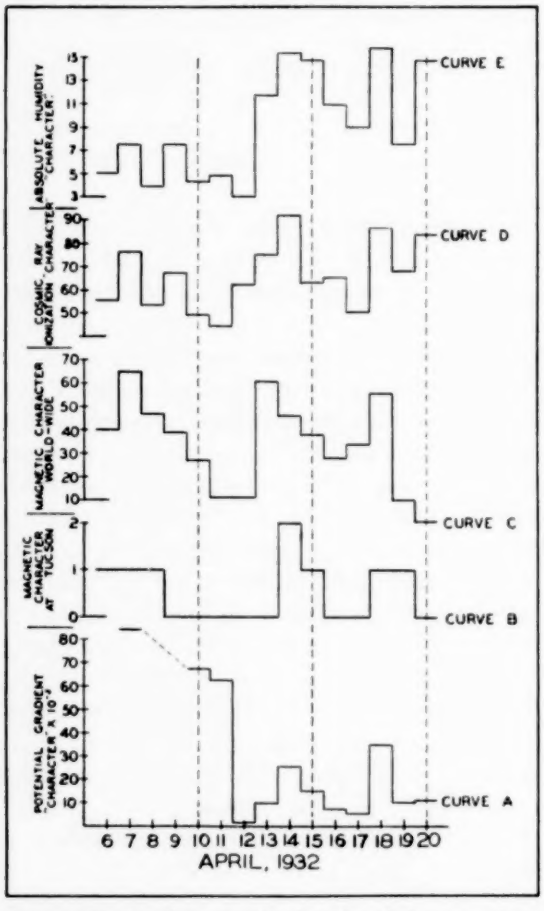

FIG. 1. Fluctuations in absolute humidity, cosmic-ray ionization, magnetic and atmospheric electric data during the fifteen-day period of our observations.

In Fig. 1, curve *B* represents the magnetic character at Tucson during the fifteen-day period of our measurements; curve *C*, the world-wide magnetic character; and curve *D*, the cosmic-ray ionization "character" at Boulder, altitude 5400 ft., latitude 40° 01′ N, longitude 105° 16′ W. The cosmic-ray "character" curve shows a considerable correspondence with the magnetic character curves. The maxima on the seventh, fourteenth and eighteenth, and the depressions in the neighborhood of the eleventh and seventeenth are rather striking. It is noticeable that the cosmic-ray ionization "character" maximum on the fourteenth corresponds precisely with the magnetic character maximum at Tucson, whereas the world-wide magnetic character maximum occurs on the thirteenth. (It should be recalled that Tucson is about 600 miles from Boulder in a direction about 30° W of S.) There are some differences between the forms of the curves, it is true, but the similarities seem too considerable to be ignored.

Inasmuch as the similarities between the magnetic and cosmic-ray ionization "character" curves were greater than had been anticipated, and to obtain some further appreciation of the significance to be attached to the "character" function of the cosmic-ray ionization, a similar function was evaluated for each of the other variables we had measured, the "character" of each being represented by the product of the average for the day by the range for the day. When each of these was plotted against the days of the month no similarities with the magnetic and cosmic-ray ionization "character" curves were apparent in the case of either the atmospheric temperature or the barometric pressure "character" curves (all ionization values had been corrected for barometric pressure variations in the manner described in the paper of reference 1)* and only a hint of correspondence in the case of the relative humidity "character" curve. The absolute humidity "character" curve *E* of Fig. 1, however, displays a very striking cor-

* The "character" curve (not shown) for *uncorrected* ionization values appears to retain the chief features common to the corrected ionization and the absolute humidity "character" curves, but may possibly be considered to resemble the barometric pressure "character" curve slightly more than does the corrected ionization "character" curve. The uncorrected ionization "character" does not correspond well with the magnetic character. Other than in this footnote, reference is made only to ionization values corrected for barometric pressure as described in the paper of reference 1.

respondence with the cosmic-ray ionization "character" curve. Curve *E* does not indicate a very large value on the seventh, as do *C* and *D*, but almost every minor irregularity of *D* is reproduced faithfully in *E*. Likewise, the atmospheric potential gradient "character" curve *A* of Fig. 1 shows some noticeable likeness to the other "character" curves. Data regarding the potential gradient were rather meager during the first several days, but the peaks on the fourteenth and eighteenth are again noticeable.

Adequate interpretation of the curves is a matter for some consideration. If further investigations over longer intervals of time and at various stations over the earth should confirm the relations apparently implied by these curves, the consequences would be many and important. That fluctuations in the cosmic-ray ionization intensity should accompany fluctuations in the terrestrial magnetic field, or the absolute humidity of the atmosphere, or the atmospheric potential gradient, or in all of them is not inconceivable. That there should be any close connection between the probably rather localized variations in the absolute humidity and the world-wide variations in the terrestrial magnetic field might not appear likely, although one can readily imagine a relation through the agency of atmospheric potential gradients and earth currents. In this connection it seems worth emphasizing that the large variations in the absolute humidity "character" curve do not correspond with those of the magnetic character curves nearly so well as do the small irregularities of the absolute humidity "character" curve with those of the cosmic-ray ionization "character" curve.

That cosmic-ray ionization disturbances might be associated with variations in the absolute humidity or the potential gradient may seem quite unlikely in view of the quite random distributions shown in Figs. 3 and 4 of the paper of reference 1. However, as was there emphasized, these diagrams could only be expected to bring out a first order dependence. If the ionization values should depend simultaneously upon several variables, the nature of this dependence would probably be indicated as in Fig. 1 of that paper only in case the effect of one of them was decidedly predominant. Moreover, a dependence of one variable upon the time rate of change or some other indirect function of another would not be brought out by these diagrams. In order to designate clearly the relations between the observed values of the three quantities whose "character" curves have been found of interest in connection with the magnetic character curves, Figs. 2 and 3 have been included. In Fig. 2 the

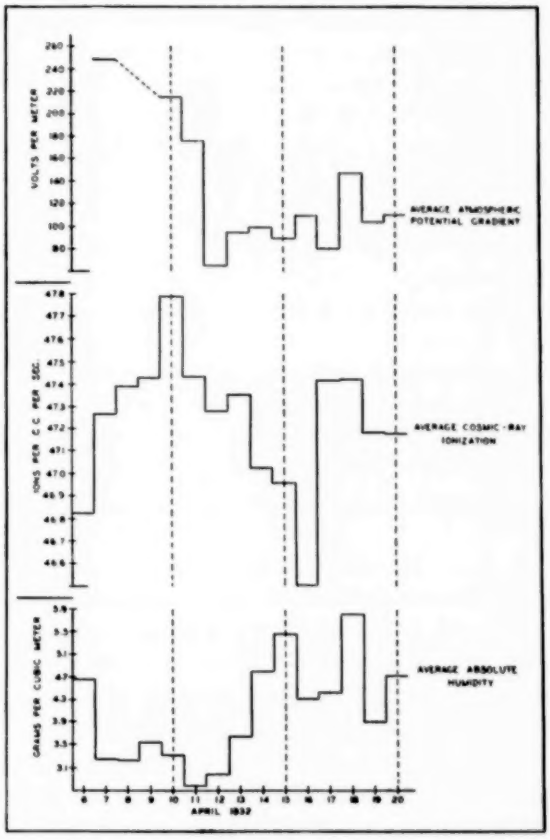

FIG. 2. Mean (Greenwich day) values of the potential gradient, the cosmic-ray ionization, and the absolute humidity during the period of our observations.†

mean (Greenwich day) values of the potential gradient, the cosmic-ray ionization, and the absolute humidity, respectively, are designated. In Fig. 3 the corresponding individual values are shown. It should be recalled that each of these is the average of (usually) three independent observations made during an interval of about an hour. Also, it should be mentioned that in these diagrams as in the calculation of the potential gradient "character," a high off-scale reading at 9.30 A.M., April 7, M.S.T., was arbitrarily assigned a value of 500 volts/meter, and a low off-scale value (incorrectly designated high in Fig. 4

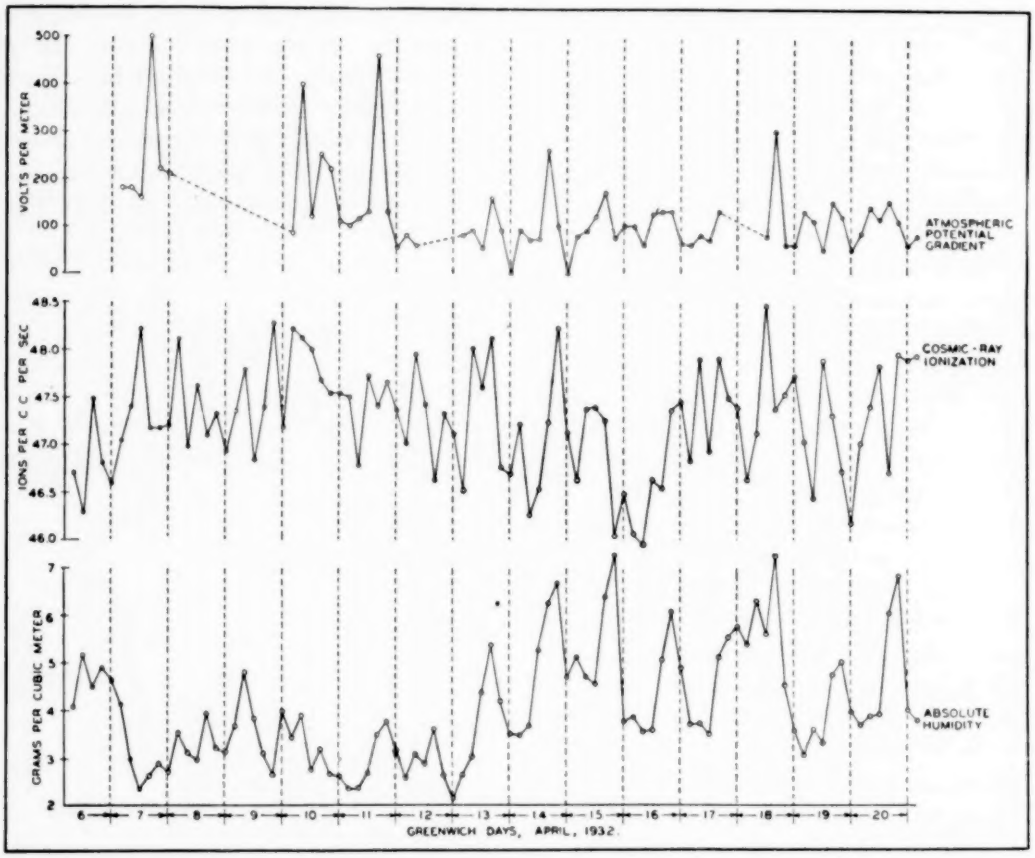

FIG. 3. The individual values corresponding to the averages of Fig. 2.*

of reference 1) at 5:30 P.M., April 14, M.S.T., was arbitrarily assigned the value, zero.

No general constant relation appears to be brought out by these curves, but there is a very noticeable inverse relation between the average ionization and absolute humidity curves of Fig. 2 during the first nine days. Later the irregularities of the two curves appear to be rather more nearly in phase than otherwise.†

The possibility of a humidity effect through the agency of insulation leakage in the apparatus will probably occur to the reader. Such a possibility

* Both in Fig. 2 and Fig. 3 of this paper and in Fig. 4 of the paper of reference 1, potential gradient values are erroneously recorded as *volts per meter*. Actually, the designated values should be divided by the reduction factor, 2.35, in order to reduce them to *volts per meter*.

† *Note added in proof.* If one plots the daily average ionization against the daily average absolute humidity (values shown in Fig. 2) for the *first ten days*, the best straight line through the points as determined by the method of least squares has a slope indicating a decrease of 0.5 per cent in the ionization accompanying an increase of one g per cubic meter in the absolute humidity. When the individual *uncorrected* or observed ionization values for the 15-day period are corrected for humidity on this basis, the ionization "character" curve (not shown) obtained with values so corrected does not appear to correspond with the barometric pressure "character" curve appreciably better than does that obtained with entirely uncorrected ionization values. This might very well be the situation even if the cosmic-ray ionization actually does depend upon the water vapor content of the atmosphere. Probably the absolute humidity at a point on the earth's surface at a particular instant is not at all representative of that at higher altitudes at that instant, whereas the average value of the humidity at the earth's surface during a whole day may be fairly representative of average conditions throughout the neighboring atmosphere during that day. If one corrects hourly ionization values on the basis of the simultaneous absolute humidity at the earth's surface, then, he may very well introduce as many errors as corrections. In order to make an adequate integrated humidity correction, one may require simultaneous humidity values extending to high altitudes and to considerable horizontal distances.

would be very unlikely for several reasons. In the first place, it was the absolute rather than the relative humidity fluctuations which yielded the "character" curve closely resembling that of the cosmic-ray ionization. Moreover, whereas the potential gradient observations depended upon actual deflections of an electrometer with its very carefully insulated system, the cosmic-ray ionization electrometer was used merely as a null instrument, the central system being maintained at all times at the potential of the specially constructed guard system described elsewhere.[5] Also, in addition to the fact that the entire cosmic-ray ionization measuring equipment with its water shield was indoors, the guard system (with the high potential system at one point) entirely surrounded the central system, and separated it mechanically from the air in the room. The air inside the guard system and adjacent to the amber and ebonite insulation of the central system was kept dry by P_2O_5. Under these circumstances, it does not seem that the absolute humidity of the outdoor atmosphere could have influenced the cosmic-ray ionization measurements by affecting the electrical insulation.

That relations between "character" curves might appear without corresponding obvious relations among the curves representing the average magnitudes of the quantities, themselves, might perhaps result from an indirect dependence of one variable upon another, or from simultaneous dependence of one variable upon two or more relatively independent variables. In the latter case, relations between the magnitude curves of the dependent and an independent variable might be apparent at one time and not at another.

Dr. Hulburt has pointed out that the apparent dependence upon magnetic activity herein discussed may not be in contradiction with the fact that Millikan[6] and Corlin[7] found no auroral effect upon the cosmic-ray ionization at latitudes of 59°N and 68°N, respectively, since the effect might be less pronounced at high latitudes, and because of the possibility (though improbable) that the aurorae in those instances might have occurred with no world-wide magnetic storms.

In passing it may be worth remarking that if the cosmic-ray ionization varies with meterological conditions for which corrections are not applied, then probable errors calculated on the basis of variations of individual observations from the average probably have very little significance.

If further observations confirm the relations herein indicated, there will be numerous consequences. As Dr. Hulburt points out, it would follow that cosmic-rays offer another tool for the study of terrestrial magnetism, particularly the external magnetic field of the earth. Also, further considerations of meteorological conditions would be necessary for correct interpretations of cosmic-ray ionization observations.

The critical feature of this treatment of the data consists of the "character" functions which have been defined. The propriety of defining such functions may not be obvious; their real significance and the implications inferred from them may be questioned, particularly in view of the limited number of observations each day. However, the similarities among the "character" curves which were obtained appear too striking to be left unmentioned.

[5] J. W. Broxon, Phys. Rev. **37**, 1320 (1931).

[6] R. A. Millikan, Phys. Rev. **36**, 1595 (1930).

[7] Corlin, Nature **130**, 245 (1932).

X-Ray Line Intensities and Cathode-Ray Retardation in Thick Targets of Silver

D. L. WEBSTER, W. W. HANSEN* AND F. B. DUVENECK, *Stanford University*

(Received April 28, 1933)

K-line intensities from thick silver targets have been measured in arbitrary units for voltages up to 180 kv, with emergence angles from 1 to 25°. A practical use of these data is the determination of the voltage which will give the maximum efficiency of line emission at any emergence angle. At 1° the best voltage is 70 kv but at 25° it is well above 180 kv. These data are also used in conjunction with data on thin targets to get information as to the retardation of cathode rays in silver. For this purpose the thick-target data are corrected to eliminate the effects of target absorption, indirect production of line rays through fluorescence and loss of cathode rays by rediffusion. The loss of energy per unit distance along the path of a cathode ray varies as the -1.4 power of the speed, just as it does in light elements according to more direct evidence collected by E. J. Williams.

I. LINE INTENSITIES

DATA on x-ray line intensities as functions of tube voltage have often been used to test theories of ionization probabilities for inner electrons. Taking rays from the thick targets generally used, such tests depend on assumptions about the law of retardation of cathode rays within the targets. While the Thomson-Whiddington law has been used practically universally for this, evidence for a change has appeared from various sources. These include x-rays, in Kulenkampff's[1] comparisons of his continuous-spectrum intensities from thick and thin aluminum, which indicate that the change in the retardation rate with speed is less rapid than that law would make it. Our present purpose is to make similar comparisons for silver, with line intensities, by using our thin-target data already published[2] and thick-target data to be presented here; and to find a more quantitative law of cathode-ray retardation.

Our thick-target data were taken in two groups, with different tubes. The first tube[3] was made of brass and glass, cemented with Dennison's "royal scarlet" sealing wax and carrying the electrodes on greased ground joints. While this tube ran smoothly even at 200 kv, it was discarded for one with no wax or grease[4] and our conclusions on cathode-ray retardation are based on the work with this second tube.

Fig. 1 shows the data of both groups. Here the $K\alpha$ line intensity for constant current is shown as a function of U, the ratio of tube voltage to K-ionizing voltage, and Θ, the angle made by the x-rays with the polished surface of the target. The dependence on Θ is due primarily to absorption in the target but there are also slight differences of scale caused by differences in reflection efficiency at different parts of the crystal, which affect any comparison of line rays from sources of different widths.

In Fig. 2 the same data are shown logarithmically and another graph is added, above those for the angles noted, for the intensity with target absorption entirely eliminated, as described below.

A straight line here would correspond to the formula[5]

$$I(U)=K(U-1)^n, \qquad (1)$$

where K and n are constants. This formula is evidently not accurate even for the case of no target absorption, though for that case it fits fairly well up to about $U=4$ with $n=1.65$.

* Now National Research Fellow at Massachusetts Institute of Technology.

[1] H. Kulenkampff, Ann. d. Physik **87**, 597 (1928), and Phys. Zeits. **30**, 515 (1929).

[2] D. L. Webster, W. W. Hansen and F. B. Duveneck, Phys. Rev. **43**, 839 (1933).

[3] D. L. Webster, H. Clark and W. W. Hansen, Phys. Rev. **37**, 115 (1931).

[4] D. L. Webster, W. W. Hansen and F. B. Duveneck, Rev. Sci. Inst. **3**, 729 (1932).

[5] D. L. Webster and H. Clark, Proc. Nat. Acad. Sci. **3**, 181 (1917); A. Jönsson, Zeits. f. Physik **36**, 426 (1926); S. K. Allison, Phys. Rev. **30**, 245 (1927); and others.

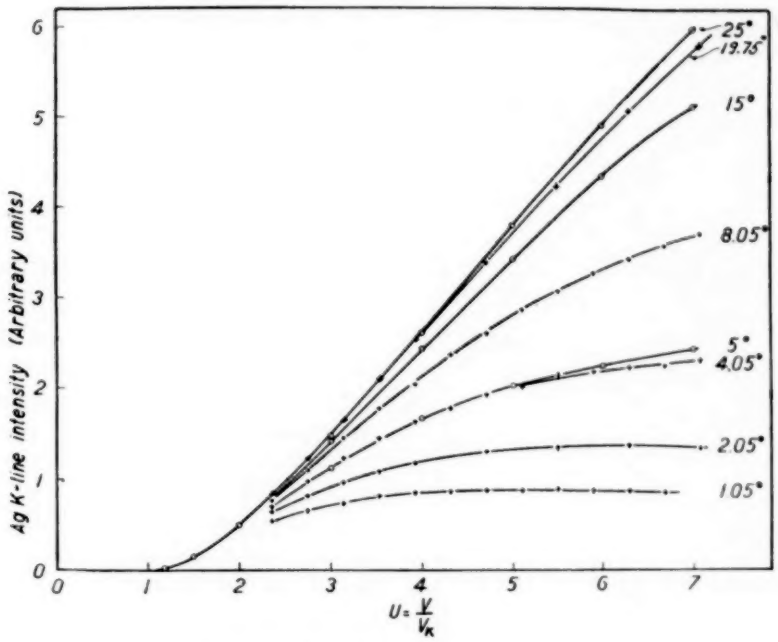

FIG. 1. Ag line intensities for constant current.

For practical uses of line rays, such as crystal analysis, it is often necessary to choose a tube voltage for maximum output at constant power, rather than constant current. In Fig. 3, therefore, we have plotted graphs on this basis. Evidently the best voltage depends greatly on the emergence angle.

II. CORRECTIONS

The comparison of thick and thin targets proposed in Section I would be more direct if the thick targets did not involve certain minor complications. One of these, obviously, is the loss of intensity by absorption of some of the rays to be measured, on their way out of the target. Another is a gain of intensity in the line-spectrum rays by fluorescence absorption of continuous-spectrum rays. A third complication is a loss resulting from the loss of some of the cathode rays by rediffusion. The next procedure is therefore to correct the observed intensities into those of an ideal thick target, not involving these complications.

To eliminate absorption of the line rays, one might perhaps attempt first to calculate the absorption from the depths at which the rays are produced, obtaining these in turn from such data as are already at hand on the retardation of cathode rays in the target material. Practically, however, this is next to impossible because in any element as heavy as silver the depths of penetration of cathode rays are limited much more by diffusion than by retardation and the combined effect of these two processes is very difficult to calculate. We are therefore using the experimental method due to Kulenkampff[6] which is based on a comparison of rays at different emergence angles. Theoretically, if all the rays could be produced at the same depth, X, their intensity would be reduced by absorption in the ratio $\exp(-\mu X \csc \Theta)$ where Θ is the emergence angle measured from the surface of the target. A graph of the logarithm of the intensity against $\csc \Theta$ would then be linear, and could be extrapolated accurately to $\csc \Theta = 0$, eliminating all target absorption. As a matter of fact, however, the rays are not all produced at the same depth and the graph is therefore not quite straight; and with an element as heavy as silver, the depths of production vary even more than the depths of penetration of cathode rays, because about a third of the line-spectrum x-rays

[6] H. Kulenkampff, Ann. d. Physik **69**, 548 (1922).

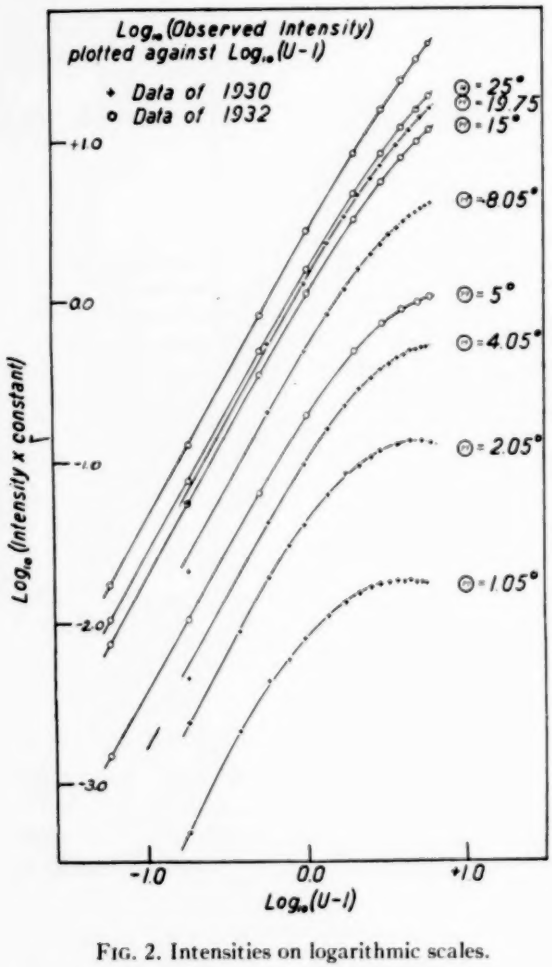

FIG. 2. Intensities on logarithmic scales.

are produced indirectly by fluorescence within the target. This departure from straightness produces some uncertainty in the extrapolation, and another source of uncertainty here is the difficulty of standardizing the units of intensity at different emergence angles. To remove this latter uncertainty, the best plan is to straighten one of the graphs arbitrarily by a proper choice of units for each emergence angle. If there was any theory for the correct curvatures of these graphs, this plan would sacrifice it and thereby lose accuracy. Without any such theory, however, it gains accuracy by reducing the curvatures of the graphs most strongly curved. The one we have chosen to straighten is that for $U=2$. The family of graphs thus obtained is shown in Fig. 4, and the intensities for csc $\Theta=0$ from this figure are those plotted as the uppermost graph in Fig. 2. Incidentally, the spacings of the graphs in Fig. 2 at $U=2$, or $\log_{10}(U-1)=0$, are proportional to csc Θ, except for the lowest two graphs, which would require too much space if plotted this way. The regularity with which the curvatures of these graphs increase with this spacing is therefore an index of the consistency of these data.

The corrections for the other two complications are by methods explained elsewhere. For the elimination of the rays produced indirectly, through fluorescence, we use the data of Hansen and Stoddard.[7] Working with palladium at an emergence angle of 90°, they find the direct rays, produced by impact ionization, to constitute 0.66 of the total line-spectrum rays at 40 kv, 0.67 at 100, and 0.68 at 180. For silver, the ratios are probably slightly lower but since our intensities are in an arbitrary unit, the only important feature of this ratio is its change with voltage. Data on silver up to 80 kv[8] indicate small changes similar to those with palladium. Here, therefore, we are simply using the palladium ratios and neglecting the small effect of target absorption on them.

For the third correction, for rediffusion, the method is that of Webster, Clark and Hansen[3] but with one notable improvement. To calculate the loss of intensity at any voltage by rediffusion, one needs to know the function giving the intensities to be found without rediffusion, at all lower voltages. Fortunately this function need not be known accurately but whereas we used very rough approximations before, we used Eq. (1) this time, with $n=1.73$. The correction is made after those for absorption and indirect rays, by multiplying the intensities as they are then by the factors given in Table I.

TABLE I. *Correction factors for rediffusion.*

U	Factor	U	Factor
1.000	1.00	3	1.26
1.056	1.01	4	1.28
1.178	1.06	5	1.29
1.5	1.16	6	1.30
2.0	1.23	7	1.31

[7] W. W. Hansen and K. B. Stoddard, Phys. Rev. **43**, 701 (1933).

[8] D. L. Webster, Proc. Nat. Acad. Sci. **14**, 339 (1928).

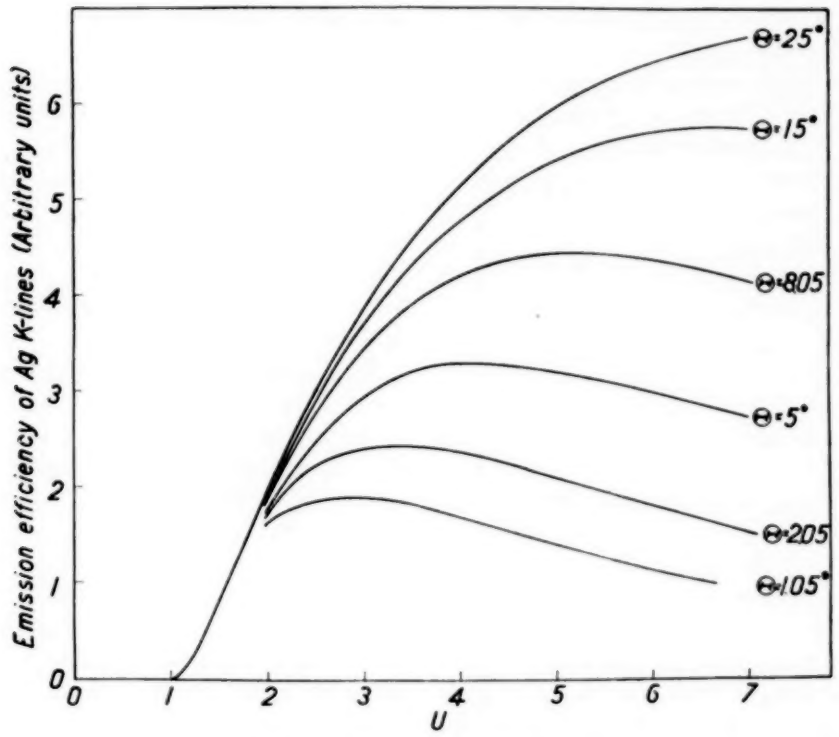

FIG. 3. Ag line efficiencies in arbitrary units.

The resulting intensities are shown logarithmically in Fig. 5. As is evident there, the corrections for indirect rays and rediffusion make the graph steeper than that of Fig. 2, which is repeated here for comparison. In fact, where the data corrected for absorption only were fitted fairly well below $U=4$ by Eq. (1) with $n=1.65$, those corrected for all three complications are fitted about equally well over the same range with $n=1.74$.

It must be noted, however, that Eq. (1) does not fit exactly with any fixed exponent. The best value of n in the immediate neighborhood of any point is of course the slope of the logarithmic graph at that point. Like the slope of any empirical graph, this is somewhat uncertain, especially near $U=1$, where the intensity is weak and also the errors in U show prominently in log $(U-1)$. Fortunately, however, we can get the slope at $U=1$ from our data on thin targets,[2] because the derivative of the thin-target intensity with respect to U is finite and not zero at $U=1$. Whatever the law of cathode-ray retardation may be, provided only that it is continuous, equations to be given below show that this behavior of thin targets requires thick targets to have n approach 2 as U approaches 1. We have therefore used this value as one of the data for plotting n against U, regarding it as more reliable than any other point near $U=1$. Above that, the values of n are computed from secants between the points of Fig. 5 and they are plotted for values of U in the middles of these intervals. The resulting graph is Fig. 6.

III. Cathode-Ray Retardation

Returning to the problem proposed in Section I, we shall now use our data on line intensities from thick and thin[2] targets to calculate the cathode-ray retardation rate. Letting U' represent the kinetic energy in terms of the ionization energy, at a distance s along the path of a cathode ray in the target, as U represents it at $s=0$, it is known that

$$i_o(U)=(dI_o(U)/dU)(-dU'/ds)_{U'=U} \qquad (2)$$

where $I_o(U)$ is the intensity from an idealized thick target, obtained as described above, and

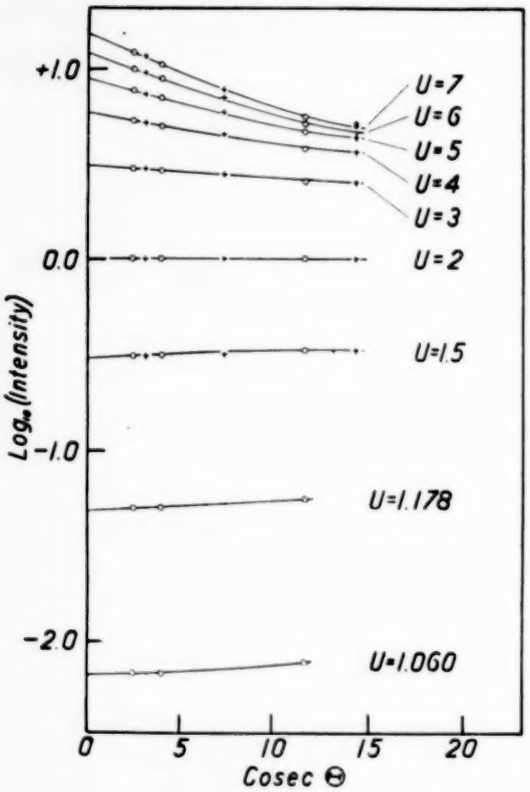

FIG. 4. Eliminating target absorption.

$i_o(U)$ is the intensity per unit thickness from a correspondingly idealized thin target. Both of these intensities are measured here in arbitrary units. Theoretically these units ought to be the same, so that they would cancel in solving for $-dU'/ds$. Practically, however, the difficulties of measuring the thickness of a thin target accurately make i_o even more arbitrary than I_o. Consequently we do not wish to commit ourselves on the absolute value of $-dU'/ds$ here beyond its order of magnitude, which was shown, in our paper on thin targets, to agree well enough with previous measurements. The objective here is rather to find how dU'/ds varies with U'.

While the data for $i_o(U)$ and $I_o(U)$ are fairly accurate, those for $dI_o(U)/dU$ are subject to the uncertainty common to all derivatives of empirical functions. In this case, this uncertainty is increased by the rapidity with which $dI_o(U)/dU$ changes with U. The logarithmic derivative shown in Fig. 6, however, changes much less rapidly and needs only to be multiplied by $I_o(U)/(U-1)$ to give $dI_o(U)/dU$. The best procedure, therefore, seems to be to eliminate the erratic errors as well as possible by reading values of these functions from the graphs of Figs. 6 and 5. Since this gives dU'/ds as a continuous function, it is plotted as such in Fig. 7. In this graph the upper limit of U is 6.5, as in Fig. 6. For the lower limit, an extension of the reasoning about the behavior of these functions near $U=1$ gives a value for dU'/ds for that point but not with the same degree of certainty, so the graph is dotted below $U=1.2$.

In much of the theoretical work done on cathode rays, relativity has been neglected, more or less of necessity, and their behavior has been described in terms of either their kinetic energy or the square of their speed, as if these quantities were equivalent. At the lower end of the range of the present data, this is not very inaccurate but at the upper end the kinetic energy varies practically as the cube of the speed. This raises a question, whether we should expect dU'/ds to be specified most simply in terms of energy or of speed.

For evidence on this point from previous work,

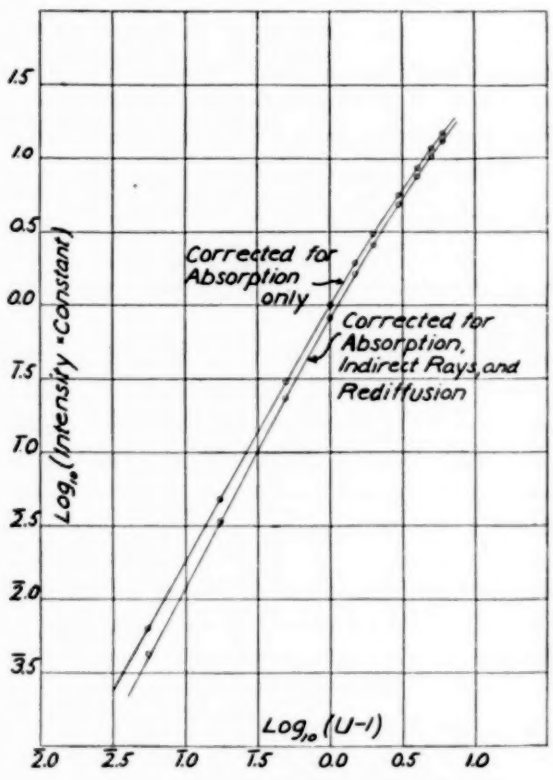

FIG. 5. Intensities after corrections.

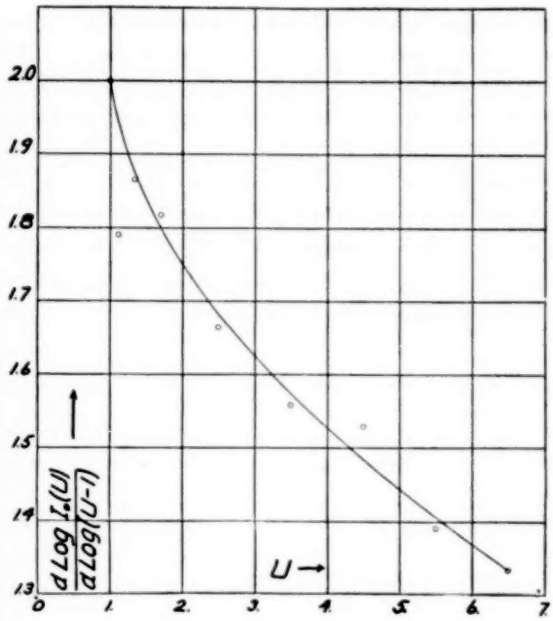

FIG. 6. n as a function of U.

an exceptionally clear case is described by Williams[9] in reviewing the work of Becker[10] on aluminum and White and Millington[11] on mica. Their data begin at $\beta=0.52$, or about 80 kv, in the middle of our range. For them a constant power of the speed, namely the -1.4 power, gives a surprisingly close proportionality to a quantity differing by only a few percent from $-dV'/ds$, even up to $\beta=0.96$. Over most of this range no constant power of the kinetic energy could imitate any constant power of the speed. For this reason we have plotted two graphs in Fig. 7, both logarithmic, against energy and (speed),[2] to show whether any proportionality occurs in our data with any power of either energy or speed.

It is evident that while neither graph is exactly linear, the speed graph is the straighter of the two. Furthermore, while the slope of the straightest part of this graph, in terms of speed rather than its square, is -1.5, slightly steeper than Williams' formula would indicate, the slope of a chord from end to end is almost exactly his exponent, -1.4.

To be sure, a different exponent is advocated by him for very low voltages, below 20 kv, where he puts the law in a form equivalent to an exponent -0.82 for the energy, or nearly -1.7 for the speed. For the region between 20 and 80 kv he has no data, but the -1.4 power holds so well from high speeds down to 80, and the exponent -1.7 differs from -1.4 so little, that it seems reasonable to expect a steady transition between them. This agrees excellently with our data—indeed too well for us to consider the agreement not partly due to chance.

For practical purposes it is often convenient to calculate in terms of voltage rather than speed and a fractional power of V' will sometimes serve for rough calculations. For the lower half of our range the best exponent is -0.67; for the upper half, about -0.45; near the middle or for the range as a whole, about -0.6.

The theoretical significance of our results becomes evident through later papers of Williams.[12] In these he made very careful analyses of the data on light elements and concluded that Bethe's[13] theory, based on nonrelativistic wave mechanics, was the best, especially if modified in certain ways based on relativity. Since most of the energy taken from the cathode rays is taken by the more easily ionized electrons in the atoms, the differences between silver and the light elements ought to be small, probably

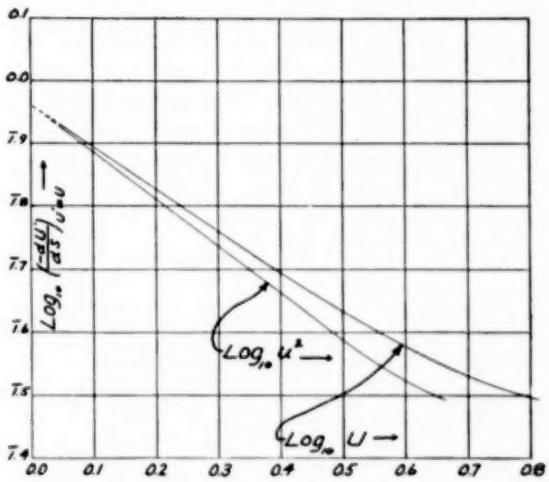

FIG. 7. Cathode-ray retardation in arbitrary units.

[9] E. J. Williams, Proc. Roy. Soc. **A130**, 310 (1931).

[10] E. Becker, Ann. d. Physik **78**, 209 (1925).

[11] P. White and G. Millington, Proc. Roy. Soc. **A120**, 701 (1928).

[12] E. J. Williams, Proc. Roy. Soc. **A130**, 328 (1931); **A135**, 108 (1932).

[13] H. Bethe, Ann. d. Physik **5**, 325 (1930).

within our present limits of error. So the similarity of our retardation function to Williams' indicates that our data, like his, favor Bethe's theory.

Sooner or later our results will probably be supplanted by others based on more direct measurements of retardation. If they confirm the law deduced here, the present measurements will no longer be needed as evidence on cathode-ray retardation but will then become evidence on the theory of thick-target x-ray emission. They will then indicate that the process of line-spectrum emission does, indeed, depend primarily on the laws of thin-target emission and cathode-ray retardation, as assumed here, with minor complications due to absorption, rediffusion and the indirect production of line rays by fluorescence and that all the important factors in the process of thick-target line emission are now recognized and approximately measured.

The Relative Abundance of Hydrogen Isotopes

WALKER BLEAKNEY AND AUSTIN J. GOULD, *Palmer Physical Laboratory and Frick Chemical Laboratory, Princeton University*

(Received June 30, 1933)

Samples of rain water collected at Princeton were decomposed by repeated passage over iron turnings heated to 510°C. The hydrogen formed was analyzed with a mass-spectrograph to determine the abundance ratio $H^2 : H^1$. The first fraction of hydrogen to be liberated from a particular sample of the water yielded a value given by $H^2 : H^1 = 1 : 6500$ while the last fraction gave 1 : 4500. Another sample was prepared in which the decomposition was carried to completion and all of the hydrogen collected. The abundance found in this sample was 1 : 5000. It is believed that this last figure represents a close approximation to the true abundance ratio for natural hydrogen. The value 1 : 30,000 previously reported by Bleakney for electrolytic hydrogen may be in agreement with these measurements when account is taken of the separation introduced by the electrolysis. A fairly extensive bibliography is given of recent work on the hydrogen isotopes.

INTRODUCTION

SINCE the discovery more than a year ago of a hydrogen isotope of mass 2 many attempts have been made to determine its true abundance in nature by estimating the relative numbers of H^1 and H^2 to be found in natural hydrogen. Large discrepancies exist, however, among the results so far obtained. From his observations on the magneto-optical effect Allison[1] believed that hydrogen had two isotopes but Urey, Brickwedde and Murphy[2] secured the first positive and quantitative evidence for the existence of an isotope of mass 2 and at that time they gave for the abundance ratio the value $H^2 : H^1 = 1 : 4000$. This was in agreement with that predicted by Birge and Menzel[3] to account for the discrepancy between the chemical atomic weight and Aston's mass determinations. Bleakney[4] shortly after confirmed their discovery by an independent method but found a much smaller abundance for H^2. Even when Urey and Bleakney studied by their respective methods the same sample of hydrogen enriched by evaporation near the triple point they failed to agree on the relative amounts of H^1 and H^2 present. Urey, Brickwedde and Murphy[5] subsequently suggested a plausible explanation for this difference when they pointed out that the error could be attributed to unequal absorption in their discharge tube thus enhancing the H^2 lines at the expense of the H^1 spectrum. Meanwhile Bainbridge[6] had succeeded in making some excellent measurements of the mass of the new isotope. Bleakney's result for the abundance, $H^2 : H^1 = 1 : 30{,}000$, was checked by the work of Hardy, Barker and Dennison[7] in which they found 1 : 35,000, and later by Tate and Smith[8] when they reported a value of the order of 1 : 30,000. Also Rank[9] succeeded in photographing the $H\gamma$ line and concluded that the abundance must be roughly of this order of magnitude.

The early work of Stern and Volmer,[10] however, indicated that H^2 cannot exist to the extent of one part in 100,000 while Menzel[11] and Unsöld[12] reached the same conclusion for the abundance of H^2 in the sun. Kallmann and

[1] F. Allison, J. Ind. Eng. Chem. **4**, 9 (1932); J. Chem. Ed. **10**, 7 (1933).

[2] H. C. Urey, F. G. Brickwedde and G. M. Murphy, Phys. Rev. **40**, 1 (1932), **39**, 164 (1932) and **39**, 864 (1932).

[3] R. T. Birge and D. H. Menzel, Phys. Rev. **37**, 1669 (1931).

[4] W. Bleakney, Phys. Rev. **41**, 32 (1932).

[5] H. C. Urey, F. G. Brickwedde and G. M. Murphy, Phys. Rev. **40**, 464 (1932).

[6] K. T. Bainbridge, Phys. Rev. **41**, 115 (1932), **42**, 1 (1932) and **44**, 57 (1933).

[7] J. D. Hardy, E. F. Barker and D. M. Dennison, Phys. Rev. **42**, 279 (1932).

[8] J. T. Tate and P. T. Smith, Phys. Rev. **43**, 672 (1933).

[9] D. H. Rank, Phys. Rev. **42**, 446 (1932).

[10] O. Stern and M. Volmer, Ann. d. Physik **59**, 225 (1919).

[11] D. H. Menzel, Pub. Ast. Soc. of the Pac. **44**, 41 (1932).

[12] A. Unsöld, Naturwiss. **20**, 936 (1932).

Lasareff[13] made an attempt to find this elusive isotope and concluded it did not exist to the extent of one part in 10^6, basing their result on the extreme rarity of the $(H^1H^1H^2)^+$ ion as compared to the ordinary triatomic ion. This result is difficult to understand since Bainbridge[6] was able to photograph the triatomic ion of mass 4 with ease which proves that this ion is readily formed. Later, Kallmann and Lasareff[14] reported the detection of H^2 in some enriched samples of hydrogen.

The wide discrepancies among the various observations began to be understandable when Washburn and Urey[15] discovered the electrolytic method of separating the isotopes. Most of the researches so far mentioned have been carried out with electrolytic hydrogen, commercial or otherwise, and the hydrogen collected was therefore enriched in the lighter isotope by an amount depending on the age of the cell from which it came. By the electrolytic method Lewis[16] and Macdonald[17] obtained a very high degree of separation and concluded from their observations that the natural abundance for H^2 was about 1 : 6500. However, shortly after the publication of this communication Lewis and Cornish[18] expressed the opinion that this value was entirely too high.

At this point it might be well to complete the bibliography of the widely scattered references dealing with this isotope even though some of the work may not have a direct bearing on the subject of this paper.* On the theoretical side have appeared papers by Eyring,[19] Eyring and Sherman,[20] Urey and Rittenburg,[21] and Polanyi.[22] Other methods of concentration have been tried by Newell and Ficklen,[23] Washburn and Smith,[24] Taylor, Gould and Bleakney,[25] Lewis and Cornish,[18] and Cremer and Polanyi.[26] Bradley and Urey[27] have studied the concentrations in natural hydrogen from several different sources. Meissner and Steiner[28] measured directly the variation of the vapor pressure of hydrogen with concentration of the heavier isotope. Ashley[29] and Lewis[30] have observed the band spectrum of the heavy isotope and deduced a spin of unity for the H^2 nucleus. Ballard and White[31] have photographed and measured several members of the Lyman series and Williams and Gibbs[32] have reported some work on the fine structure of the spectrum of the heavy isotope. Lukanow and Schütze[33] have obtained spectra by the parabola method of the negative ion H^{2-}. Recently, also, the H^2 atom has been used as a new projectile in disintegration studies by Lewis, Livingston and Lawrence.[34]

A knowledge of the true abundance of the two

[13] H. Kallmann and W. Lasareff, Naturwiss. **20**, 206 (1932).

[14] H. Kallmann and W. Lasareff, Naturwiss. **20**, 472 (1932).

[15] E. W. Washburn and H. C. Urey, Proc. Nat. Acad. Sci. **18**, 496 (1932).

[16] G. N. Lewis, J. Am. Chem. Soc. **55**, 1297 (1933).

[17] G. N. Lewis and R. T. Macdonald, J. Chem. Phys. **1**, 341 (1933).

[18] G. N. Lewis and R. E. Cornish, J. Am. Chem. Soc. **55**, 2616 (1933).

* See also the following references which were either overlooked or were published after this paper was written: E. W. Washburn, E. R. Smith and M. Frandsen, J. Chem. Phys. **1**, 288 (1933); H. L. Johnston and D. H. Dawson, Naturwiss. **21**, 495 (1933); G. N. Lewis and F. H. Spedding, Phys. Rev. **43**, 967 (1933); G. N. Lewis and R. T. Macdonald, J. Am. Chem. Soc. **55**, 3057 (1933); F. H. Spedding, C. D. Shane and N. S. Grace, Phys. Rev. **44**, 58 (1933); H. C. Urey, G. M. Murphy and F. G. Brickwedde, J. Chem. Phys. **1**, 512 (1933); J. Kendall, J. Am. Chem. Soc. **55**, 2612 (1933).

[19] H. Eyring, Proc. Nat. Acad. Sci. **19**, 78 (1933).

[20] H. Eyring and A. Sherman, J. Chem. Phys. **1**, 345 (1933).

[21] H. C. Urey and D. Rittenburg, J. Chem. Phys. **1**, 137 (1933).

[22] M. Polanyi, Naturwiss. **21**, 316 (1933).

[23] I. L. Newell and J. B. Ficklen, J. Am. Chem. Soc. **55**, 2167 (1933).

[24] E. W. Washburn and E. R. Smith, J. Chem. Phys. **1**, 426 (1933).

[25] H. S. Taylor, A. J. Gould and W. Bleakney, Phys. Rev. **43**, 496 (1933).

[26] E. Cremer and M. Polanyi, Zeits. f. physik. Chemie **B19**, 443 (1932).

[27] C. A. Bradley and H. C. Urey, Phys. Rev. **40**, 889 (1932).

[28] W. Meissner and K. Steiner, Zeits. f. Physik **79**, 601 (1932).

[29] Muriel F. Ashley, Phys. Rev. **43**, 770 (1933).

[30] G. N. Lewis and Muriel F. Ashley, Phys. Rev. **43**, 837 (1933).

[31] S. S. Ballard and H. E. White, Phys. Rev. **43**, 941 (1933).

[32] R. C. Williams and R. C. Gibbs, June Meeting, Am. Phys. Soc., Chicago, 1933.

[33] H. Lukanow and W. Schütze, Zeits. f. Physik **82**, 610 (1933).

[34] G. N. Lewis, M. S. Livingston and E. O. Lawrence, June Meeting, Am. Phys. Soc., Chicago, 1933. Also Phys. Rev. **44**, 55, 56 (1933).

isotopes in natural hydrogen is of fundamental importance and the discordant results already reported leave much to be desired. Before the question is settled the abundance must be measured in a variety of natural sources of hydrogen by a trustworthy method which introduces no change in the concentration during the process. The present work was undertaken as a first step toward this objective.

Preparation of the Samples

All of the present work was done on samples of rain water collected at Princeton and purified by distillation from alkaline permanganate in an all-Pyrex still. The water was decomposed by repeated passage over iron turnings heated to 510°C. Fig. 1 is a diagram of the apparatus used

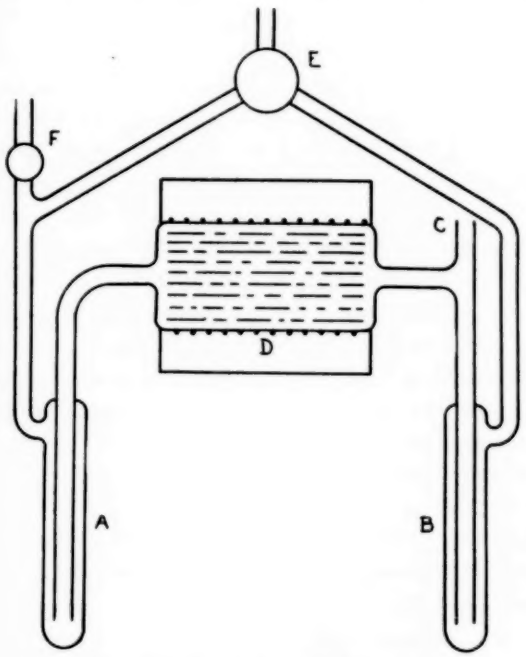

Fig. 1. Diagram of decomposition apparatus.

for the decomposition. *A* and *B* are small traps which may be surrounded by liquid air. *D* is a connecting tube packed with iron turnings, wound with resistance wire, and insulated with a heavy layer of asbestos. In order to obtain fairly pure iron free from carbon the turnings were prepared from a piece of Norway iron. *F* leads to a mercury diffusion pump backed by an oil pump. *E* is a three-way stopcock leading to an automatic Sprengel pump.

In the first experiment 0.3 cc of water was placed in *B* through the opening *C* after which tube *C* was sealed off. *B* was cooled in liquid air and the entire system evacuated through *F*. Stopcock *F* was then closed, stopcock *E* turned in such a position that the Sprengel pump exhausted the system through *A*, and the liquid air removed from *B* and placed around *A*. In this way some of the water vapor passing over the iron turnings at 510° was decomposed, the undecomposed portion frozen out at *A*, and the hydrogen formed removed and collected by the Sprengel pump. After all the water had evaporated from *B*, stopcock *E* was turned to connect the Sprengel pump with *B* which was again chilled while *A* was allowed to warm up to room temperature. This process of distilling the water back and forth over the hot iron was repeated until all of the water in the system was decomposed. We designate as sample I the first 30 cc of hydrogen collected and sample II the last 30 cc. In the second experiment 0.05 cc of water was decomposed as before except that all of the hydrogen formed was collected in one sample which we have called sample III.

Method of Measurement

The instrument used to determine the relative numbers of the isotopes was a mass-spectrograph which has already been described by Bleakney[35] in a previous number of this journal. In order to distinguish between the many possible combinations of two isotopes to form monatomic, diatomic and triatomic hydrogen ions it is necessary to determine the e/m ratio and to study the intensity as a function of pressure. This procedure has been described by Bleakney[4] in detail in his first work on hydrogen isotopes. Briefly the method is to measure the number of $(H^1H^1)^+$ ions in order to determine the pressure and then find the intensity of the peak corresponding to ions of mass 3 which consists of the two kinds $(H^1H^2)^+$ and $(H^1H^1H^1)^+$. They are proportional to the first and second powers of the pressure respectively. Hence if we let p be the intensity of the $(H^1H^1)^+$ ion (always much stronger than any other) and let I be the number of ions of mass 3 we have $I=ap+bp^2$ or $I/p=a+bp$, which is the equation of a straight line whose intercept a is the ratio

[35] W. Bleakney, Phys. Rev. **40**, 496 (1932).

$H^1H^2 : H^1H^1$. The ratio $H^2 : H^1$ is of course just half this value.

The hydrogen was admitted to the positive ray apparatus through a fine capillary leak while a rapid diffusion pump exhausted this chamber at such a rate that the pressure maintained there was of the order of 10^{-5} mm Hg. This pressure could be regulated by adjusting the pressure of the source. Sufficient time was given for equilibrium to be sensibly established before any readings were taken.

Results

The curves for I/p plotted as a function of p for the three samples are shown in Fig. 2. Sample II, the last fraction to be liberated in the first experiment, shows a higher concentration of the heavy isotope than sample I and we conclude that the method of preparation is a selective one. Sample III in which the dissociation was carried to completion falls directly between the other two, as expected, and furnishes an excellent check on the reliability of the measurements. Taking the intercept of curve C we obtain for the relative abundance of the isotopes in rain water

$$H^2 : H^1 = 1 : 5000$$

with perhaps a probable error of ten percent. This value is about six times as great as the one previously reported by Bleakney.[4] The authors feel confident, however, that the discrepancy is due to a real difference in the samples tested and is not to be ascribed to errors of measurement. As a further check a sample of ordinary commercial electrolytic hydrogen was examined and the results are shown by curve IV which gives a result of about 1 : 25,000. This agrees with the earlier work of Bleakney. The fractionation factor of 5 for separation by the electrolytic method reported by Lewis and Macdonald[17] would seem to account almost perfectly for these results, but it is surprising that the samples of commercial hydrogen used by various observers should yield such a low concentration since this would imply that they all came from comparatively new cells. It would seem quite likely that if there were any selective reaction in the method of preparing the samples of hydrogen for this experiment it would be in a direction tending to decrease the concentration of the heavy isotope because of its lower zero point energy, and hence we believe the abundance found is certainly not too low. We hope to continue these experiments during the next year.

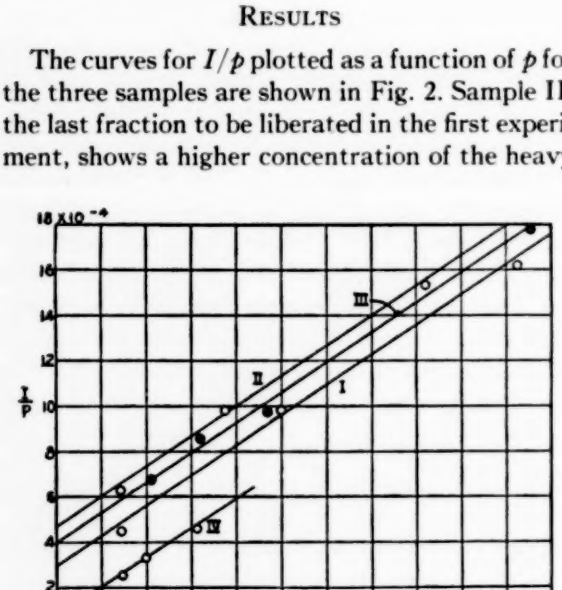

FIG. 2. The ratio I/p plotted as a function of p. The intercept on the vertical axis gives the ratio $H^1H^2 : H^1H^1$. Curves I and II represent the first and last fractions decomposed and curve III represents a sample completely decomposed. Curve IV represents a sample of commercial electrolytic hydrogen.

The Effect of Exchange on the Scattering of Slow Electrons from Atoms

PHILIP M. MORSE AND W. P. ALLIS, *Massachusetts Institute of Technology*

(Received May 8, 1933)

Reasons are given why the Born approximation is incapable of dealing with the scattering of slow electrons. Since this approximation assumes that the sine of the phase angle δ equals δ, the results computed by the Born method become completely unreliable when δ is greater than $\pi/2$. Exact solutions then must be obtained. Equations are set up, including exchange effects, for the best possible wave function for an electron scattered from hydrogen or helium when the complete wave function is of the separable type usually used in atomic theory. These equations are solved on the differential analyzer to find the best possible curves for the δ's, for the angle distribution of scattering and for the total cross section, for this type of wave function. The check with experiment for helium is good, the maximum discrepancy in any of the δ's being only ten degrees. No data for atomic hydrogen are available. The small error introduced by the use of separable wave functions (neglect of polarization) is discussed. The conclusions are that exchange effects are not important for electron energies greater than 30 volts, and below this energy have an appreciable effect only on the angle distribution curves, and not on the cross section curves. An analytic solution of the equations, valid for any atom having closed electronic shells, is obtained for a simplified form of atomic wave function and potential. The results confirm the above conclusions, and also show that exchange is less important in scattering from heavy atoms than from light ones.

INTRODUCTION

IN the past several years a number of fairly satisfactory methods have been devised for the treatment of the bound states of atomic electrons; but, although numerous attempts have been made, no correspondingly satisfactory methods have been found for the treatment of states involving one or more unbound electrons being scattered by an atom. This is essentially due to the fact that the interesting property of a bound state is its energy, and the energy matrix for bound states is pleasantly insensitive to changes in the shape of the wave functions. On the other hand, the interesting property of an unbound wave function is its distribution-in-angle, and the integral of this distribution, the cross section. This property is quite sensitive to changes in the wave function; a choice of function which is a little in error may give a completely erroneous scattering curve.

It is not difficult to see the reason for this sensitiveness if we expand the wave function in a series of spherical harmonics times radial functions $R(r)/r$. If there is no atom at the origin, then the R corresponding to the λ'th spherical harmonic will have an asymptotic form $\sin(kr-\lambda\pi/2)$, where k^2 is the electron's initial kinetic energy (atomic units are used throughout this paper). When the atom is present the radial function becomes more complicated, but its asymptotic value becomes $\sin(kr-\lambda\pi/2+\delta_\lambda)$, differing from the R when no atom is present only by a shift in phase, δ_λ.

These shifts in phase for the different values of λ completely determine the distribution in angle and cross section for scattering of the electron. The current scattered[1] per unit solid angle at an angle θ from the initial direction, per unit primary current density is

$$f^2(\theta)=\sum_{\lambda,\,\lambda'}(2\lambda+1)(2\lambda'+1)(\sin\delta_\lambda/k)(\sin\delta_{\lambda'}/k)\cos(\delta_\lambda-\delta_{\lambda'})P_\lambda P_{\lambda'} \tag{1}$$

and the cross section for scattering is

$$q=4\pi\sum_\lambda(2\lambda+1)(\sin\delta_\lambda/k)^2. \tag{2}$$

Now when the λ'th radial function has several oscillations inside the atom, a slight error in its

[1] See Morse, Rev. Mod. Phys. **4**, 577 (1932) for a general discussion. This paper will be called (I) hereafter.

form can easily produce an error in δ_λ of more than $(\pi/2)$, and the resulting values of f^2 and q will therefore be considerably in error.

A more detailed discussion of the behavior of δ_0 for an electron in a spherically symmetric field $V(r)$ will illustrate some of these facts. If we express the coefficient of P_0/r by means of the functions $\mu(r)$ and $A(r)$ such that $R_0 = A(r) \sin(kr+\mu(r))$, and arrange the relation between A and μ so that (dR/dr) will equal $kA(r)\cos(kr+\mu)$, then the equation which μ must satisfy is

$$-k(d\mu/dr) = V(r)\sin^2(kr+\mu). \qquad (3)$$

The value of μ for r very large is equal to the phase shift δ_0 which we need to compute f^2 and q. We also must have μ approach zero as r approaches zero.

Now Eq. (3) is a particularly intractable one, and one usually tries to solve it by approximate methods. The obvious method is to set μ equal to zero on the right-hand side of the equation, when

$$-\mu(r) = \int_0^r V(r)\sin^2(kr)dr/k. \qquad (4)$$

If we now set $\sin\delta_0/k$, which is needed for Eqs. (1) and (2), equal to $\mu(\infty)/k$, we have the Born approximation.[2] There are thus two approximations made in obtaining the Born formula, and both of them are *only valid when* $\mu(r)$ *is always small compared to* $\pi/2$. When k is large enough this is true, and the approximation is not a bad one, but when k is small the neglect of μ on the right side of (3) may cause the $\sin^2$ term in (4) to be unity at a place where it should be zero and *vice versa;* and the assumption that $\sin\delta_0$ is nearly equal to $\mu(\infty)$ is also a bad one.

The discrepancy becomes quite marked when k is quite small. The approximate Eq. (4) indicates that μ should increase fairly uniformly with r, reaching some constant value when r becomes great enough so that $V(r)$ is practically zero (the outside of the atom). But the correct solution of (3) for small k is very different. It is a sort of "step function," remaining nearly zero as r increases from zero, then suddenly jumping to a value π, remaining at that value for a while, then jumping to a value 2π, and so on, until the outside of the atom is reached, after which it is practically independent of r. The number of "steps" depends on the size and depth of the atomic potential hole, and as one increases this size and depth, keeping k constant, more steps appear, each one showing itself by a sudden increase in δ_0 by π. A curve showing the behavior of $\mu(r)$ for a simple form of potential field[3] is shown by the solid line in Fig. 1. The dotted line gives

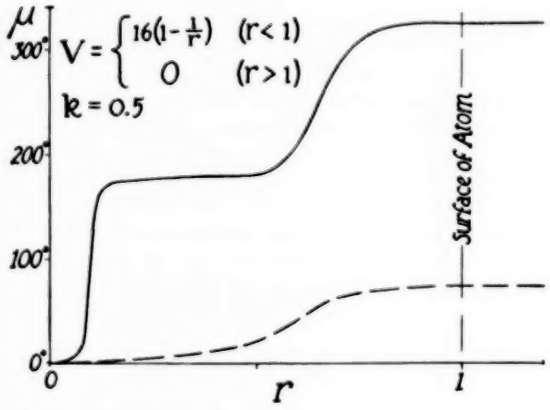

FIG. 1. Phase function $\mu(r)$ for a simple form of potential field. Solid line gives exact solution, dotted line gives corresponding Born approximation.

the behavior of the approximate function given in (4). The same sort of a discussion can be made for λ other than zero. The larger λ is, the larger V must be before a step appears in the δ_λ.

So we are forced to view with considerable skepticism the use of any scattering formula obtained by the Born method for small values of k, and to use the formula (if we must) with considerable trepidation. Unfortunately it does not seem possible to get along entirely without the Born approximation in the treatment of the collision of an electron and an atom. If the atom were just a potential field as far as the incoming electron is concerned, an exact solution could be obtained for the δ_λ's by a not impossibly great expenditure of energy. But the atom is not just a potential field, its electrons can be excited or can change places with the incoming electron.

In the treatment of inelastic collisions there seems at present no feasible method better than the Born method, bad as it is; but in the treat-

[2] See (I), page 589.

[3] See (I), page 581, and also Allis and Morse, Zeits. f. Physik **70**, 567 (1931).

ment of the exchange effects in elastic collisions, it is possible to obtain a better solution.

Hydrogen and Helium

The elastic collision of an electron and a hydrogen atom can be represented by a stationary state function where one electron is bound and the other is not. An exact solution would give a wave function which could not be separated into factors involving the coordinates of just one of the electrons, as the atomic electron's function would depend on the position of the unbound electron, and *vice versa*. However, separable wave functions work very well for bound states, so that it is interesting to find out if, in at least one case, they give fairly good approximations for the δ_λ's of an unbound state. If agreement is satisfactory in that case, it will be worth investigating others; if not, methods must be devised for the solution of nonseparable equations before further advance can be made.

By a method entirely analogous to that used by Fock[4] in atomic problems one can show that the best possible solution for the hydrogen atom plus electron problem having the separable form

$$\psi=\varphi(1)\chi(2)\pm\varphi(2)\chi(1) \tag{5}$$

will be when the atomic wave function φ is a solution of

$$(\nabla^2+2/r-E_a)\varphi=0, \tag{6}$$

and where the wave function χ of the scattered electron is a solution of

$$(\nabla^2+k^2-V(r_1))\chi(1)=\pm\varphi(1)\left[2\int\varphi(2)\chi(2)\frac{dv_2}{r_{12}}+(k^2-E_a)\int\varphi(2)\chi(2)dv_2\right]. \tag{7}$$

The function V is the combined potential of the nucleus and of the atomic electron. Since we shall deal with the scattering from normal hydrogen we have

$$V(r)=-2e^{-2r}(1+r)/r.$$

The plus sign in (5) and (7) corresponds to the symmetric function and therefore to the singlet state, while the minus sign corresponds to the antisymmetric function and to the three triplet states. The total cross section will equal $(\frac{1}{4})$ times the singlet cross section plus $(\frac{3}{4})$ times the triplet one.

In the antisymmetric case $\chi=\varphi$ makes ψ zero and hence satisfies (7) identically. $\chi+a\varphi$ is therefore as good a solution[5] as χ and we can make use of this to orthogonalize φ and χ and thus eliminate the second integral on the right of (7).

If we now set

$$\chi=\sum_\lambda P_\lambda(\cos\theta)R_\lambda(r)/r,$$

the R's must satisfy the equations,

$$\left(\frac{d^2}{dr^2}-\frac{\lambda(\lambda+1)}{r^2}-V+k^2\right)R_{\lambda s}=\frac{4\pi}{2\lambda+1}\varphi\left[2r^{\lambda+1}\int_r^\infty r^{-\lambda}\varphi R_{\lambda s}dr-2r^{-\lambda}\int_r^\infty r^{\lambda+1}\varphi R_{\lambda s}dr+\left(r^{-\lambda}-\frac{k^2-1}{2}\delta_{0\lambda}\right)2\int_0^\infty r^{\lambda+1}\varphi R_{\lambda s}dr\right] \tag{8}$$

for the symmetric case, and

$$\left(\frac{d^2}{dr^2}-\frac{\lambda(\lambda+1)}{r^2}-V+k^2\right)R_{\lambda a}=-\frac{4\pi}{2\lambda+1}\varphi\left[2r^{\lambda+1}\int_r^\infty r^{-\lambda}\varphi R_{\lambda a}dr-2r^{-\lambda}\int_r^\infty r^{\lambda+1}\varphi R_{\lambda a}dr+(1-\delta_{\lambda 0})2r^{-\lambda}\int_0^\infty r^{\lambda+1}\varphi R_{\lambda a}dr\right] \tag{9}$$

for the antisymmetric case.

The best separable wave function for scattering from helium corresponds to the antisymmetric case only, and must satisfy an equation of the form of (9), where φ is the Hartree wave

[4] Fock, Zeits. f. Physik **61**, 126 (1930).

[5] Feenberg, Phys. Rev. **42**, 17 (1932).

function for helium and V is the corresponding potential.

An analytic solution of (8) and (9) for any but the most rudimentary forms of φ and V seems quite impossible. Several approximate solutions[5, 6] have been carried through, but these all have the same inherent defects which were brought out in the discussion of the Born approximation. It is possible, however, to solve these equations mechanically. We have obtained exact solutions of (8) and (9), and of these equations without the right-hand sides, on the differential analyzer.[7] From them were computed the δ_a's for the antisymmetric, the δ_s's for the symmetric, and the δ_n's for the no-exchange case. Fig. 2 gives curves of these quantities as functions of k for hydrogen, and Fig. 3 gives them for helium[8] (the δ_s's were not computed for helium, since they are not needed). It is to be noticed that the effect of exchange in the case of hydrogen

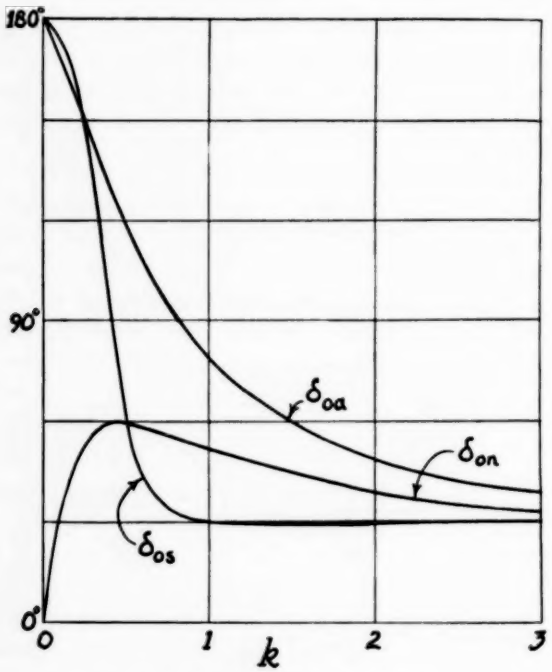

FIG. 2. Phase shifts for hydrogen.

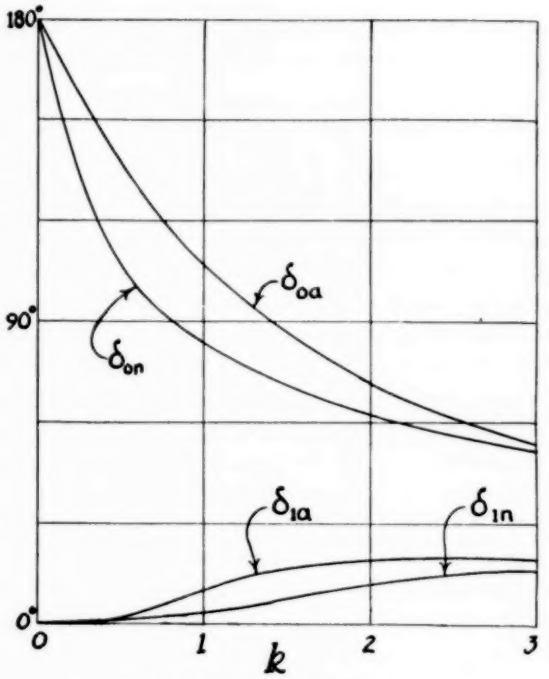

FIG. 3. Phase shifts for helium.

introduced an extra step in the $\mu(r)$ function, making δ_{0a} approach 180° instead of 0° as k goes to zero. It is obvious that the usual approximate methods of computing exchange cannot cope with so drastic an alteration of the δ curve.

The only experimental data available are for helium.[9] Since both sets of data on angle scattering check with each other, it seems reasonable to consider them as fairly correct, although probably the amount measured for small angles is larger than the true atomic scattering curve, due to multiple scattering, and to possible spreading of the primary beam. The data on cross section are for total cross section, and therefore larger than the elastic cross section for large values of k.

Fig. 4 gives curves of the angle distribution for several different accelerating potentials. The solid lines are the values computed when exchange is included, the dotted lines the values when exchange is neglected, and the circles are the experimental points. Fig. 5 gives the corresponding curves for cross section as a function of

[6] Oppenheimer, Phys. Rev. **32**, 361 (1928); Massey and Mohr, Proc. Roy. Soc. **A132**, 605 (1931).

[7] V. Bush, J. Frank. Inst. **212**, 447 (1931).

[8] The Hartree atomic functions for helium were computed on the differential analyzer by S. H. Caldwell (paper to appear shortly). The writers are indebted to Mr. Caldwell for his kindness in supplying these data.

[9] For angle scattering, see Bullard and Massey, Proc. Roy. Soc. **A133**, 637 (1931); Ramsauer and Kollath, Ann. d. Physik **12**, 529 (1932); and Hughes, McMillen and Webb, Phys. Rev. **41**, 154 (1932). For cross section, see Normand, Phys. Rev. **35**, 1217 (1930).

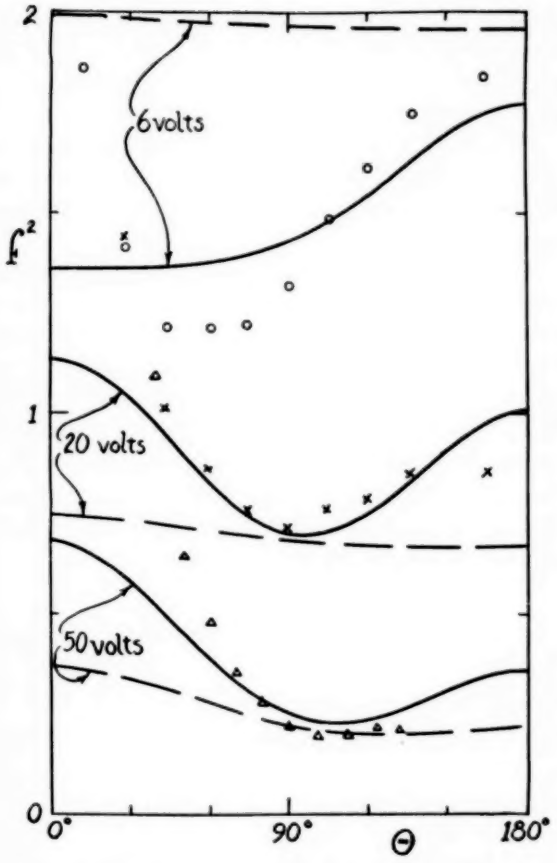

FIG. 4. Angle distribution of scattered electrons, f^2, for helium. Solid line, computed with exchange. Dotted line, computed without exchange. Circles and crosses, experimental data by Ramsauer and Kollath. Triangles, experimental data by Bullard and Massey (multiplied by a single arbitrary constant, since Bullard and Massey do not give absolute magnitudes).

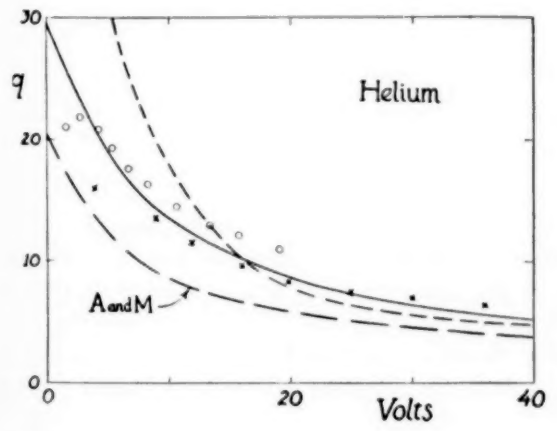

FIG. 5. Elastic cross section of helium. Circles, experimental data by Ramsauer and Kollath; crosses, data by Normand.

electron velocity in square root volts. The curve marked A and M is that computed[4] for a considerably cruder form of potential field, without exchange.

It is seen that the check with experiment is better for the curves computed including exchange than for the curves neglecting exchange. For instance, the exchange angle scattering curves for small velocities exhibit the curious phenomenon that more electrons are scattered backward than forward, a phenomenon found experimentally. It is also seen that curves for the cross section check better than the curves for angle distribution; and that the effect of exchange is much more important in the angle distribution curves than in the cross section curves. This is due to the fact that the angle distribution curves are sensitive to the magnitude of the terms involving products of two different spherical harmonics (especially the term in P_0P_1), and these terms integrate out to zero when the cross section is computed. One might say that exchange distorts the distribution of the electrons which are scattered without causing any great change in their total number.[10]

The check for the angle distribution is not particularly good, but this only shows the extreme sensitivity of the angle distribution to the form of the wave functions. If the values of δ_{1a} be increased only slightly, with a maximum change of less than 10°, *the check with experiment is wellnigh perfect.* This corresponds to a 1 percent change in the abscissa of the wave function where the phase shift was measured. As this difference is much larger than the error within which the machine will repeat itself, it is not unreasonable to assume that it is due to the fact that separable wave functions were used instead of the correct nonseparable ones.

As a matter of fact, it seems surprising that the discrepancy is so small. If we attempt to estimate the effect of the "nonseparableness" by an equivalent polarization field, we find that this field is of the same order of magnitude as the atomic field V, and is many times larger than V at large distances. The addition of a field of any such size would change the δ's, not by the needed 10°, but by 180° or twice 180°, and the curves

[10] See (I), page 615.

for f^2 and q would be of a completely different character from the experimentally determined ones, as Holtzmark has already noticed.[11]

It is not hard to see that a "polarization field" is a very poor way of including the effect of non-separability. To obtain such a field we assume that φ, and therefore E_a depend parametrically on the position of the unbound electron, but that χ is independent of the position of the atomic electron. The polarization field is obtained by computing the change of φ and of E_a produced by a stationary electron at a certain distance away and then computing the effect of this distortion on the field in which the unbound electron travels. An argument analogous to that used by Born and Oppenheimer[12] in discussing the motions of electrons and nuclei in diatomic molecules can be used to show that such an approximation is quite bad when the incoming particle is an electron. Thus, it is not likely that the method suggested by Feenberg[5] to include "polarization" will be successful.

However, it does not seem possible at present to go beyond these rather negative remarks in discussing the error due to the use of separable wave functions.

To conclude, Figs. 2 and 3 show that exchange effects become unimportant for electronic energies larger than 30 volts ($k>2$) for helium and hydrogen. This is about the limiting value of k at which the Born approximation has any validity at all. Consequently, the correction for exchange is always smaller than the errors inherent in the Born method and it is senseless to add the exchange terms when using it. This conclusion applies, of course, only to elastic scattering.

Many Electron Problems

The extension of Eq. (9), for the case of any atom consisting of closed shells, is not difficult.[13, 5] If the atomic wave function is a determinant involving N pairs of electrons, each pair having a wave function

$$\varphi_\nu(r)=A_{m,\,l,\,n}e^{im\varphi}\sin^m\theta P_l^m(\cos\theta)R_\nu(r)/r$$

and opposing spins, then each of these N functions is orthogonal to the others, and is a solution of the equation

$$\left[\nabla_1^2+E_\nu+\frac{4N}{r_1}-V(r_1)\right]\varphi_\nu(r_1)=-\sum_{\mu=1}^{N}2\varphi_\mu(r_1)\int\varphi_\mu(r_2)\varphi_\nu(r_2)\frac{dv_2}{r_{12}}$$

$$=-2\sum{}'A^2_{0,\,l,\,n}\frac{R_\mu}{r_1}\int P_l(\cos\theta_{12})\frac{R_\mu(r_2)\varphi_\nu(r_2)}{r_2r_{12}}dv_2, \quad (10)$$

where $\sum'$ is a sum over all the different values of l and n in the atom. The potential

$$V(r_1)=4\sum_{\mu=1}^{N}\int\varphi_\mu^2(r_2)\frac{dv_2}{r_{12}}.$$

Therefore, each atomic electronic wave function is an eigenfunction of the same equation. The wave function χ is also a solution of (10), and is therefore orthogonal to all of the atomic functions φ. The kinetic energy k^2 must of course be substituted for the negative atomic energy E_ν when (10) is used to find χ.

As the sum $\sum'$ indicates, the incident electron can exchange only with electrons of same spin and m-value, and since there is only one such in each shell, the effect of exchange increases not as

[11] Holtzmark, Zeits. f. Physik **48**, 239 (1928).

[12] Born and Oppenheimer, Ann. d. Physik **84**, 457 (1927).

[13] See Fock, Zeits. f. Physik **81**, 195 (1933); Lennard-Jones, Proc. Camb. Phil. Soc. **27**, 469 (1931).

the number of electrons but as the number of shells. We shall show that the effect of the inner shells is negligible so that only one or two terms on the right of (10) are worth keeping. (10) then reduces practically to the form of (9) but with a very much larger field V.

In order to study how the effect of exchange varies with the field V, we have studied a very simple form of (9) which has analytic solutions. Although the simplifications are extreme, previous calculations neglecting exchange have shown that the scattering is not at all sensitive to the shape of the potential field, provided the "atomic size factor" is not changed. Therefore, one can expect that the behavior of this solution will correspond in its general aspects to the actual case. If we set

$$V=\begin{cases}-V_0 & (r<r_0)\\ 0 & (r>r_0)\end{cases}\qquad \varphi=\begin{cases}(3/4\pi r_0^3)^{\frac{1}{2}} & (r<r_0)\\ 0 & (r>r_1)\end{cases}$$

it is found that

$$\frac{R_\lambda}{r^{\frac{1}{2}}}=\begin{cases}[s_\lambda J_{\lambda+\frac{1}{2}}(s_\lambda r)/J_{\lambda-\frac{1}{2}}(s_\lambda r_0)]-[t_\lambda J_{\lambda+\frac{1}{2}}(t_\lambda r)/J_{\lambda-\frac{1}{2}}(t_\lambda r_0)] & (r<r_0)\\ C_\lambda J_{\lambda+\frac{1}{2}}(kr)+D_\lambda J_{-\lambda-\frac{1}{2}}(kr) & (r>r_0)\end{cases}$$

is a solution of (9) provided that s_λ and t_λ are roots of the equation

$$y^4-(V_0+k^2)y^2-6/r_0^3=0.$$

C_λ and D_λ are determined by the requirement of continuity of value and slope of R_λ at $r=r_0$, and

$$\delta_\lambda=(-)^\lambda \tan^{-1}(D_\lambda/C_\lambda).$$

There is an error, of course, in that φ is not a solution of the "nuclear field" corresponding to V and hence is not orthogonal to R_0 but it is believed that this does not vitiate the results.

It is found that δ_λ is a function of an electron velocity parameter $x=kr_0$, an atomic size factor $\beta=r_0(V_0)^{\frac{1}{2}}/2$, and an exchange parameter r_0 (which is the size of the atomic wave function). Except in the exchange effect, the radius of the atom only enters in terms of the parameters x and β. In other words, except for the exchange, potential fields having quite different values of r_0 but having the same value of β would give scattering curves of exactly the same form when plotted as functions of x. The parameter r_0 is therefore a sort of exchange parameter, and when it becomes zero the right-hand side of (9) becomes zero, reducing to the form obtained for any value of r_0 when exchange is neglected.

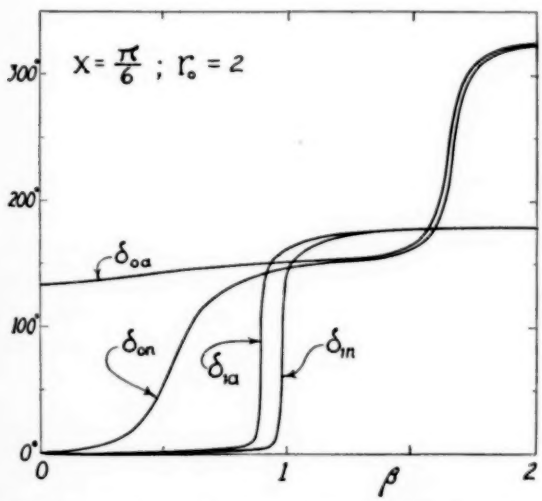

FIG. 6. Phase shifts with and without exchange for a simple atomic model, as functions of the atomic size factor β.

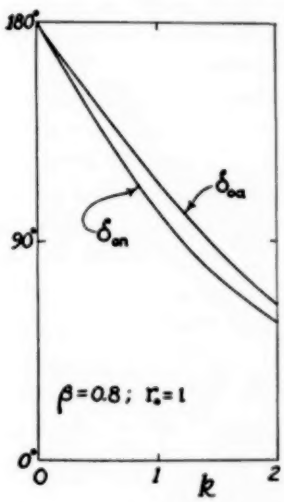

FIG. 7. Phase shifts with and without exchange for the simple model appropriate to helium.

We thus see immediately that the effect of exchange depends on the spread of the atomic wave function, becoming negligible for electrons concentrated in a small space. Nor is it difficult to show that this is true for any form of potential field and atomic wave function. Exchange with atomic electrons in inner shells is therefore extremely unlikely.

Fig. 6 gives plots of δ as a function of the atomic size factor β for $\chi=\pi/6$. It can be seen that the difference between the δ's with and without exchange decreases as β increases, showing that exchange with each electron is less effective in larger atoms than in smaller ones. This, combined with the fact that the electrons in inner shells play practically no rôle in exchange, makes it quite likely that the total exchange effect is smaller for heavy atoms than for light ones.

To show that this crude model of the atom is yet capable of correct results, we give in Fig. 7 phase-defect curves for the parameters appropriate to helium $\beta=0.80$, $r_0=1$. These are to be compared with the correct curves from the machine solution, given in Fig. 3.

In conclusion, we wish to thank Mr. S. H. Caldwell and the staff of the differential analyzer for their care in solving this problem.

The Effect of Temperature on the Emission of Electron Field Currents from Tungsten and Molybdenum*

A. J. AHEARN, *Bell Telephone Laboratories*

(Received June 15, 1933)

Electron field currents from the central portion of long molybdenum and tungsten filaments about 2.7×10^{-3} cm in diameter have been studied. The field currents were first made stable to about 5 percent by long-continued conditioning treatments of temperature and high voltage under high vacuum conditions. Thermionic emission measurements gave the values 4.32 and 4.58 volts for the work function of the molybdenum and tungsten, respectively, in good agreement with the accepted values for the clean metals. Emission measurements were then made at fields varying from about 5×10^{5} volts/cm to about 1×10^{6} volts/cm and at temperatures varying from 300°K to about 2000°K. Down to about 1600°K the thermionic currents completely masked the field currents. Thermionic emission values below 1600°K were obtained by extrapolation. Thus the field currents at the lower temperatures were separated from the thermionic currents. Where necessary, corrections were made for the decrease in the voltage gradient accompanying the thermal expansion of the filament. The field currents were found to be independent of temperature to within 5 percent from 300°K to 1400°K. At temperatures higher than 1400°K the data are consistent with the assumption that the current consists of a thermionic current plus a current which is independent of temperature. However, because of the exponential change of thermionic current with temperature a small effect of temperature on the field current could not be distinguished at temperatures higher than 1400°K. From the theory of Fowler and Nordheim, β, a factor introduced by surface irregularities, is found to be 120 for the tungsten cathode and 47 for the molybdenum one. Thus for tungsten, Houston's theory of the temperature effect is in approximate agreement with the negative results of these experiments.

INTRODUCTION

THE effect of temperature on electron field currents was originally investigated by Millikan and Eyring.[1] With a thoriated tungsten cathode they first observed a decrease of the critical gradient, i.e., the value of the field strength at the surface just sufficient to produce a perceptible outflow of electrons, at about 1100°K. This was interpreted as an effect of temperature on field currents rather than as the onset of a perceptible thermionic current. Since it is not known whether in respect of thermionic properties the metal would behave like a tungsten surface which is clean or one which is contaminated with free thorium, this interpretation is not free from question.

DeBruyne[2] used tungsten in similar studies. On the basis of measurements by Pforte[3] and DeBruyne[4] he calculated the thermionic emission from the Richardson equation and the theory of the Schottky effect.[5] Subtracting this from the measured currents he obtained what he regarded as the field current emission and plotted it as a function of field strength and temperature. He then represented the variation of field currents with field strength at temperatures from 293°K to 1944°K by a single curve about which the points are rather widely scattered. It is concluded that within the experimental error, the field currents are independent of temperature from 293°K to 1944°K.

There are two serious possibilities of error in this proposed way of distinguishing the field current and the thermionic current. In the absence of direct measurements, the correct value for the work function of the cathode to be used in the Richardson equation is uncertain. Then there are the usual difficulties in a determination of the absolute magnitude of the filament temperature which is necessary for estimating the thermionic

* Presented before the American Physical Society in Washington, D. C., April, 1933.

[1] Millikan and Eyring, Phys. Rev. **27**, 51 (1926).

[2] DeBruyne, Proc. Camb. Phil. Soc. **24**, Part 4, 518 (1928).

[3] Pforte, Zeits. f. Physik **49**, 46 (1928).

[4] DeBruyne, Proc. Roy. Soc. **A120**, 423 (1928).

[5] Schottky, Phys. Zeits. **15**, 872 (1914).

emission. These are serious since the absolute magnitude of both the work function and the temperature are involved exponentially.

By drawing separate lines through the data taken at each separate temperature, Millikan and Lauritsen[6] obtain a series of curves from the DeBruyne[2] data which they believe shows an increase of field current with temperature.

In the latest publication on this subject, DeBruyne[7] calculates that the thermionic emission from fully activated thoriated tungsten would explain the current increase which Millikan and Eyring[1] interpreted to be a field current temperature effect. He then automatically obtained a continuous record of the field currents at a given field as a tungsten filament was alternately heated to various temperatures and cooled to room temperature. Below 1600°K his records do not show a consistent temperature variation greater than the spontaneous fluctuations in the current. The increase in current at 1600°K is attributed to thermionic emission. DeBruyne concluded that while there may be a temperature effect on field currents no real variation has yet been observed.

The contradictory deductions from the above experiments occur because it is uncertain whether the cathode surface is clean or contaminated and because the thermionic emission correction is uncertain. I therefore investigated the effect of temperature on field currents from filaments of tungsten and molybdenum of which the surfaces were proved by study of their thermionic emission to be clean. The correction due to the thermionic emission was determined by extrapolation of the measurements. In this way the uncertainty as to the exact value of the work function, the temperature, the applied field and the variation of current with field is minimized.

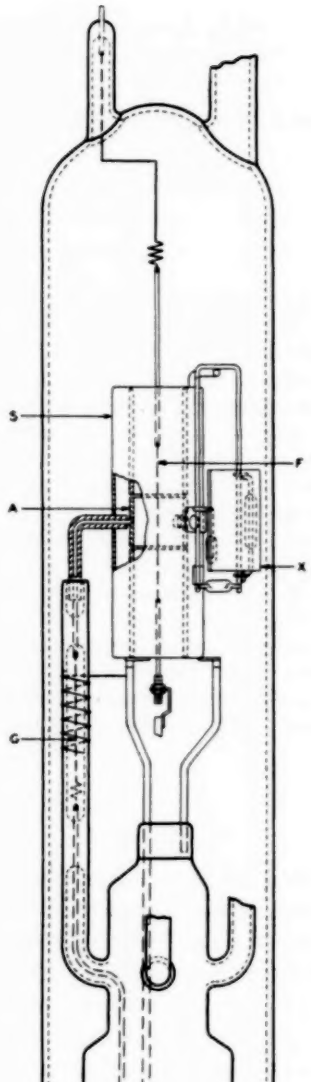

FIG. 1. The experimental tube.

APPARATUS

The experimental tube is shown in Fig. 1. The anode A is a nickel cylinder 2 cm long and 2 cm in diameter. The cathode consists of a filament F about 2.7×10^{-3} cm in diameter and 6 cm long, and is mounted on the axis of the cylindrical anode. The average applied field in volts/cm is obtained by multiplying the applied voltage by the factor G, the approximate value of which is 100 cm^{-1}. To prevent a displacement of the filament by the strong electric field, a certain tension is applied to it by means of the calibrated spring and the bolt and nut arrangement shown. In this way the tension is decreased as the temperature is increased and the filament does not pull apart. The anode has cylindrical guard rings 4 cm long

[6] Millikan and Lauritsen, Phys. Rev. **33**, 598 (1929).
[7] DeBruyne, Phys. Rev. **35**, 172 (1930).

and 2 cm in diameter. End effects due to filament leads, end cooling of the filament, and distortion of the electric field at the ends of the anode are in this way eliminated. A cylindrical shield S attached to these guard rings completely surrounds the outside of the anode. The electrical lead from the anode is completely shielded by quartz and glass until it passes through the glass envelope. The guard ring G on the glass tubing encasing this lead prevents any surface leakage of electrons from reaching the anode A. Throughout the experiments, currents to the anode A are the only ones measured. The guard rings and shield S are such that the only currents which can reach the anode come from the central portion of the filament which is uniformly heated and at which the average electrical field is constant and known.

Voltages up to about ten thousand volts were used. Steady d.c. voltages were obtained from a 220-volt a.c. source by means of transformers, rectifiers and filters. The voltage was measured with an ordinary high resistance voltmeter in series with the proper resistors.

Current measurements were made with a d.c. vacuum tube amplifier and a series of grid leaks. These measurements ranged from about 10^{-12} amp. to 10^{-4} amp.

The filament temperature was determined from the temperature heating current data of Worthing[8] for molybdenum and Jones and Langmuir[9] for tungsten. The filament heating current was measured with a standard resistance and a Leeds and Northrup Type K Potentiometer. The filament diameter was determined from the mass of a measured length of the wire.

High vacuum technique of the sort already reported[10] was employed in the pumping of the tubes. Before the tubes were removed from the pumps some field currents were drawn from the cathodes. After the tubes were removed from the pumps, the filaments were heated at high temperatures for many hours, sufficient to age them according to the procedure of Worthing[8] and Jones and Langmuir.[9]

The filaments were also conditioned by applying voltages at least as high as were used in any of the subsequent measurements. These first applications of the high voltage produced extensive fluorescence on the glass walls of the tube, the shield S and the inside surface of the anode A and its guard ring cylinders. The fluorescence on the glass was blue, that on the metal (nickel) red. In both cases, the patches of light were quite intense and fluctuated much both in position and intensity. Some patches were quite diffuse and some quite sharply defined. Usually the fluorescence which appeared at any given voltage would soon vanish if the voltage continued unchanged, although this was not always so. These fluorescence effects emphasize the importance of the shield S of the experimental tube.

Eventually, the high temperature and high voltage treatment established conditions such that at a given voltage the field current was constant to within about 5 percent over periods of hours and was not affected by temperature treatments at 2000°K. Throughout the temperature studies recorded here the pressure was about 1 or 2×10^{-8} mm Hg.

Method

When this stability of the field currents was established the effect of temperature on field currents was investigated as follows. The thermionic characteristics of the cathodes were first measured to insure that they agreed with those for clean surfaces. With the field kept at some constant value, current measurements were then made by varying the temperature from about 300°K to about 2000°K. After each temperature setting above 300°K the filament would be reduced to 300°K (room temperature) for a current measurement. In this way any small trend in the room temperature value of the field current, due to whatever cause, was recorded. Current and voltage were always measured together. Measurements of this sort were made on molybdenum from 8×10^5 volts/cm to 1×10^6 volts/cm and on tungsten from 5×10^5 volts/cm to 1×10^6 volts/cm.

Results for Tungsten

Fig. 2 gives the thermionic characteristics of the tungsten filament. The average value for the

[8] Worthing, Phys. Rev. **28**, 190 (1926).

[9] Jones and Langmuir, G. E. Review **30**, No. 6, June, 1927.

[10] Ahearn, Phys. Rev. **38**, 1858 (1931).

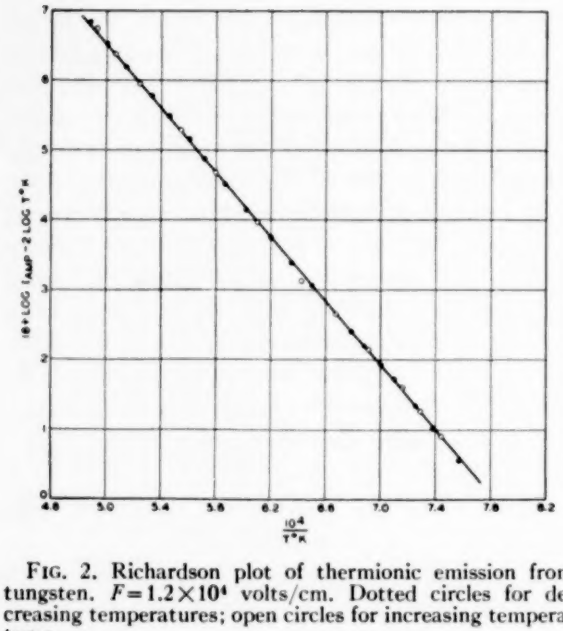

FIG. 2. Richardson plot of thermionic emission from tungsten. $F=1.2\times10^4$ volts/cm. Dotted circles for decreasing temperatures; open circles for increasing temperatures.

work function Φ is 4.58 volts and for the constant A of the Richardson equation 73 amp./cm^2 deg^2. This value of Φ agrees well with 4.52 volts, the average of the most satisfactory data on tungsten.[11] The field current measurements are therefore characteristic of a clean tungsten surface.

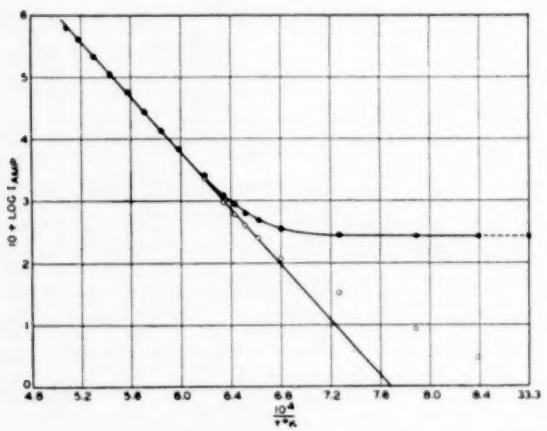

FIG. 3. Electron emission from tungsten at $F=9.47\times10^5$ volts/cm. Dotted circles are experimental points; open circles show the difference between measured currents and current at 300°K.

Figs. 3 and 4 give emission-current *vs.* temperature data at two values of the applied field,

[11] Dushman, Rev. Mod. Phys. **2**, 394 (1930).

[12] Bridgman, Phys. Rev. **34**, 1411 (1929).

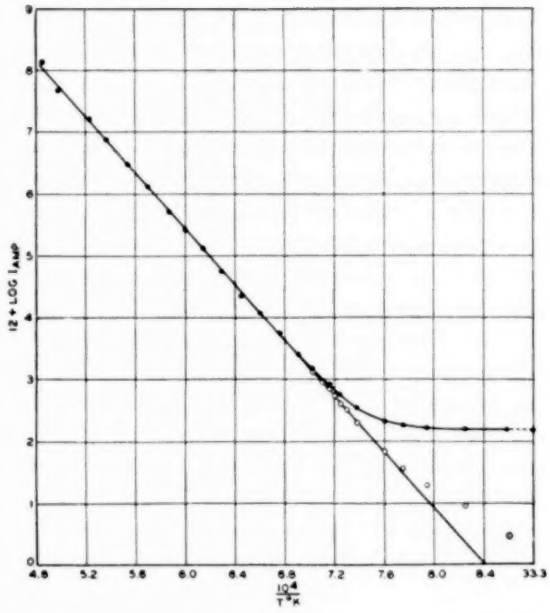

FIG. 4. Electron emission from tungsten at $F=5.42\times10^5$ volts/cm. Dotted circles are experimental points; open circles show the difference between measured currents and current at 300°K.

the coordinate system being that familiar in thermionics in which points lie along a straight line if they conform to the Richardson equation. One infers that down to about 1600°K for one field strength and down to 1400°K for the other, the thermionic current completely submerges the field current, for the data lie along a straight line when plotted according to the Richardson equation. This linear portion of the experimental curve is extrapolated to lower temperatures and assumed to give the values of the thermionic emission there. The difference between the experimental curve and this extrapolated curve is interpreted as the field current. Corrections to the field required by voltage variations or thermal expansion[12] of the filament are negligible for the tungsten data. In Table I these field current values are expressed as percentages of the field current at room temperature. At the lower temperatures, these percentages have an approximately constant value near 100 percent. However, at the higher temperatures they depart from this constant value. This is easily understood from Figs. 3 and 4. As the experimental and extrapolated curves approach each other, the error involved in a determination of the difference in their ordinates increases.

The points marked with open circles on Fig. 3 are obtained by subtracting the room temperature value of the field current from the observed currents at the various temperatures. If the field current is independent of temperature, these differences should be values of the thermionic current and accordingly the points should be on the extrapolated straight line. As a matter of fact they fall nicely on the extrapolated straight line down to 1450°K. At lower temperatures the amounts by which these points are displaced from the straight line are well within the experimental error in their determination. For example consider the point at $10^4/T=7.3$. This calculated thermionic emission is 8 percent of the total current measured while the straight line predicts that the thermionic emission would be 3 percent of this total current. Since the experimental error in the current measurements is about 5 percent this seemingly large discrepancy between the two values of the thermionic emission is not significant. Thus in Figs. 3 and 4 there is determined a temperature T_L above which the calculated thermionic emission agrees as well with the Richardson equation as do the direct measurements of the thermionic emission as shown in Fig. 2. Therefore it follows that above T_L the data are consistent with the assumption that the measured current consists of a thermionic current plus a field current which is independent of temperature. However, because of the exponential change of thermionic current with temperature a small effect of temperature on the field currents could not be distinguished. This analysis was made on all of the data given in Table I where T_L is located by the horizontal lines.

TABLE I. *Tungsten cathode. Ratio of field current at temperature T to that at 300°K.* T_L (indicated by the horizontal lines) is the temperature above which the measured emission minus the emission at 300°K is described by the Richardson thermionic emission formula.

Field, (v/cm) $\times 10^{-6}\rightarrow$		5.31	5.36	5.42	6.25	6.25	7.00	7.00	7.10	7.10	7.63	7.95	7.95	8.65	8.65	9.47	9.47	9.64	10.56
$10^4/T$ (°K)	T (°K)																		
33.3	300	100	100	100	100	100	100	100	100	100	100	100	100	100	100	100	100	100	100
9.5	1050																	96	
9.4	1065																		
9.3	1075																		
9.2	1085																		
9.1	1100																	99	
9.0	1110																		
8.9	1125																		
8.8	1135			101	97	99	101					103						102	
8.7	1150			100	98	98		101											
8.6	1165		107	100	99	98													
8.5	1175		107	103	100	98				106	107		106		101				
8.4	1190		107	103	100	98	100	102		106	107		106			101	104		105
8.3	1205	106	107	103	101	98				106	107		104					106	
8.2	1220	104	107	104	102	97				106	107		107		103				
8.1	1235	106	107	102	102	97				106	103		107						
8.0	1250	109	107	99	103	97	100	106	104	106	103	103	107	111	106		100	105	
7.9	1265	111	107	100	103	96	100		104	108	110		107	111	107	100	102	105	
7.8	1280	111	107	101	103	97	100		108	106	110		104	110	107	104	104	105	
7.7	1300	112	107	107	103	96	100		108	108	110		104	109	105	104	106	105	
7.6	1315	112	107	111	104	96	101	106	108	108	112	102	109	108	103	104	107	105	
7.5	1335	114	107	114	105	97	103	106	108	111	112	102	109	109	105	102	105	105	
7.4	1350	124	107	124	105	97	105	108	108	114	112	102	111	109	107	106	105	105	
7.3	1370	143	107	137	105	99	108	109	112	118	112	103	114	112	110	108	108	105	96
7.2	1390	162	107	170	103	101	113	111	125	123	107	103	121	112	110	108	108	110	100
7.1	1410	190	111	209	109	101	117	116	117	133	118	103	121	110	111	108	108	110	100
7.0	1430	267	111	235	112	95	120	122	129	141	121	102	123	108	111	104	108	110	95
6.9	1450					85	120	128	142	157	129	102	128	106	107	104	106	110	93
6.8	1470					60	114	125	154	168	146	98	137	101	101	98	103	114	93
6.7	1490						114	125	158		148	87	156	95	91	96	101	110	95
6.6	1515										143		191	82		87	91	109	101
6.5	1540										143					70	77	113	103
6.4	1560																	109	94
6.3	1590																	95	
6.2	1610																		
Average below T_L		106	105	103	100	98	101	103	104	106	105	102	109	107	105	101	103	103	99
Average ratio 103%																			

Below T_L the effect of temperature on field currents can be determined from Table I. When these data are averaged, equally weighing all parts of the temperature range below T_L, a value of 103 percent is obtained. If this value were 100 percent it would mean, of course, that the field currents were completely independent of temperature.

Results for Molybdenum

Fig. 5 shows the early history of one particular molybdenum cathode. On the ordinate the logarithm of field current is plotted. The applied field had the constant value 8.05×10^5 volts/cm. One sees that, during the portion of the filament history given here, the "field current activity" decreased by a factor of about 35,000. A large decrease in activity of this sort is always observed during the early stages of treatment of a filament. However, just as shown in Fig. 2, one type of treatment sometimes increases the activity while again it may produce a decrease. This applies quite generally to all the types of treatments shown in Fig. 2. At times in the early history of a filament with a constant applied voltage, spontaneous increases of as much as 30,000 would occur. In some of these cases the current would be reduced to its former value by heating the filament to only 1000°K for a few minutes.

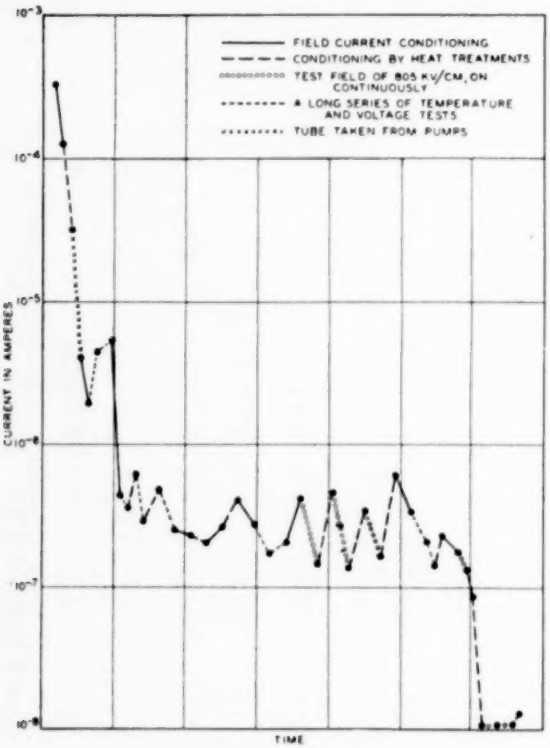
FIELD CURRENT CONDITIONING
CONDITIONING BY HEAT TREATMENTS
TEST FIELD OF 805 KV/CM, ON CONTINUOUSLY
A LONG SERIES OF TEMPERATURE AND VOLTAGE TESTS
TUBE TAKEN FROM PUMPS
CURRENT IN AMPERES
TIME

Fig. 5. Early life history of a molybdenum filament. A test field of 805 kilovolts/cm was used. The time extended over about 20 days.

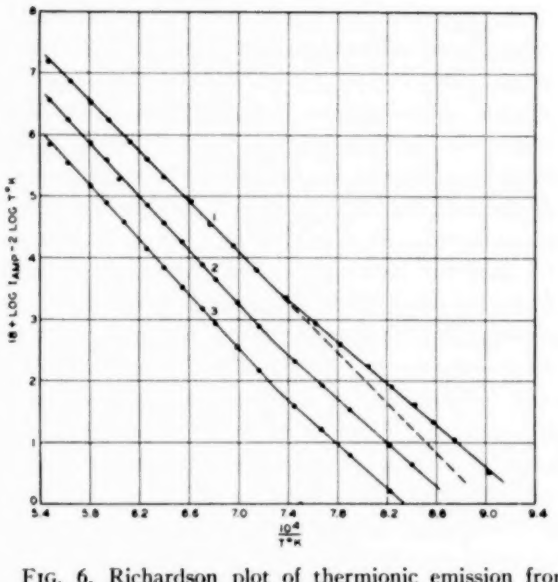

Fig. 6. Richardson plot of thermionic emission from molybdenum. Curve 1, $F=4.4\times10^5$ volts/cm; curve 2, $F=1.0\times10^4$ volts/cm; curve 3, $F=1.0\times10^3$ volts/cm. Add 0.6 to ordinate.

Fig. 6 shows the thermionic characteristics of the molybdenum filament, where the data are plotted according to the Richardson thermionic emission equation. The electric fields were 10^3, 10^4, and 4.4×10^5 volts/cm, values much too small to give field currents measurable in this experiment. The data are not fitted by a single straight line but require two straight lines which intersect at about 1400°K. The slope of the low temperature line in all three cases is 20 percent lower than that of the high temperature one. The explanation of this nonlinearity is not yet known and will be further investigated.* It cannot be attributed to end cooling of the filament because such an effect would produce an increase in slope.

A contamination of the filament by gases at the lower temperatures might produce such an

* This same nonlinearity has again appeared in similar measurements which have just been made on another molybdenum filament.

effect. There is, however, no definite evidence in favor of this idea. A thermionic emission measurement at one of these low temperatures immediately after hours of heating at the highest temperature gave a point on the curve of Fig. 6. Furthermore a measurement made at a low temperature after the filament had been at room temperature many hours gave a point on the curve also.

Regardless of the explanation of this nonlinearity, it is clear that, given the thermionic data above 1400°K, one does not obtain the correct values below 1400°K by extrapolating the straight line. Instead, one must insert a straight line whose slope is 20 percent less than that for the emission above 1400°K.

The high temperature portions of these curves give for the work function Φ the value 4.32 volts and for the constant A of the Richardson equation 200 amp./cm^2 deg^2. Dushman[11] chose 4.41 electron-volts as the average of the most reliable data for the work function of clean molybdenum. The more recent measurements of DuBridge and Roehr[13] give the value 4.15. My value of 4.32 is in good agreement with the average of these measurements. The field current measurements are therefore characteristic of a clean molybdenum surface.

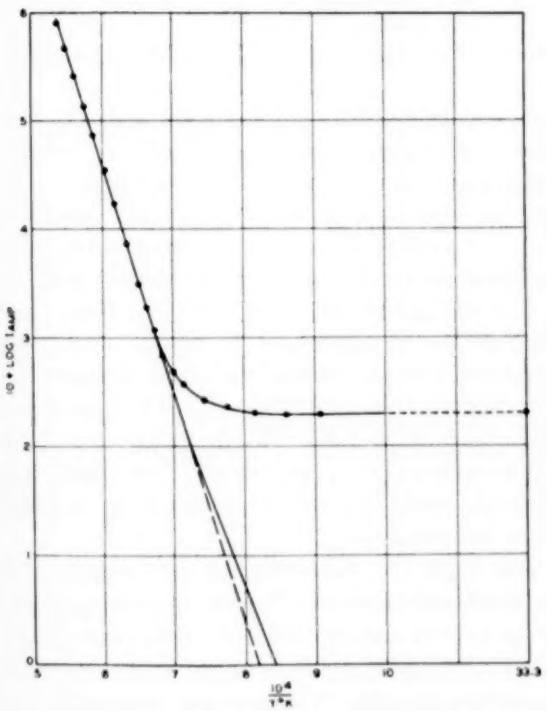

FIG. 7. Electron emission from molybdenum at $F=1.05\times10^6$ volts/cm. The intersecting straight lines give the thermionic emission.

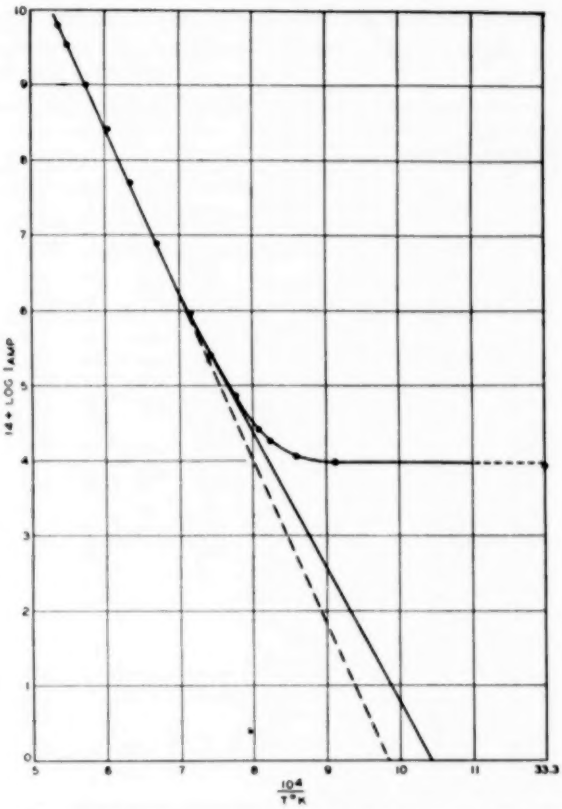

FIG. 8. Electron emission from molybdenum at $F=8.13\times10^5$ volts/cm. The intersecting straight lines give the thermionic emission.

Figs. 7 and 8 give emission current *vs.* temperature data for the highest and lowest fields used. One observes that down to about 1400°K or 1500°K, depending on the applied field, the thermionic current completely submerges the field current since the data lie on a straight line according to the Richardson equation. We draw a line whose slope is 20 percent smaller and which intersects the other line at about 1400°K, extrapolate it, and assume that it gives the values of the thermionic current at these lower temperatures. The current corresponding to the difference between the experimental curve and this extrapolated curve for the thermionic emission is assumed to be the field current. In Table II, its

[13] DuBridge and Roehr, Phys. Rev. **42**, 52 (1932).

TABLE II. *Molybdenum cathode. Ratio of field current at temperature T to that at 300°K.* T_L (indicated by the horizontal lines) is the temperature above which the measured emission minus the emission at 300°K is described by the Richardson thermionic emission formula.

Field, (v/cm) $\times 10^{-4} \rightarrow$		8.05	8.05	8.13	7.97	7.97	8.13	8.75	8.75	8.75	8.75	8.75	9.46	9.46	9.46	9.56	10.4	10.4	10.4
$10^4/T$(°K)	T(°K)																		
33.3	300	100	100	100	100	100	100	100	100	100	100	100	100	100	100	100	100	100	100
9.5	1050	100	97	106	110	106	107	114	100	102	97	100	104	105	100	100	103	106	100
9.4	1065	100	94	107	110	106	108	114	100	102	97	100	104	105	100	103	103	106	105
9.3	1075	101	97	107	110	108	108	114	100	102	97	100	104	105	100	103	103	106	105
9.2	1085	101	94	107	112	108	108	114	100	102	97	102	104	105	100	103	103	106	105
9.1	1100	101	94	107	112	108	108	114	100	102	97	102	104	105	105	103	103	106	105
9.0	1110	100	89	107	110	110	107	118	99	102	95	102	104	105	105	103	103	106	105
8.9	1125	100	84	106	110	106	107	118	99	102	95	102	104	105	105	103	103	106	100
8.8	1135	99	100	106	110	106	106	121	99	102	95	102	104	105	105	105	103	106	100
8.7	1150	97	89	106	112	104	106	121	99	102	95	102	104	105	105	105	103	106	100
8.6	1165	94	51	105	118	100	105	118	99	100	95	102	104	105	110	105	103	106	100
8.5	1175	91	41	105	120	94	102	121	99	98	95	102	109	105	110	103	103	106	100
8.4	1190	86	35	105	128	88	99	118	97	98	97	102	109	105	110	103	103	106	100
8.3	1205	75	27	105	130	81	98	111	96	97	95	103	109	105	110	103	103	106	100
8.2	1220	65		107	125	73	90	100	95	94	95	102	109	105	110	103	103	106	105
8.1	1235	48		103	122	56	79	86	93	92	94	102	109	105	110	103	103	106	105
8.0	1250	29		103	100	38	61	64	90	89	90	98	104	105	110	100	103	106	105
7.9	1265			103	100		37		89	84	86	92	104	100	110	100	100	106	105
7.8	1280			103	75				87	81	81	84	100	95	105	95	100	106	105
7.7	1300			115					85	78	73	75	100	95	105	92	97	112	105
7.6	1315			161					85	72	69	62	104	89	110	92	97	112	105
7.5	1335								87	67	64	55	100	89	110	89	90	112	110
7.4	1350								87	62	48	31	109	84	115	89	87	112	105
7.3	1370								100	94	64	47	114	95	130	92	80	118	105
7.2	1390								163	156		94	155	110	175	100	80	130	105
7.1	1410								125				136	89	175	89	77	124	100
7.0	1430												114		150	70	73	112	84
6.9	1450																60	82	63
6.8	1470																40	30	32
Average below T_L		98	94	106	110	105	106	115	99.5	102	96	101	105	103	106	102	102	104	103
Average ratio 103%																			

values, corrected for changes in the applied field because of voltage variations and expansion of the filament on heating, are expressed as percentages of the field current at room temperature. Several sets of data at each of the applied fields used are given. Just as in the data on tungsten, the temperature T_L is indicated by the horizontal lines. From Table II one can calculate the effect of temperature on the field currents from molybdenum. When these data are averaged equally weighing all parts of the temperature range below T_L a value of 103 percent is obtained.

DISCUSSION

These phenomena then are the field-current *vs.* temperature characteristics of clean surfaces, where the work function of the surface in comparison with that known to be characteristic of a clean surface is taken as the criterion of cleanliness. The measurements presented here extend over a considerable range of field and temperature thus giving a wide assortment of relative magnitudes of field current and thermionic current as well as a wide range of field currents. Tables I and II show that the results are quite independent of the value of the applied field.

One sees as in Figs. 3 and 4 and in Tables I and II that the temperature T_L above which the measured current minus the room temperature field current falls on the thermionic line decreases with decreasing field. No doubt if one made measurements at a sufficiently low field this linearity could be extended down to a much lower temperature.

The data for tungsten and molybdenum in Tables I and II below T_L give an average value of about 103 percent for the ratio of the high temperature field currents to the field currents at room temperature. This cannot necessarily be interpreted as a 3 percent temperature effect because the experimental errors amount to 5 per-

cent. It is true that the percentages given in Tables I and II are largely above 100 percent. It is possible that when the filament temperature is raised the filament bows enough to give a small increase in the average applied field. However, there is no evidence that the filament bows on being heated.

Theory *vs.* Experiment

Houston[14] developed a formula for field currents as a function of field strength and temperature, which in working form is as follows.

$$I = Ge^{-B/F}(HF^2 + D\Phi T^2), \qquad (1)$$

where F is the field in volts/cm, T is the temperature in degrees (absolute), $H = 2.52 \times 10^{-24}$, $D = 6.67 \times 10^{-16}$, Φ is the work function in electron-volts. The ratio $R = D\Phi T^2/HF^2$ determines the effect of temperature on field currents. At a field of 10^6 volts/cm, where most of the experiments on the temperature effect have been performed, Eq. (1) predicts an increase in field current of about one thousand percent from 300°K to 1000°K. The order of magnitude of the effects observed experimentally, is predicted by the theory at a field of about 10^8 volts/cm.

This discrepancy may be explained by assuming that because of surface irregularities, over the effective areas of emission the field is greater than the average field by a factor of about 100.

Fowler and Nordheim[15] obtain the following formula for field currents.

$$I = 6.2 \times 10^{-6} \frac{\mu^2}{(\Phi+\mu)} \Phi^{\frac{1}{2}} F^2 e^{-6.8 \times 10^7 \Phi^{3/2}/F}. \qquad (2)$$

Stern, Gossling and Fowler[16] set $F = \beta F_m$, where F_m is the average field calculated from the average dimensions of the filament and β is a factor introduced by the surface irregularities. Thus from Eq. (2) they get the following relations.

$$(d \log_{10} C/F_m^2)/dF_m^{-1} = (-2.94 \times 10^7 \Phi^{3/2})/\beta \qquad (3)$$

$$\log A = \log C - \log 6.2 \times 10^{-6} - \log \frac{\mu^2}{(\Phi+\mu)} \Phi^{\frac{1}{2}} - 2 \log \beta F_m + \frac{2.94 \times 10^7 \Phi^{3/2}}{\beta F_m}, \qquad (4)$$

where C is the total current in amperes, A is the emitting area in square centimeters, μ is the usual parameter of the electron distribution in the Fermi-Dirac statistics, Φ is the work function of the metal in electron-volts, F_m is the applied field in volts/cm.

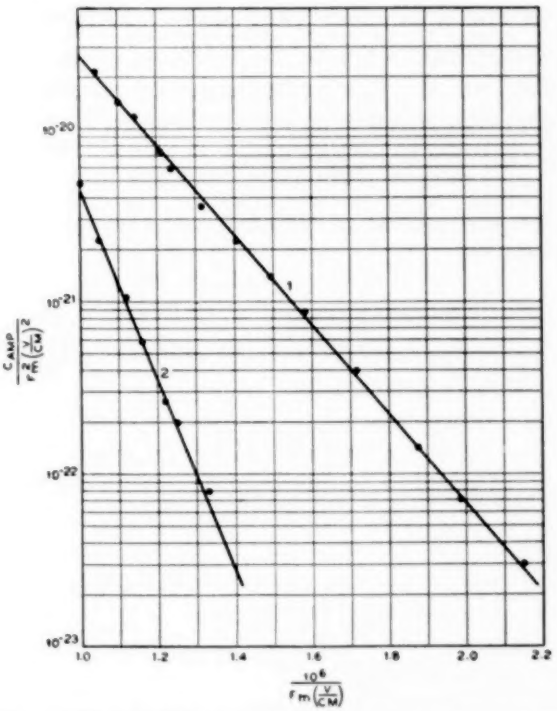

Fig. 9. Electron field currents from pure tungsten and molybdenum. Curve 1, tungsten; curve 2, molybdenum.

The 300°K data embodied in Tables I and II are shown in Fig. 9. From it the values of β and A given in Table III are obtained by using Eqs. (3) and (4). Published data of others[2, 17, 18] yield for tungsten,* values of β ranging from 24

Table III.

	β	A
Tungsten	120	1×10^{-13} cm²
Molybdenum	47	1×10^{-12} cm²

[14] Houston, Phys. Rev. **33**, 361 (1929).

[15] Fowler and Nordheim, Proc. Roy. Soc. **A119**, 172 (1928).

[16] Stern, Gossling and Fowler, Proc. Roy. Soc. **A124**, 699 (1929).

[17] Millikan and Lauritsen, Proc. Nat. Acad. Sci. **14**, 45 (1928), Fig. 2.

[18] Piersol, Phys. Rev. **31**, 441 (1928), Fig. 3.

* Φ was assumed to be 4.6 electron-volts in these calculations.

to 210. Values of β as high as 200 were obtained early in the life of some of my molybdenum* filaments. Eq. (1), with $\beta = 120$, predicts a temperature effect of from 10 to 30 percent at 1000°K for the range of fields used with tungsten. Experiment shows this effect to be less than 5 percent. For molybdenum the theory predicts a temperature effect of 50 percent or more contrasted with the negative results of the experiment.

If one could make field-current temperature measurements at a value of βF_m as low as 10^6 volts/cm, the large effect predicted could be definitely verified or disproved. Measurements of this sort are being attempted.

* Φ was assumed to be 4.3 electron-volts in these calculations.

Conclusion

These measurements therefore clearly demonstrate that electron field currents from clean tungsten and molybdenum are independent of temperature to within 5 percent from 300°K to about 1400°K. Furthermore above 1400°K the data are consistent with the assumption that the measured current consists of a thermionic current plus a field current which is independent of temperature. However, the rapid rise of thermionic current with temperature would make it impossible to discern a small effect of temperature on field currents at temperatures higher than 1400°K.

The author is indebted to Mr. R. R. Sullivan for some of the preliminary measurements on molybdenum and to Drs. M. J. Kelly and H. E. Mendenhall for criticisms and suggestions during the course of the experiments.

Absorption Spectra of the Samarium Ion in Solids. III. Absorption of $Sm(BrO_3)_3 \cdot 9H_2O$ and a Partial Energy-Level Diagram for the Sm^{+++} Ion as It Exists in Crystalline $Sm(BrO_3)_3 \cdot 9H_2O$

FRANK H. SPEDDING AND RICHARD S. BEAR, *Chemical Laboratory, University of California*

(Received March 7, 1933)

The absorption spectrum of $Sm(BrO_3)_3 \cdot 9H_2O$ has been studied at four temperatures between 20° and 298°K. The temperature variation in the absorption intensities is used to determine the location of excited lower levels situated at 39 and 68 cm^{-1} above the basic one. Other levels from 100 to 230 cm^{-1} above the normal state are probable. Between 78° and 20° many lines show a marked change, becoming double at the lower temperature. This is shown to be compatible with a splitting of the levels into new ones at 0, 37, 45, 67 and 82 cm^{-1}. Selection rules are indicated which show two apparently independent sets of these levels; 0, 37, 82 and one group of high levels; and 0, 45, 67 and another group of upper levels. This low-temperature splitting may be due either (1) to actual removal of degeneracy or (2) to development of two types of Sm^{+++} ion, differing in crystal environments. Either effect could presumably be caused by small changes in the crystal dimensions and symmetry. The hexagonal bromate shows less extension and complexity of upper multiplets and the excited lower levels are closer to the basic one than in the less symmetrical monoclinic chloride previously studied.

THIS is the third of a series of papers describing the effects of chemical composition and crystal symmetry on the energy levels of Sm IV (Sm^{+++} ion) in the solid state. In the previous papers[1] the absorption spectra of monoclinic crystals of $SmCl_3 \cdot 6H_2O$ have been described. It was demonstrated at that time that the absorption lines result from transitions between several lower levels and higher ones, the latter being grouped in multiplets. The behavior of these multiplets with temperature variation strongly indicates that they are composed of components which have resulted from the splitting of one or more excited levels by the electric fields of the neighboring ions in the crystal (a crystal Stark effect). This conclusion is in excellent agreement with the discoveries of Spedding and Nutting[2] concerning the nature of the excited levels of the Gd^{+++} ion in various salts. It will also be substantiated in this and subsequent papers.

The lines arising from the excited lower levels are readily distinguished, not only by the frequently occurring constant energy differences of the spectrum, but also by the behavior of the lines with temperature variation. As is well known, the intensity of a line is proportional to the number of atoms in the energy state from which it originates, and that number in turn depends on the temperature according to the Boltzmann relation. Because of this fact, as the temperature is lowered the intensities of lines arising from excited lower levels become less, and below a certain critical temperature, which depends on $\Delta\nu$, such lines become too faint to be observed.

This paper deals with the absorption spectra of hexagonal crystals of $Sm(BrO_3)_3 \cdot 9H_2O$ as shown by single crystals and by conglomerates of small crystals. In general the spectra resemble those described for the chloride and behave in a similar manner with regard to temperature shifts of multiplets and lines within them, changes in distinctness and intensity, etc. We shall describe only the points wherein the two spectra differ and shall refer the reader to the previous paper for general details.

Experimental Part

The bromate was prepared by the addition of a $Ba(BrO_3)_2$ solution to one of $Sm_2(SO_4)_3$ in a slightly less than equivalent amount. The $Sm(BrO_3)_3$ solution was then evaporated and the hydrated crystals extracted and purified by re-

[1] Spedding and Bear, Phys. Rev. **42**, 58 (1932); **42**, 76 (1932).

[2] Spedding and Nutting, Phys. Rev. **38**, 2294 (1931); J. Am. Chem. Soc. **55**, 496 (1933).

crystallization. The crystals were measured by Dr. A. Pabst of this university. His preliminary results were as follows: The crystals are hexagonal prisms with very ragged multiple terminations by hexagonal pyramid faces. From the measurement of four crystals the angle $(10\bar{1}0) : (10\bar{1}1)$ was found to be 57°1′. This gives an axial ratio of 0.5620.

The samarium was from the same lot that had been used for the chloride preparation and was of such purity that no lines of other rare earths were observed. In addition to photographing single crystals with 3 to 6 mm absorbing paths, conglomerates of 5 to 10 mm in thickness were used. The differences between the spectra for the two cases were less than with the chloride, since the low-lying levels are much closer to the basic one. Even at hydrogen temperatures (20°) the population in these states is appreciable, making extreme absorbing layers unnecessary.

The apparatus and methods used in photographing the spectra at low temperatures have been described previously.[1]

Results

In Fig. 1 are reproduced the photographs of the spectra observed at 20°, 78°, 169° and 298°K, and in Table I are given measurements of the positions of lines and bands at these temperatures. Between 78° and 20° occurs a remarkable phenomenon which we have observed so far only for the bromate. Practically all the lines split into two components, the red one of which is almost certainly complex (see Fig. 2). Above 78° the spectra behave similarly to the other samarium salts that we have studied.[3] The shift in position with temperature variation and the widening of the multiplets at lower temperatures may perhaps be slightly greater in the bromate case than in the chloride.

The multiplets of excited energy levels, and consequently the low-temperature multiplets of the spectrum, on the whole obey rules that are similar to those found by Spedding and Nutting[2] for the Gd^{+++} ion. In crystals of higher symmetry the over-all spread of the spectral multiplets is less and frequently the number of components fewer than in crystals of less symmetry. The samarium bromate multiplets, however, are shifted to the red with respect to those of the chloride, while with the gadolinium salts the opposite is true. In some cases the samarium bromate multiplets seem to have more components than the corresponding ones in the chloride. This is almost certainly an illusion, since the extra lines may arise from the excited lower levels. In the case of the chloride these lines are absent at 20°K, while in the bromate they can be quite intense at that temperature as a result of the smaller separations between these low levels. Another factor which tends to complicate matters is an apparent difference in the selection rules that are effective in the two salts. Thick conglomerates (long optical path) of the chloride tend to bring out many faint lines, causing the appearance of the spectrum to be markedly changed from that of a single crystal. In the bromate only a few new lines appear.

The lower levels of the ion in the bromate are also "pulled-in" from their chloride position.[4] Fig. 3 shows an energy-level diagram of several of the multiplets whose individual lines could be most satisfactorily studied. Lines arising from the low excited levels were identified, as before with the chloride, not only by their constant energy differences but also by their temperature

[3] This is also true below 78° if only the red components of the doublets at 20° are considered. On the other hand, the violet components shift quite markedly to the shorter wave-lengths, which is contrary to the usual behavior. As a result, at 20° the "center of gravity" of a doublet frequently appears to have reversed the direction of temperature shift. This phenomenon may account for an apparent reversal between 78° and 20° in the direction of displacement of several diffuse lines that are probably unresolved doublets of this type.

[4] The close proximity of the low excited levels to the basic one makes the bromate spectrum an excellent example of a type whose temperature variation has frequently been erroneously reported in the literature. When spectroscopic instruments of low dispersion are employed related high and low-temperature lines appear to form an unresolved band. On account of the fading of the former and the increasing intensity of the latter type of line as the temperature is lowered, such a band may appear to shift to shorter wave-lengths, whereas the individual lines themselves may be actually displaced in the opposite direction. That the movement of multiplets and most lines is to longer wave-lengths at low temperatures has now been confirmed in this laboratory for quite a few gadolinium and samarium salts.

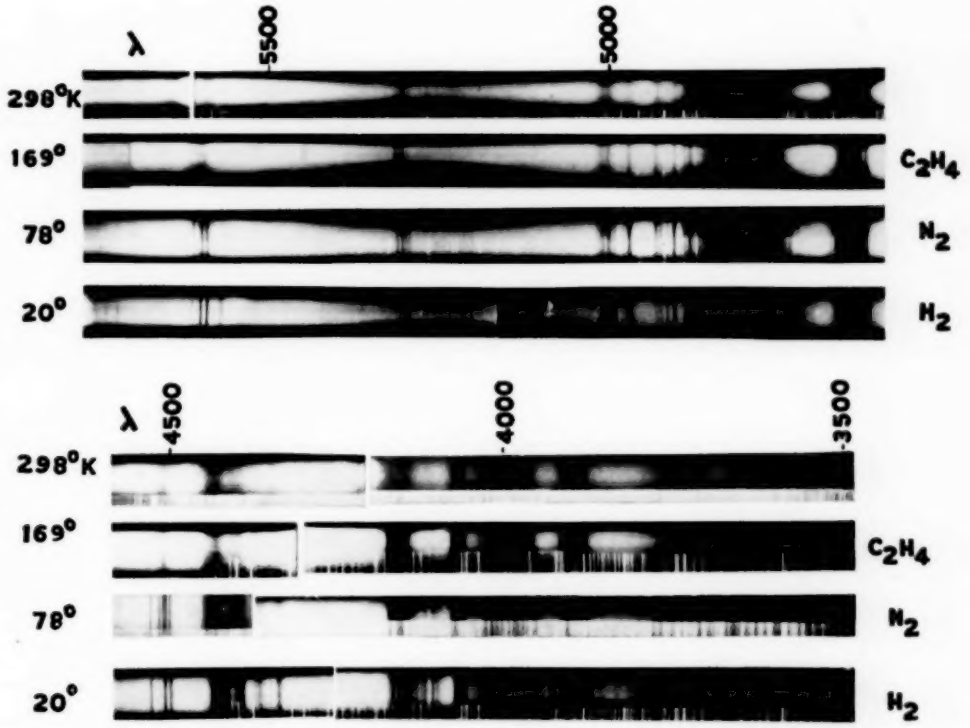

FIG. 1. Conglomerate absorption of $Sm(BrO_3)_3 \cdot 9H_2O$. The substances at whose boiling points the spectra were photographed are indicated on the right, the corresponding temperatures on the left. The three conspicuously simple multiplets on the long wave-length end are considered in more detail in Figs. 2 and 3.

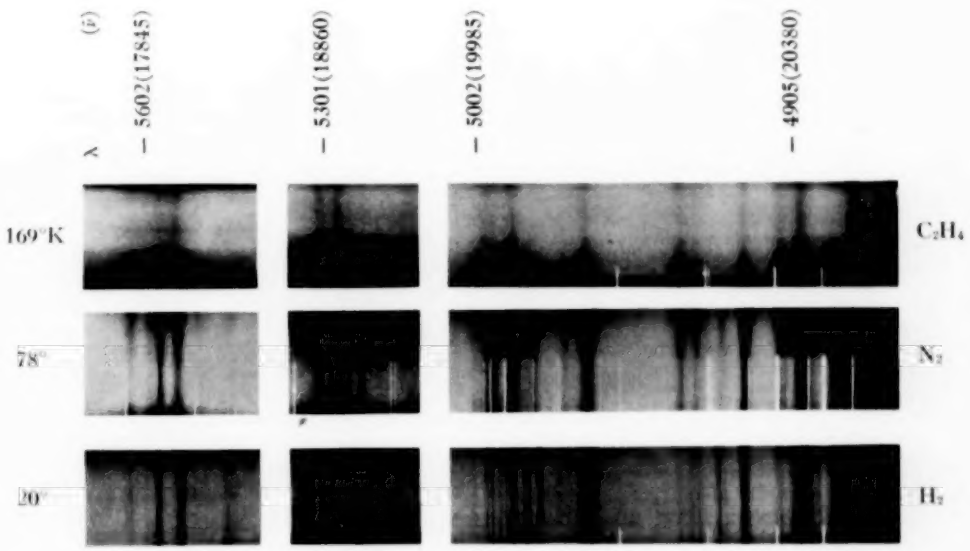

FIG. 2. Selected multiplets of $Sm(BrO_3)_3 \cdot 9H_2O$ absorption. Several of the multiplets of simplest structure are shown here magnified. The temperatures are given on the left, these being the boiling points of the substances on the right. Above are quoted wave-lengths and wave numbers for purposes of orientation with respect to the other figures and tables.

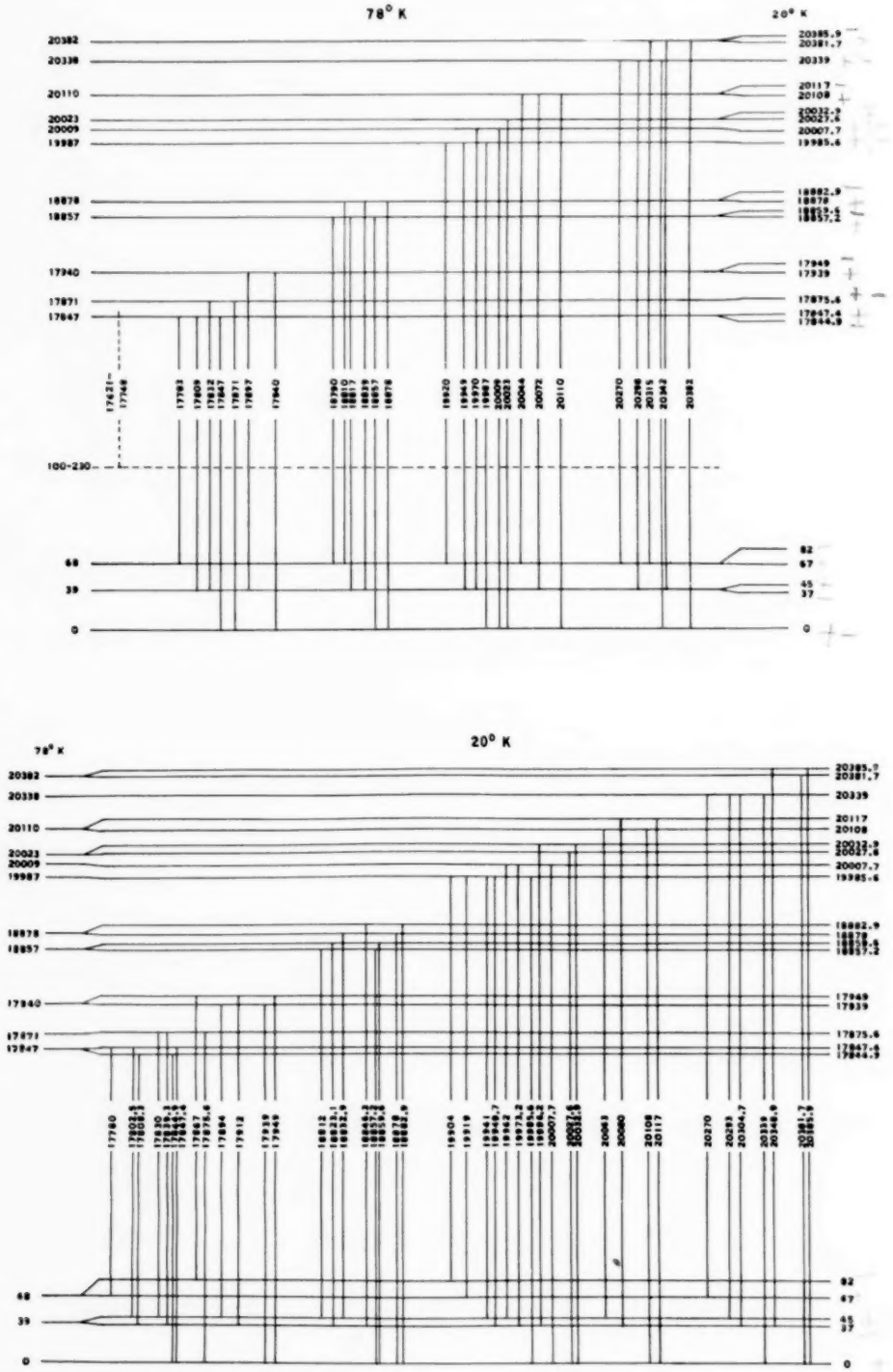

FIG. 3. Energy levels of $Sm(BrO_3)_3 \cdot 9H_2O$. Fig. 3a shows the levels needed to account for the multiplets of Fig. 2 at 78°K. The dotted lines indicate indistinct levels and transitions which are most evident at ethylene temperature (for other examples see text). In Fig. 3b are given the same levels after the changes which occur between 78° and 20°. The figures are wave numbers (cm^{-1}).

TABLE I. *Conglomerate absorption lines and bands of* $Sm(BrO_3)_3 \cdot 9H_2O$.

H (Type) = high-temperature line; L (Type) = low-temperature line; HL (Type) = probably both types overlap; R. T., E. T., N. T., H. T. = columns for room, ethylene, nitrogen, and hydrogen temperatures, respectively; Int. = columns of intensity and character of the lines. Intensity is estimated very roughly on a scale of 10, with very faint or doubtful lines given as 0; s, vs, indicate degrees of increasing sharpness; se, indicates that a line that is somewhat broader than a truly single line would be expected to be has sharp edges; nd, d, vd = degrees of increasing diffuseness; b = broad line or band, used most frequently with bands; "2," "3" = possibly double or triple, respectively. Primed values represent band edges; c, centers.

R. T. $\bar{\nu}$ (cm^{-1})	E. T. $\bar{\nu}$ (cm^{-1})	N. T. $\bar{\nu}$ (cm^{-1})	Int.	Type	H. T. λ (A)	H. T. $\bar{\nu}$ (cm^{-1})	Int.
	17621′	17308	2d	L	5776.0	17309	3s
	17637′	17352	0d	H?			
	17649′	17374	2d	L	5754.2	17374	3d
	17734′	17415	2d	L	5740.7	17415	3d
	17749′	17465	2d	L	5724.1	17465	3d "2"
	17782′	17783	1d	H	5622.6	17780	6
	17792′			H	5615.65	17802.5	2nd
	17804′	17809	4d	H	5613.80	17808.3	2s
				?	5611.6	17815.3	0
				?	5609.1	17823.5	0
	17819′	17832	3d	H	5606.9	17830	2d
17836′	17835c			H	5604.05	17839.3	1s
	17845′	17843′			5602.6′	17844′	
				L	5602.30	17844.9	10s
		17847	9d	L	5601.50	17847.4	10s
	17853′	17850′			5601.0′	17849′	
				?	5598.8	17856	0
	17866′	17867′		?	5595.35	17867.1	1nd
17877′		17871	9d	L	5592.65	17875.6	10se
	17886′	17875′					
		17897	2d	H	5588.5′	17889′	1d
					5585.7′	17898′	
	17905′			H	5582.0′	17910′	1d
					5580.4′	17915′	
	17930′				5574.1′	17935′	
		17940	2d	L	5572.9	17939	4d
					5572.0′	17942′	
				L	5569.8	17949	3d
	17952′	18790	0	H			
	18786′	18810e	4d	H	5314.3	18812	2d
	18797′	18817e	4d	H			
18811′	18807′			H	5311.15	18823.1	2s
18824′	18818′	18839	8d	H	5308.40	18832.9	4d
18840′	18836′			H	5304.60	18846.3	4s
	18845′				5302.7′	18853′	
18852′		18857	4d	L	5301.55	18857.2	9s "3"
	18859			L	5300.85	18859.6	9s "3"
					5300.5′	18861′	
				?	5298.5	18868	0
	18879	18878	4d	L	5295.8	18878	9d "2"
				L	5294.35	18882.8	9s
	19012.6	19008.4	2nd	?	5260.4	19005	0s
	19020.7	19018.1	1nd	?			
	19166	19163.9	3nd	L	5216.85	19163.0	4s
				?	5212.8′	19178′	0vd
					5210.0′	19189′	
	19209	19211.6	4nd	L	5203.40	19212.7	5s
		19650	0s	L	5087.5	19651	0nd
				H	5022.7	19904	0d
	19918′	19920	3d	H	5018.9	19919	2d
19931′		19938′					
	19941′			H	5013.4	19941	3d
19956′		19949	5vd	H	5011.20	19949.7	3s
	19957′	19958′		H	5008.0	19962	2d
		19970	4d	H	5005.30	19973.2	2s
19986′	19983′	19987	9d	LH	5002.20	19985.6	9sc
	19996′			H	4999.55	19996.2	1nd
20003′		20009	1d	L	4996.70	20007.7	9se "2"
	20023	20023	4d	L	4991.70	20027.6	7s
				L	4990.40	20032.9	7s
		20044	0d	H			
	20065′	20067′		H	4983.0	20063	1vd
		20072	3d	H			
	20083′	20076′		H	4978.7	20080	1vd
20107′	20106′	20105′			4972.8′	20104′	
				L	4971.8	20108	10d "2"
		20110	8d	L	4970.9′	20111′	
20125′	20120′	20117′		L	4969.6	20117	9d

R. T. $\bar{\nu}$ (cm^{-1})	E. T. $\bar{\nu}$ (cm^{-1})	N. T. $\bar{\nu}$ (cm^{-1})	Int.	Type	H. T. λ (A)	H. T. $\bar{\nu}$ (cm^{-1})	Int.
20269′	20269′	20270	4d	H	4931.9	20270	1d
20290′	20279′	20298	4d	H	4926.5	20293	2d
	20303			H	4923.60	20304.7	2nd
20322′		20315	1d "3"	H			
	20338′	20342	2d	LH	4915.4	20339	3d
	20352′			H	4912.90	20348.9	2nd
20378′	20379′	20378′			4905.70′	20378.7′	
		20382	9d	L	4905.00	20381.7	10s
20394′	20389′	20387′			4904.00	20385.9	10s
					4903.60′	20387.5′	
				L	4896.5′	20417′	0d
					4893.5′	20430′	
20438′	20442′	20439′	8	H	4890.9	20440	1d
20457′	20452′	20450′	8d	H	4889.1	20448	2d
		20472′		L	4884.3	20468	2d
20475′	20478′		9vd		4882.2′	20477′	
20493′	20489′	20492′		L	4878.6′	20492′	9d "2"
					4876.9′	20499′	
				L	4872.95	20515.7	3nd
	20526′	20526′			4870.6′	20526′	
	20536′		4db	H	4866.6	20543	3d
		20550′			4863.8′	20554′	
				L	4863.0	20558	1d
20559′	20563′	20563′			4861.4′	20565′	
	20583′		8db	L	4858.0′	20579′	10vd
20591′		20593′		L	4855.3	20590	9vd
					4852.0′	20604′	
20612′	20614′	20611′	4d	H	4849.6	20615	2d
	20626′	20623′			4845.8′	20631′	
		20637′		H	4844.7	20636	3vd
20644′			5d	H	4842.7	20644	4vd
		20650′			4841.4′	20649′	
20667′	20666′	20664′		L	4837.8	20665	3d
	20682′		9db		4835.5′	20675′	
20693′		20683′		L	4834.4	20679	10vd
	20700′	20695′		L	4830.1	20698	10vd
	20719′		9db	L	4828.2′	20706′	10vd
		20723′			4822.3′	20731′	
20762′	20765′	20745	2d	L	4818.9	20746	7d
20802′	20799′	20768′	9db	L	4814.7′	20764′	10vd
	20829′	20800′			4804.8′	20807′	
	20858′	20829′	9vdb	L	4797.7′	20838′	10vd
	20878′	20864′			4790.1′	20871′	
	20898′	20872′	7vdb	L	4787.8′	20880′	8vd
	20915′	20896′			4784.1′	20897′	
	20931′	20909′	6vdb	L	4780.0′	20915′	7vd
	20947′	20930′			4776.8′	20929′	
	20967′	20945′	9vdb	L	4773.6′	20943′	10vd
		20962′			4767.5′	20970′	
	20990′	20978′		L	4764.2′	20984′	9vd
21004′					4760.5′	21000′	
	21016′		8wvd	L	4758.1′	21011′	8vd
		21024′			4752.7′	21035′	
	21046′	21047′			4749.2′	21050′	6vd
			5wd	L	4745.4′	21067′	
	21089′	21091′		L	4740.5	21089	4vd
21104′	21116′	21115′			4736.4′	21107′	
	21133′	21135′	8vd	L	4733.2′	21121′	9vd
					4729.3′	21139′	
		21173′	3d	L	4720.9′	21176′	5vd
		21186′			4718.5′	21187′	
				L	4713.7′	21209′	1vd
					4708.9′	21230′	
21254′				L	4704.0	21252	1vd
				L	4693.3	21301	1vd
				L	4682.2′	21351′	1vd
					4677.4′	21374′	

TABLE I. (*Continued*).

R. T. $\tilde{\nu}$ (cm^{-1})	E. T. $\tilde{\nu}$ (cm^{-1})	N. T. $\tilde{\nu}$ (cm^{-1})	Int.	Type	H. T. λ (A)	H. T. $\tilde{\nu}$ (cm^{-1})	Int.
					4669.3′	21411′	
21438′	21439′	21442c	9d	H	4661.7	21445	2vd
	21456′	21472	10d	H	4657.5c	21465c	7d
	21471′			H	4653.9	21481	7d
	21486′			HL	4650.5	21497	5vd
21512′	21518′	21509	8vd	L	4647.5	21511	10vd
21539′	21530′	21532′	8vd	L	4643.4	21530	10vd
	21541′	21548′					
	21547′				4636.3′	21563′	
21578′	21573′	21567	8d	L	4634.2′	21573′	10d
	21585′	21585	8d	L	4631.5′	21585′	
21594′		21600	8d	H	4629.4	21595	5d
21614′	21608′			H	4626.6	21608	7d
		21622′			4623.6′	21622′	
21633′	21634′	21634′	10vd	L			10vd
	21645′	21648′					
21656′		21659′			4616.7′	21654′	
	21707′	21719	0	L	4605.4′	21707′	1vd
	21734′				4600.1′	21733′	
		21812	1d	L	4583.7′	21810′	2d
					4581.4′	21821′	
		21833′	0	L	4578.2′	21837′	1d
		21852′			4575.6′	21849′	
		21872′					
		21891′	0	L	4568.2	21885	1d
		21904′					
		21921′	0	L	4562.0	21911	1d
				L	4555.3	21946	1d
				H	4551.4	21965	1d
	21974′	21974.7	2nd	H	4549.0	21977	1d
21983′	21985′	22003.3	2nd	H	4544.6	21998	1d
22002′	22004′			H	4541.8	22011	1d
22016′	22016′			L	4535.80	22040.7	8s
22028′		22043.0	6nd	L	4535.10	22044.0	8s
22049′	22048			L	4534.30	22048.5	8s
22072′	22075′	22076	2d	H	4531.2′	22063′	0
	22086′				4528.2′	22078′	
22106′	22104′	22104	3d	H	4523.75	22099.4	2nd
				H	4521.20	22111.8	2nd
22122′	22117′	22117	1d	H	4519.5	22120	0
22142′	22142′	22136′			4515.2′	22141′	
		22144	8d	LH	4514.3	22145	9d "2"
22159′	22152′	22152′			4513.5′	22150′	
22176′	22181′	22179′			4506.9′	22182′	
		22185	6d	L	4505.9	22187	8d
22197′	22193′	22191′			4504.9′	22191′	
		22242	0	H?			
		22276	0	H?			
		22319	0	H?			
		22341′	0	?	4473.5′	22348′	0
		22367′			4469.3′	22360′	
				L	4466.2′	22384′	0
					4463.2′	22399′	
	22426′	22420′		H	4459.2′	22419′	1d
22449′					4457.2′	22430′	
		22446′		H	4454.1	22445	1s
	22462′		8db	H	4452.4	22453	1s
				H	4451.3	22459	1s
		22470′		H	4449.7	22467	1s
					4448.5′	22473′	
	22477′			H	4448.3	22474	2d
	22490′	22480′		H	4447.2	22480	2d
			8d	L	4445.30c	22489.3c	9s
22508′	22507′			L	4442.50	22503.5	9s
		22512′		L	4440.85	22511.9	8s
22527′	22527′		8d	L	4438.85c	22522.0c	8nd
		22528		L	4437.90c	22526.8c	8nd
					4436.3′	22535′	
	22548′			L	4435.4	22540	10d
22558′		22545	8d	L	4433.3	22550	10d
					4432.5′	22554′	
		22568	8d	L	4430.4c	22565c	8d
				L	4429.1c	22572c	8d
22581′	22587′	22581′	8d	L	4426.35	22585.6	9nd
		22601′		L	4423.95	22597.8	8nd
				L	4421.6	22610	2d
22643′	22639′			L	4418.80	22624.3	4nd
		22642	6wd	H	4412.5	22657	0
		22661′					
		22669	7d	H	4410.6	22666	2d
22676′	22680′	22674′					
22702′	22700′	22699′			4405.0′	22695′	
		22708	8d	L	4403.7	22702	10d
	22715′	22712′		L	4401.8	22712	10d
					4400.8′	22717′	
		22726′	8d		4398.7′	22728′	
22737′					4397.7	22733	d
		22742′			4396.6′	22739′	

R. T. $\tilde{\nu}$ (cm^{-1})	E. T. $\tilde{\nu}$ (cm^{-1})	N. T. $\tilde{\nu}$ (cm^{-1})	Int.	Type	H. T. λ (A)	H. T. $\tilde{\nu}$ (cm^{-1})	Int.
22809′	22802′	22798′		L	4386.4	22791	1d
				L	4382.4	22812	1d
		22829′		L	4379.1	22829	2d
					4375.4′	22849′	
22860′	22856′		3wvd	L	4374.1	22856	3d
		22872′		L	4371.2c	22871c	2vd
				L	4368.3	22886	1d
				L	4363.1	22913	1d
22930′	22929′	22931c	3d	H	4359.6	22931	2d
	22939′			H	4357.0	22945	3d
	22952′	22960	3d	H	4352.6	22968	2d
	22966′	22976c	3d	H	4350.0	22982	0
22985	22983′	Faintly evident		L	4347.2	22997	2d
23011′	23007′				4345.1′	23008′	
		23012	6d	L	4344.2	23013	7d
	23018′				4343.3′	23017′	
23031′		Faintly evident		L	4340.7c	23031c	2d
	23660′				4338.7′	23042′	
	23701′	23391.6	1vs	L	4274.10	23390.3	1vs
	23742′	23744	0	H			
	23783′	23776	0	H			
	23818′	23830	1d	H			
	23843′	23859	2d	H	4190.45	23857.2	2nd
	23859′			H	4188.60	23867.6	2nd
23877′	23877′	23898.8	8nd	L	4182.70c	23901.4c	9s
	23900′	23908′		L	4182.15c	23904.5c	9s
	23908′		10db	L	4179.45c	23919.9c	9nd
		23928′		L	4178.70c	23924.3c	9nd
	23925′	23940′		L	4175.4	23943	10d
23943′	23933′		10db	L	4173.6	23953	10d
	23943′	23962′		L	4171.95	23962.8	3nd
	23964′			L	4170.85	23969.3	2nd
		23980.9c	8nd	L	4168.75	23981.2	9nd
23987′	23982	23987.3c	8nd	L	4167.40	23988.9	10nd
				L	4165.55c	23999.8c	3nd
24013′	24015′	24006′			4163.2′	24013′	
			9db	L	4162.5	24017	10d
	24029′	24028′		L	4160.7	24028	10d
					4159.8′	24033′	
	24041′	24038′		L	4158.7′	24039′	10b
			10db		4156.4′	24053′	
	24060′	24060′		L	4155.3	24059	10d
				L	4153.6	24069	10d
24080′	24076′			L	4151.6	24080	8d
	24093′	24082′			4150.8′	24085′	
		24101	3vd	L	4147.8	24103	3d "2"
					4147.3′	24105′	
	24111′			L	4146.00c	24112.8c	4nd
		24119′		L	4144.95c	24119.0c	4nd
	24134′			L	4143.30	24128.6	3nd
			4db	L	4140.95	24142.3	4nd
24148′				L	4139.3	24152	4d
	24161′	24168′		L	4137.4	24163	4d
				L	4135.90	24171.9	2nd
				L	4132.60c	24190.9c	3nd
	24197′	24199	4d	L	4131.25	24198.8	4nd
24203′	24213′			L	4129.80c	24207.4c	3nd
	24220′			L	4128.15c	24217.2c	3nd
24234′	24233′	24226	5d	L	4126.90	24224.5	5nd
					4123.9′	24242′	
				L	4122.70	24249.1	3nd
				L	4120.5	24262	2d
24278′	24280′			L	4118.7	24273	3d
					4116.5′	24286′	
	24298′	24290	5d	L	4115.6	24291	6d
24316′	24319′				4114.8′	24296′	
				L	4112.6	24309	4d
	24336′	24331	4d	L	4108.5′	24333′	5d "2"
					4107.9′	24337′	
				L	4105.5	24351	3d
				L	4103.9	24365	1d
				L	4099.8	24385	1d
				L	4096.6	24404	1d
				L	4093.8	24420	0
				L	4091.3	24435	0
24459′				L	4088.6	24452	0
	24469′	24463.2	8nd	H	4086.15	24466.0	5nd
		24478′		?	4084.55	24475.7	1vs
	24483′		9d	H	4082.6	24487	8d
	24498′	24495′		H?	4080.85c	24497.9c	6nd
	24507′	24504′		H?	4079.5	24506	8d
24513′				H?	4078.65	24511.0	8nd
			8bd	H?	4077.55	24517.6	8nd
	24521′			H?	4076.70	24522.8	8nd
		24535′		L	4075.8′	24528′	9d
24540′	24535′				4074.2′	24538′	
		24541′	9d	H	4073.6′	24541′	
	24546′	24557′					10b
	24559′	24566c	8d	L			
	24565′	24574c	8d	L	4067.1′	24581′	

TABLE I. (*Continued*).

R. T. $\tilde{\nu}$ (cm^{-1})	E. T. $\tilde{\nu}$ (cm^{-1})	N. T. $\tilde{\nu}$ (cm^{-1})	Int.	Type	H. T. λ (A)	H. T. $\tilde{\nu}$ (cm^{-1})	Int.
††24593′	†24579′	24588.9	8nd	L	4065.85e	24588.2e	9nd
	24588			L	4065.05e	24593.1e	9nd
				L	4056.8′	24643′	2d
					4054.2′	24659′	
				L	4051.8′	24674′	2d
					4048.8′	24692′	
24715′				L	4044.5′	24718′	4vd
					4041.5′	24740′	
				L	4038.1′	24757′	3vd
	24775′				4034.8′	24777′	
		24783′			4032.7′	24790′	
				L	4029.9	24807	4d
			9db	L	4027.2e	24824e	10d
	24958′	24953′			4006.3′	24953′	
				L	4004.3	24966	7vd
	25007′	25008	6vd	L	3997.8	25007	7vd
	25028′	25051	5bd	L	3989.6′	25058′	
25038′	25040′		6d	L	3987.4′	25072′	7d
	25061′	25079			3985.5′	25084′	
	25076′	25093	8d	L	3984.5′	25090′	9d
	25099′				3982.7′	25102′	
	25115′	25118	8d	L	3981.2′	25111′	9d
	25127′				3978.9′	25126′	
			8d	L	3978.2′	25130′	9d
	25137′	25139			3976.1′	25143′	
	25150′			L	3974.6	25153	8d
	25179′	25165	2vd	L	3971.6	25171	2d
	25195′	25188	4vd	L	3968.50	25191.2	8nd
	25215′	25221e	8d	L	3965.1′	25213′	9d
	25234′				3961.1′	25238′	
25251′				L	3958.0	25258	6d
		25265′			3957.1′	25264′	
				L	3956.25	25269.4	2nd
				L	3954.3	25282	4d
		25336	2d	H	Faintly evident		
		25373	3d	L	3939.75	25375.1	6nd
				L	3935.3	25404	3d
		25425	4d	L	3932.7	25421	6d
				L	3930.2	25437	6d
25484′	25488′	25480′	8d	H	3922.2	25489	6d
	25502′	25498′					
25512′		25505′	8d	H	3919.80	25504.4	4nd
25527′	25538	25524′		H	3917.8	25517	6d
	25546′	25534	7d	H	3914.3′	25540′	
25573′	25559′	25549	9d	HL			9vd
		25564	7d	HL	3908.8′	25576′	
				L	3906.7	25590	9d
25613′	25614′			L	3904.4	25605	8d
	25625′	25619	9d	L	3902.7′	25616′	
	25633′			L	3900.7′	25629′	10d
	25645′	25638e	9d	L	3900.0′	25634′	10vd
25661′					3897.9′	25648′	
				L	3896.55	25656.6	6nd
25694′	25695	25669	4d	L	3893.50	25676.5	4nd
		25693	4d	L	3891.15	25692.0	4nd
					3889.3′	25704′	
25721′	25723			L	3888.5	25710	8d
	25733′	25719	9d	L	3886.3	25724	10d
25755′	25744′	25737	9d	L	3883.9	25740	10d
					3882.8′	25747′	
		25758.7	5nd	L	3880.80	25760.5	9nd
		25776.2	5nd	L	3878.65	25774.8	8nd
				L	3877.45	25783.0	8nd
		25809	3d	L	3873.0	25812	6d
		25845′	0	L	3867.9′	25846′	2d
		25864′			3865.1′	25865′	
	25882′	25881′	0	L	3860.4′	25897′	2d
	25904′	25909′			3857.2′	25919′	
				L	3840.2′	26033′	2vd
					3834.1′	26074′	
26324′	26327	26321.1	2s	H			
	26362	26352.1	1s	H			
26388′				L	3787.65	26394.1	3nd

R. T. $\tilde{\nu}$ (cm^{-1})	E. T. $\tilde{\nu}$ (cm^{-1})	N. T. $\tilde{\nu}$ (cm^{-1})	Int.	Type	H. T. λ (A)	H. T. $\tilde{\nu}$ (cm^{-1})	Int.
26509′				L	3771.9	26505	2d
		26549	8d	H	3766.4	26543	6d
	26558			H	3764.6	26556	6d
	26570′	26565′		L	3762.7′	26560′	8nd "2"
					3761.30e	26579.2e	
				L	3758.8	26597	9db
	26631′			L	3755.4	26621	9db "2"
	26641′		9db	L	3753.0′	26638′	10db
	26676′				3747.7′	26675′	
	26687′			L	3746.4′	26685′	9d "2"
					3744.1′	26701′	
	26712′	26714′		L	3742.8	26710	3d
	26729′	26723′	9db	L	3741.6′	26719′	9db
	26750′	26751′			3737.1′	26751′	
	26815′	26812	7d	H			
	26838′	26833	8d	L	3725.5	26834	8d
	26859	26857	8d	L	3722.8	26854	8d
	26892	26888	6d	H†	3718.5	26885	4d
				H†	3716.6	26899	6d
	26928	26926	8d	L	3713.8	26919	8d
				L	3712.0	26932	9d
26982′				L	3710.4	26944	7d
		26962	4d	L	3706.9	26969	7d
		26994	3d	L	3702.7	27000	6d
			4d	L	3698.4′	27031′	6d
		27042			3695.6′	27052′	
27260′	27268′	27273	7d	H			
	27288′	27302	8d	H	3662.5	27296	6d
	27297′			H	3661.1	27306	6d
27325′	27317′			H	3659.5	27319	6d
			8d	L	3657.5′	27334′	9d
	27344	27340			3655.9′	27346′	
		27359	8d	L	3654.7′	27354′	9d
	27363				3652.9′	27368′	
27421′	27457′	27453′					
	27488′	27481′	9d	H	3638.2	27478	8d
	27499′	27492′	8db	L	3636.3′	27493′	
	27524′	27512′					
	27541′	27584′	8db	L			8wb
	27571′	27617′					
	27591′	27637′	8db	L			
	27621′	27662′			3600.0′	27770′	
	27634′	27809′		L	3597.9	27786	6d
	27663′		8db	L	3593.2	27822	6db
27739′	27810′	27862′		L	3589.2	27854	8db
27837′	27866′	27886′		L	3583.8e	27896e	8d
	27879′		8db	L	3581.25	27915.3	8s
27924′	27919′	27926′		L	3579.75e	27927.0e	8e
					3573.6′	27975′	
		28055	2d	H			
	28067	28087	6d	H	3560.2	28080	4d
				H	3558.5	28094	4d
	28094	28125	9d	L	3554.50e	28125.2e	9s
				L	3553.85e	28130.6e	9s
	28130	28159	9d	L	3550.50′	28156.9′	9se
					3549.00′	28168.8′	
28153′	28163	28178	3d	H			
28197′	28184	28207	5d	H	3544.6	28204	4d
				H	3542.8	28218	4d
		28244	8d	L	3538.9	28249	8d
	28250	28283	8d	L	3534.0	28288	8d
28287′	28289			L	3513.7	28452	0
28303′				L	3511.5	28470	0
		28640	5d	H	3490.9	28638	4d
	28643			H	3489.35	28650.5	4vs
28657′		28673	6d	L	3486.6	28673	6d
	28673			L	3485.05	28686.0	4vs
28692′				L	3483.35	28699.8	4vs
28761′		28782	5d	H	3473.3	28783	3d
	28788	28812	5d	L	3469.5	28814	5d
28811′	28817	28845	5d	L	3465.2	28850	5d
28842′	28841′						

behavior. Tables II and III give examples of the constant intervals found. The lower levels of the diagram and tables account for all of the important lines of the multiplets considered and for most of the high-temperature lines in other parts of the spectrum. The complexity of the other multiplets seems to be the chief factor hindering attainment of complete agreement.

TABLE II. *Prominent "low-temperature" lines and their "high-temperature" satellites (78°K).*

L.-t. line	Satellite *A*	$\Delta\tilde{\nu}_A$	Satellite *B*	$\Delta\tilde{\nu}_B$
17847	17809	38	17783	64
17871	17832	39		
18857	18817	40	18790	67
18878	18839	39	18810	68
19987	19949	38	19920	67
20009	19970	39		
20110	20072	38	20044	66
20382	20342	40	20315	67
21509	21472	37	21442	67
21641	21600	41		
22043.0	22003	40	21975	68
22144	22104	40	22076	68
22185			22117	68
22708	22669	39	22642	66
23898.8	23859	40	23830	69
24588.9	24549	40		
26926	26888	38		
27340	27302	38	27273	67
28125	28087	38	28055	70
28244	28207	37	28178	66

The lines at nitrogen temperatures are somewhat more diffuse for the bromate than for the chloride. This probably results from the fact that the lines already have started to split apart. At hydrogen temperature the splitting is so pronounced that at first sight the spectrum seems to present an entirely different appearance. All of the levels evidently have split into two components. This splitting amounts to from 5 to 15 cm^{-1} for the lower levels and is somewhat less for the extreme upper ones. Of the two components resulting from each of the lower levels the one with higher energy appears not to be single (uncertain for the 67–82 pair). It is probably double and may be still more complex. Of particular interest is the fact that after the levels have split all the lines resulting therefrom cannot be referred to common upper levels, except in cases where it is obvious that the low temperature lines in question are complex and are not completely resolved. As a result, the levels 0, 45, and 67 seem to be associated with one set of excited levels and 0, 37 and 82 with another.[5] Only a few lines arising from the excited lower level at 82 cm^{-1} are observed, since the lines are very faint because of the low population in this state at 20°K. Because of this low intensity the above rule has not as much confirmation for this level as might be desired, though the behavior described is certainly true of the 37 and 45 levels.

It is not at all certain just what causes this splitting of the levels, though in any case the effect is probably brought about by a slight change in the crystal structure. The symmetry of the field about the Sm^{+++} ion may become less at the lower temperatures, causing the levels to be less degenerate. On the other hand, the selection rules mentioned above suggest that in the crystalline change some of the samarium ions in the unit cell have become different from the others (with respect to field), and that in a mole of ions in the crystal one has a fraction of a mole of one type of Sm^{+++} and the remainder of another kind.[6]

Any crystalline change that might bring about this effect is small, however, as appears from the fact that the bromate crystals show no pronounced tendency to crack when they are suddenly cooled, nor do they undergo crystal transitions during prolonged exposures at low temperatures.

There is some evidence that other lower levels exist. New lines make their appearance at liquid ethylene temperature, though they are quite diffuse and faint. The probabilities of transitions from such levels seem to be small and only a few of them appear. Thicker absorbing layers tend to bring these lines out more strongly, but in any case they are hard to measure accurately (see dotted level and band of Fig. 3). The most

[5] It will be noticed that the method employed here cannot determine whether the basic level, 0, is or is not split at low temperatures. The diagram, Fig. 3, is based upon the assumption that it is not. If the low-temperature doublets were all of the same separation, one might conclude that the high upper levels are not split and that the basic one has divided this much. However, according to our measurements such cannot be the case, even if there is some splitting in the normal level. This ground state probably does split similarly to the next higher one, though it does so in smaller amount.

[6] The ions in a crystal of $SmCl_3 \cdot 6H_2O$ must all have the same energy states, since no such selection rules have been found for that salt.

TABLE III. *Prominent "low-temperature" lines and their "high-temperature" satellites (20°K).*

L.-t. line	A_I	$\Delta\tilde{\nu}_{A_I}$	A_{II}	$\Delta\tilde{\nu}_{A_{II}}$	B_{II}	$\Delta\tilde{\nu}_{B_{II}}$	B_I	$\Delta\tilde{\nu}_{B_I}$
17844.9 (I)	17808.3	36.6						
17847.4 (II)			17802.5	44.9	17780	67		
17875.6 (I, II)	17839.3	36.3	17830	46				
17939 (II)			17894	45				
17949 (I)	17912	37					17867	82
18857.2 (II)			18812	45				
18859.6 (I)	18823.1	36.5						
18878 (II)			18832.9	45				
18882.9 (I)	18846.3	36.5						
19985.6 (I, II)	19949.7	35.9	19941	45	19919	67	19904	82
20007.7 (I, II)	19973.2	34.5	19962	46				
20032.9 (I)	19996.2	36.7						
20108 (II)			20063	45				
20117 (I)	20080	37						
20339 (I, II)	20304.7	34	20293	46	20270	69		
20385.9 (I)	20348.9	37.0						
20485 (I, II)	20448	37	20440	45				
20679 (I, II)	20644	35	20636	43				
21511 (?)			21465	46	21445	66		
22040.7 (IIa)			21998	43 } 44.5	21977	64 } 65.5		
22044.0 (IIb)			21998	46 }	21977	67 }		
22048.5 (I)	22011	38					21965	84 −
22145 (I, II)	22112	33	22100	45				
22187 (I, II)					22120	67		
22489.3 (I, II)	22453	36	22445	44	22425	64		
22503.5 (I, II)	22467	37	22459	45				
23013 (I, II)			22968	45	22945	68	22931	82
23901.4 (II)			23857.2	44.2				
23904.5 (I)	23867.6	36.9						
24533 (I, II)	24497.9	35	24487	46	24466.0	67		
26579.2 (I, II)	26543	36						
28125.2 (II)			28080	45				
28130.6 (I)	28094	37						
28249 (I, II)	28218	31	28204	45				

The Roman numerals refer to the two components formed at 20° from single lines at 78°.

definite cases of such lines are those at 23,660 to 23,783 (see Table I). Judging from these bands the levels would be separated from the basic one by about 100 to 230 cm^{-1}, probably existing as two doublets with centers at 140 and 220 cm^{-1}.

CONCLUSIONS

The absorption spectra of $Sm(BrO_3)_3 \cdot 9H_2O$ crystals are composed of lines that originate in transitions from a basic state and other low ones to excited levels which are grouped in multiplets. These multiplets probably arise from excited levels that are split apart in the electric field of the crystal. The over-all splitting of these high levels is somewhat less than in the monoclinic chloride.

The separations of the lower levels are also less than in the chloride, being chiefly from 39 to 68 cm^{-1} as compared with 145 to 217 cm^{-1} in the chloride, though greater intervals probably also occur in both. The existence of more than three such levels in the samarium salts makes the assumption of more than one low-lying electronic state, as advocated by one of us,[7] highly probable.[8]

[7] Spedding, J. Am. Chem. Soc. **54**, 2593 (1932).

[8] The basic level of Sm^{+++} as predicted by Hund is a $^6H_{5/2}$ and should yield only $J+\frac{1}{2}$ or 3 levels in an electric field.

Charge Distributions for the Normal Atoms from Boron to Neon

F. W. BROWN, J. H. BARTLETT, JR., AND C. G. DUNN, *University of Illinois*

(Received June 16, 1933)

Hartree functions have been obtained for normal boron. The energy parameters of the $1s$, $2s$, and $2p$ electrons are found to be 15.50, 0.910, and 0.446 respectively. By use of the function for the normal electron configurations of B, O, F, and Ne, and an interpolation process, single-electron wave functions for normal carbon and nitrogen have been found. Values of the radial functions of the $1s$ and $2s$ electrons at $r=0$ for the atoms B, F and Ne have also been tabulated.

INTRODUCTION

FOR many purposes, especially for the theory of hyperfine structure and for the theory of isotopic displacement, a knowledge of accurate wave functions associated with atomic energy levels is highly desirable. The theory is at present quite incomplete, however, since no satisfactory relativistic treatment of the many-body problem has as yet been given, and since one does not even know how to obtain the exact solutions of the nonrelativistic wave equation for more than one electron.

By means of a variational method, Hylleraas[1] has been able to approximate (from above) to the energy of the normal helium atom. The successive approximations converge quite rapidly toward a limit, and this limit is in very good agreement with the experimental value. Unfortunately, this is not an absolutely convincing proof of the agreement between theory and experiment, since the theory does not furnish an estimate of the maximum amount of error[2] which may be involved in the variational method. At present, one can only hope that this error is so small as to be practically negligible. In other words, the wave functions of Hylleraas are to be assumed as not very different from the rigorous solutions of the differential equation.

It would be of interest (and may be necessary in the future) to extend the work of Hylleraas to atoms with more than two electrons. Until this is done, however, the most convenient procedure consists in using single-electron wave functions, and forming the approximate wave functions by combining linearly products of single-electron functions (with due regard for the Pauli exclusion principle). Usually, the linear combinations are restricted to a certain electronic configuration, such as $(1s)^2(2s)^2(2p)^2$, unless there is need for considering the perturbative effect of nearby configurations.

The best single-electron wave functions obtainable from central fields are those found by the Hartree[3] method (when modified as proposed by Slater[4] and Fock[5]). The determination of such functions for any arbitrary configuration is a problem of considerable magnitude, and will probably be solved by means of interpolation processes. A beginning in this direction has been made by Slater,[6] who has fitted Hartree curves by means of simple analytic wave functions, and has plotted the parameters involved as a function of the atomic number. Interpolated values for these parameters will give a first approximation to the single-electron wave functions for an atom of intermediate atomic number. A rather serious objection to this method arises when one considers that excitation or ionization generally causes the core electrons to redistribute themselves so that the final wave functions are quite different[7, 8] from the initial ones. Again, if one

[1] E. A. Hylleraas, Zeits. f. Physik **54**, 347 (1929).

[2] See H. Bateman, *Partial Differential Equations*, 1932, p. xix, for a recital of attempts to estimate such errors.

[3] D. R. Hartree, Proc. Camb. Phil. Soc. **24**, 89 (1928).

[4] J. C. Slater, Phys. Rev. **35**, 210 (1930).

[5] V. Fock, Zeits. f. Physik **61**, 126; **62**, 795 (1930).

[6] J. C. Slater, Phys. Rev. **42**, 33 (1932).

[7] D. R. Hartree and M. M. Black, Proc. Roy. Soc. **A139**, 311 (1933).

[8] J. H. Bartlett, Jr., and J. J. Gibbons, Chicago meeting, Am. Phys. Soc., June, 1933, paper No. 57.

knows the Hartree functions beforehand, it is usually better[8] in perturbation calculations to carry through numerical integrations rather than to attempt to find accurate analytic functions of the exponential type, and to use these in the integrations.

For the normal atoms of neon,[9] fluorine,[9] and oxygen,[7] Hartree wave functions have already been calculated. In the present paper, similar functions for normal boron are tabulated, and it is shown how, by an interpolation method, one may obtain quite accurate wave functions for the normal carbon and nitrogen atoms.

Self-Consistent Field for Normal Boron

For normal boron, the variation equations obtained by minimizing[10] the total energy of the atom are

$$-f_1''+2(-5/r+F_0^{11}+2F_0^{22}+F_0^{33})f_1 -2F_0^{21}f_2-F_1^{31}f_3=\lambda_{11}f_1+\lambda_{21}f_2,$$

$$-f_2''+2(-5/r+2F_0^{11}+F_0^{22}+F_0^{33})f_2 -2F_0^{12}f_1-F_1^{32}f_3=\lambda_{12}f_1+\lambda_{22}f_2,$$

$$-f_3''+2(-5/r+1/r^2+2F_0^{11}+2F_0^{22})f_3 -2F_1^{13}f_1-2F_1^{23}f_2=2\lambda_{33}f_3.$$

The notation is the same as used previously.[9] In the solution of the equations the exchange terms involving F_l^{ik} and λ_{ik}, where $i\neq k$, were neglected. All equations were put in the form

$$f''+[\epsilon-2v+l(l+1)/r^2]f=0,$$

where ϵ is the energy parameter (expressed as a multiple of the ionization potential of hydrogen) and $-v$ is the potential of the central field acting on the electron.

The values obtained for ϵ were 15.50, 0.910 and 0.446 for the $1s$, $2s$, and $2p$ electrons, respectively. The normalized functions f_1, f_2, and f_3 are given in Table I.

Table I. *Normalized radial functions for boron.*

r	f_1	f_2	f_3	r	f_1	f_2	f_3
0	0	0	0	1.5	0.037	−0.716	0.564
				1.6	.025	−.720	.570
0.01	0.196	0.043	0	1.7	.018	−.716	.573
.02	.374	.082	0.001	1.8	.012	−.707	.574
.03	.535	.117	.002	1.9	.008	−.694	.573
.04	.678	.148	.004	2.0	.006	−.676	.570
				2.2	.003	−.633	.560
.06	.922	.201	.008				
.08	1.114	.242	.013	2.4	.001	−.583	.544
.10	1.263	.273	.020	2.6	0	−.532	.524
.12	1.373	.294	.028	2.8		−.478	.503
.14	1.458	.309	.036	3.0		−.428	.481
.16	1.514	.317	.045	3.2		−.381	.456
.18	1.549	.320	.055	3.4		−.336	.431
.20	1.566	.317	.065	3.6		−.296	.405
.22	1.567	.310	.076	3.8		−.259	.379
.24	1.557	.300	.087	4.0		−.227	.355
.26	1.539	.286	.098				
.28	1.507	.271	.109	4.5		−.160	.297
.30	1.472	.253	.121	5.0		−.111	.244
				5.5		−.076	.199
.35	1.365	.200	.152	6.0		−.052	.161
.40	1.243	.139	.183	6.5		−.035	.129
.45	1.112	.074	.214	7.0		−.023	.120
.50	0.985	.006	.245	7.5		−.016	.080
.55	.865	−.061	.275	8.0		−.010	.063
.60	.754	−.127	.303	8.5		−.007	.049
.65	.653	−.191	.328	9.0		−.004	.038
.70	.563	−.252	.353				
.8	.416	−.364	.399	10.		−.002	.023
.9	.299	−.458	.440	11.		−.001	.014
1.0	.214	−.537	.473	12.		0	.008
1.1	.152	−.599	.500	13.			.005
1.2	.107	−.647	.523	14.			.003
1.3	.075	−.681	.542	15.			.001
1.4	.053	−.704	.555	16.			0

Interpolated Functions for Normal Carbon and Nitrogen

In order to compare a single-electron wave function for boron, say $P(2s)$, with a similar wave function for neon, it has proved very convenient to stretch both abscissa and ordinate, so that the new radius is a constant multiple of the old radius. The stretching factor for the ordinates is determined so that the wave function remains normalized. That is, if $\int_0^\infty f^2dr=1$, then the factor c is chosen to satisfy $\int_0^\infty (cf)^2d(ar)=1$, where a is the stretching factor for the radius. Solving, $c^2=1/a$.

If r_m denote the abscissa of a maximum, then it is found that $1/r_m$, which is proportional to the effective nuclear charge near the maximum, is

Table II. *Reciprocals of positions of maxima.*

	$1s$	$2s$ inner	$2s$ outer	$2p$
Ne	9.81 (9.80)	12.03 (12.05)	1.407 (1.406)	1.572 (1.563)
F	8.79 (8.77)	10.74 (10.75)	1.251 (1.251)	1.374 (1.379)
O	7.77 (7.77)	9.45 (9.43)	1.095 (1.093)	1.176 (1.177)
C	6.75	8.16	0.939	0.978
N	6.63	6.87	.773	.780
B	4.71 (4.72)	5.58 (5.59)	.627 (0.625)	.582 (0.582)

[9] F. W. Brown, Phys. Rev. **44**, 214 (1933).

[10] See reference (9), Eq. (24).

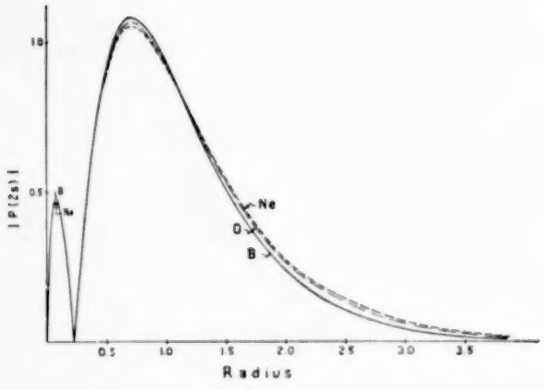

FIG. 1.

very closely a linear function of the atomic number. This is shown in Table II. The numbers in parentheses correspond to the Hartree functions already calculated, and the other numbers are those (read from a straight line graph) used to determine the stretching factors for interpolating.

On plotting the functions for B, O, and F stretched to correspond to Ne, fitting the positions of the maxima from the straight line graph, one finds that the function curves have nearly the same shape, and are such that oxygen comes between boron and fluorine (with the spacing between oxygen and boron about three times that between O and F). For the 1*s* and 2*s* functions neon also comes in the right order with about the right spacing, but for the 2*p* functions neon lies out of order, which is probably to be expected since the position of the maximum for Ne is not on the straight line. Plots of some of the stretched 2*s* and 2*p* functions are shown in Figs. 1 and 2. The radius is measured in atomic units.

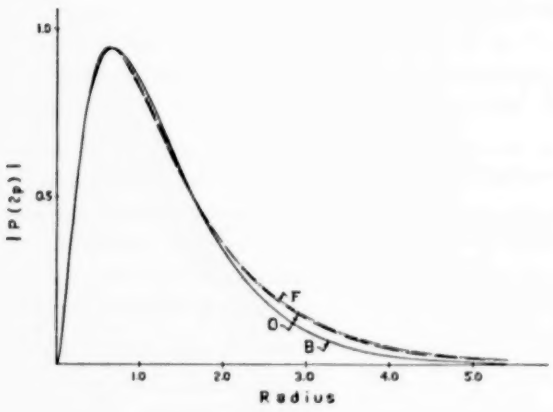

FIG. 2.

TABLE III. *Normalized radial functions for carbon and nitrogen.*

	C			N		
r	f_1	f_2	f_3	f_1	f_2	f_3
0	0	0	0	0	0	0
0.01	0.255	0.056	0.001	0.325	0.072	0.002
.02	.490	.109	.003	.613	.137	.004
.03	.694	.155	.004	.858	.193	.006
.04	.867	.195	.006	1.065	.240	.013
.06	1.154	.257	.014	1.385	.310	.024
.08	1.370	.301	.025	1.609	.355	.042
.10	1.517	.331	.038	1.761	.381	.059
.12	1.629	.348	.051	1.846	.390	.084
.14	1.691	.356	.066	1.877	.384	.107
.16	1.721	.354	.082	1.878	.367	.132
.18	1.728	.343	.100	1.851	.343	.158
.20	1.715	.328	.118	1.799	.310	.186
.22	1.688	.309	.137	1.728	.274	.213
.24	1.644	.285	.156	1.653	.233	.241
.26	1.585	.257	.175	1.569	.187	.266
.28	1.530	.227	.195	1.484	.141	.294
.30	1.465	.194	.214	1.393	.094	.320
.35	1.299	.104	.261	1.177	−.035	.386
.40	1.123	.009	.307	0.975	−.155	.448
.45	0.963	−.083	.351	.789	−.271	.498
.50	.814	−.176	.394	.638	−.381	.544
.55	.681	−.263	.433	.510	−.476	.585
.60	.569	−.340	.467	.409	−.560	.622
.65	.474	−.412	.497	.320	−.637	.653
.70	.391	−.484	.523	.249	−.697	.680
.8	.260	−.597	.572	.149	−.788	.717
.9	.170	−.681	.611	.091	−.842	.736
1.0	.111	−.737	.636	.054	−.868	.744
1.1	.073	−.775	.651	.032	−.871	.743
1.2	.046	−.795	.661	.018	−.855	.734
1.3	.029	−.799	.664	.012	−.828	.720
1.4	.018	−.791	.662	.007	−.791	.701
1.5	.012	−.774	.657	.004	−.751	.677
1.6	.008	−.749	.648	.002	−.707	.653
1.7	.005	−.721	.637	.001	−.662	.627
1.8	.003	−.690	.623	0	−.617	.603
1.9	.002	−.657	.606		−.570	.577
2.0	.001	−.623	.590		−.525	.550
2.2	0	−.551	.555		−.445	.498
2.4		−.481	.517		−.374	.447
2.6		−.417	.480		−.309	.401
2.8		−.360	.442		−.255	.357
3.0		−.309	.404		−.209	.318
3.2		−.261	.369		−.172	.280
3.4		−.221	.336		−.141	.250
3.6		−.187	.307		−.114	.221
3.8		−.158	.278		−.093	.195
4.0		−.132	.250		−.076	.171
4.5		−.086	.195		−.044	.123
5.0		−.054	.149		−.025	.089
5.5		−.033	.112		−.015	.065
6.0		−.020	.085		−.010	.046
6.5		−.013	.063		−.006	.033
7.0		−.007	.047		−.002	.024
8.		−.004	.027		−.001	.013
9.		−.002	.015		0	.006
10.		−.001	.008			.002
11.		0	.004			.001
12.			.002			0
13.			.001			
14.			0			

Since these functions lie in the correct order one can interpolate to get the stretched functions for N and C. From the stretched functions one easily obtains the normal functions, using stretching factors from Table II. The tabulated values of these functions are given in Table III.

These functions are probably almost as accurate as would be obtained by carrying out the Hartree process. The maximum possible error in the interpolation is estimated to be 0.005.

For the convenience of those engaged in hyperfine structure calculations the values of f_1/r and f_2/r at $r=0$ have been tabulated for B, F, and Ne in Table IV.

TABLE IV. *Values of f_1/r and f_2/r at $r=0$.*

Atom	f_1/r	f_2/r
B	20.6	4.53
F	51.8	11.74
Ne	60.9	13.72

CONCLUSION

As a result of the present work accurate single-electron wave functions are now available for all of the normal atoms up to and including neon.[3, 11]

It seems probable that interpolation methods such as we have used will prove to have a fairly wide range of applicability, enabling one to obtain single-electron wave functions with a minimum of effort.

[11] Slater (reference 9) lists Be as one of the atoms for which Hartree wave functions have been determined. Professor P. M. Morse has also informed one of us (J.H.B.) that, by means of a variational method, he has obtained accurate wave functions for normal lithium.

Density of Energy in the Universe

S. A. KORFF,* *Mount Wilson Observatory and California Institute of Technology, Pasadena, California*

(Received June 22, 1933)

The density of radiant energy given off by stars and luminous matter in the universe is computed and is found to be 6.91×10^{-3} erg/sq. cm/sec. as received by the earth. In interstellar space, 10^6 light years from the nearest spiral nebula, the energy density will be between 2×10^{-5} and 2×10^{-4} erg, the former value representing energy from all known nebulae and the latter an extrapolation to the 25th magnitude, further extrapolation being forbidden by red-shift considerations. The latter figures are considerably smaller than the cosmic-ray energy densities found by Millikan and others.

IT is interesting to consider the available data on the density of energy in the universe. We shall examine first the energy in the form of "starlight."

Pettit and Nicholson[1] have determined the amount of energy received from a zero magnitude star of spectral type AO, reduced to the zenith at Mount Wilson (elev. 5800 ft). They find it to be 17.3×10^{-12} calorie/sq. cm/min. This figure is believed to be accurate to 4 percent. If we take the total number of stars in the sky as equivalent to 1092 first magnitude stars, we shall receive from these 5.24×10^{-3} erg/sq. cm/sec. This simple calculation assumes (a) Seares's star counts, and (b) that all of the "equivalent first magnitude" stars are of emissivity corresponding to type AO. We shall examine these two assumptions in turn, and correct for atmospheric extinction.

The figure 1092 equivalent first magnitude stars is due to the star counts of Seares,[2] who by the "selected areas" method has evaluated the total number of stars in the sky of various magnitude down to the 19th, and gives estimates for 20th and 21st magnitudes. Since over three-quarters of the total starlight comes from stars brighter than the 15th magnitude, changes in the counts of stars of fainter magnitudes which the telescopes of the future may bring out, will not alter this figure by a large factor. From a study of the total light of the night sky, corrected for atmospheric (auroral) radiation, scattering and zodiacal light, Van Rhijn[3] finds the energy incident upon the earth to be that corresponding to 1440 stars of first magnitude (accuracy 10 percent). This value is larger than the 1092 generally given, since it includes light from stars fainter than 20th magnitude and light from various types of nebulae. We may call this "total energy" and let the figure 1092 correspond to "known starlight." Yntema similarly finds from the total energy 1350 first magnitude stars. The accuracy of these two values, however, is not nearly as good as that of Seares's 1092.

If we assume Van Rhijn's value of the total stars as equivalent to 1440 of first magnitude, we receive from these 6.91×10^{-3} erg; while Regner[4] calculates from Eddington's data on the density per cc of radiant energy 5.75×10^{-3}. In view of the inaccuracies affecting these determinations, the two figures may be considered as in agreement.

We shall next show that Pettit and Nicholson's value and the "equivalent first magnitude" is indeed typical and representative for stars of various spectral classes. Consider now three most general types of stars (1) hot stars, surface temperature 23,000–11,000°, spectral types O to AO; (2) moderate stars, temperatures 11,000 to 5500°, types AO–GO, and (3) cool stars, 5500 to 2000° and types GO to M. Types *N*, *R* and *S* are very rare, faint and neglected. The Henry Draper

* National Research Fellow.

[1] E. Pettit and S. B. Nicholson, Mt. Wilson Contributions, 369; Astrophys. J. **68**, 279 (1928).

[2] F. H. Seares, P. J. Van Rhijn, M. C. Joyner and M. L. Richmond, Mt. Wilson Contributions, 301; Astrophys. J. **62**, 373 (1925).

[3] Van Rhijn, Groningen Publ. 31, 1921.

[4] E. Regner, Zeits. f. Physik **80**, 666 (1933). A. S. Eddington, *Internal Constitution of the Stars.*

Catalog[5] contains 225,000 stars of magnitudes brighter than 9.5. These stars are collected in the groups according to the general spectral type above, and are listed in Table I. It is obvious that the total amount of light (L) received from any group of stars is given by the equation

$$L=1.205\times10^{-5}N/2.512(\exp)(m_v+H+\Delta m_r),$$

where N is the number of stars in that group (from Table I), m_v the photovisual magnitude of the star, H the heat index and Δm_r is the difference between bolometric and visual magnitude. (The factor H takes care of the lack of visual sensitivity in the red, while Δm_r is the correction for the absorption of the intense violet of the hotter and red of the cooler stars, and represents the reduction to no atmosphere.) The numerical factor is Pettit's energy determination reduced to ergs/sq. cm/sec. The total energy obtained in this way for all stars in the Henry Draper Catalog is 1.87×10^{-3} erg. The total of all stars here listed is equivalent to about 148 of zero magnitude. The energy as computed in the second paragraph of this note of 148 stars of zero magnitude is 1.78×10^{-3} erg. It is clear, then, that the estimate of type AO as typical is reasonably accurate, and that excessive radiation from very hot stars compensates approximately for feeble radiation from cooler ones. Thus the total energy received from a star of type AO is not very different from the amount received from a star of type F or G, commonly considered to represent the "average spectral type."

TABLE I.

Spectral type	N Br than 6.25	6.25–8.25	8.25–9.25	Ftr. than 9.25	H	Δm_r
(1) O to AO	2009	10,730	16,647	17,802	0.01	1.9
(2) AO to GO	2064	18,457	34,838	32,944	0.1	0.65
(3) GO to M8	2522	22,729	36,414	25,407	1.2	0.5

Table of stars in various spectral classes from Draper Catalog, and heat indices H and corrections to no atmosphere Δm_r. The value of Δm_r becomes large for hot stars (2.8 for BO) and has a minimum (0.41) at G5.

Millikan[6] finds the density of cosmic radiation energy to be 3.2×10^{-3} erg/sq. cm/sec. This is a little more than half the figure for starlight. The solar system, however, occupies a unique position since it is within a vast stellar system or huge spiral nebula. If we consider the amount of radiation crossing a square centimeter area at a distance of 8.7×10^5 light years from a typical nebula, the Andromeda, the integrated total luminosity of which[7] is equal to that of a fourth magnitude star, we obtain from it, crossing a square centimeter in a second 3.0×10^{-7} erg.

According to Hubble[8] nebulae occur in space with a mean density of 1 per each 3×10^{16} cubic parsec. This corresponds to a linear distance between cube centers of very nearly 10^6 light years. Now this latter distance is only slightly in excess of the distance between our own system and the Andromeda nebula, and hence the energy received from the Andromeda nebula will be typical of that received at a mean distance in space of 10^6 light years from the nearest nebula.

The number of nebulae is given by the equation

$$\log N_m=0.6\,m-9.2,$$

where N_m is the number of nebulae of magnitude m. It follows at once that the nebulae brighter than the 20.3rd magnitude give an energy equal to about 1.7 stars of zero magnitude; while the energy at limiting magnitude 25.3 will be ten times as great. Consequently the total energy crossing a square centimeter at a typical point in space 10^6 light years from the nearest nebula will be 2.05×10^{-5} ergs/sq. cm/sec. received from all known nebulae, up to the present limit of the 100-inch telescope; while an extrapolation to the 25th magnitude yields a tenfold higher value. Further extrapolation is not warranted for presumably the red-shift will limit the number of nebulae and energy received from them.

The value 2×10^{-5} is more representative of the amount of radiant stellar energy in space, at a vast distance from nebulae or star clouds. If, as Millikan has emphasized, cosmic rays are of the same energy-density in distant space as here, then cosmic radiation is by far the most preponderant energy in the universe.

[5] Harvard Observatory Bulletin 226.

[6] R. A. Millikan and G. H. Cameron, Phys. Rev. **31**, 930 (1929). See especially preceding paper.

[7] Russell, Dugan and Stewart, *Astronomy*, Vol. **2**, p. 854.

[8] E. Hubble and M. L. Humason, Mt. Wilson Contributions, 427; Astrophys. J. **74**, 43 (1931).

Some Remarks on the Frequency Dependence of Superconductivity and Ferromagnetism

RAYMUND SÄNGER,* *Norman Bridge Laboratory of Physics, California Institute of Technology*

(Received April 24, 1933)

An attempt is made to explain the frequency dependence of superconductivity and ferromagnetism as a further consequence of the skin effect, assuming the existence of a surface layer which shows neither superconductive nor ferromagnetic properties. The existence of this surface layer may be in some way connected with the results of recent theoretical investigations on crystal structure involved in the ideas of Epstein on ferromagnetism and in Zwicky's conception of a secondary structure.

I. INTRODUCTION

RECENTLY Wien[1] explained the discrepancy between the values of ferromagnetic permeability of iron computed on the one hand from the resistance of a wire and on the other hand from its inner self-induction at very high frequency. He explains this discrepancy as due to the fact that in the first case we are dealing with electric field lines, while in the second case with magnetic field lines, the latter passing through parts of the wire lying much closer to the surface than the electric lines. Wien also conjectured that the entire phenomenon of the vanishing of ferromagnetic properties at a wave-length of a few centimeters could be only a further consequence of the skin effect. The actual vanishing of ferromagnetic properties at these wave-lengths would also be difficult to understand from a modern theoretical point of view as included in Heisenberg's theory and more positively in the complemental considerations of Epstein's[2] work on ferromagnetism.

Very similar are the facts about the frequency dependence of superconductivity as observed by McLennan[3] and his coworkers, who found that superconductivity becomes affected at a frequency of about 10^7 sec.$^{-1}$. We will therefore restart the problem commenced by Wien, modifying the picture a bit by assuming simply that a conductor possesses a surface layer which shows neither superconductivity nor ferromagnetism. Accordingly we study the ohmic resistance and the inner self-induction of a superconducting or ferromagnetic conductor, in the form of a straight wire, for very high frequency.

In order to calculate for high frequency ν the ohmic resistance R' and the inner self-induction L_i per unit of length for a straight wire possessing a surface layer of different electric and magnetic properties from those of the core of the wire, we may use the results of Försterling's[4] theory concerning the propagation of electric waves along a straight metallic wire surrounded by a conducting cylindrical shell. If the penetration depth is small compared with the radius r of the wire (in other words the usual critical quantity $\kappa=\pi r(\mu\sigma\nu)^{\frac{1}{2}}$ for the skin effect is greater than 1), Försterling finds[5]

$$R'=\frac{1}{c_0 r}\left(\frac{\mu_2}{\sigma_2}\nu\right)^{\frac{1}{2}}(a-b);$$
$$\nu L_i=\frac{c_0}{2\pi r}\left(\frac{\mu_2}{\sigma_2}\nu\right)^{\frac{1}{2}}(a+b), \tag{1}$$

where

$$a=\frac{1-\Delta^2 e^{-2\eta}}{1+\Delta^2 e^{-2\eta}-2\Delta e^{-\eta}\cos\eta};$$

* International Research Fellow.

[1] M. Wien, Ann. d. Physik **8**, 899 (1931), also R. Michels, Ann. d. Physik **8**, 877 (1931).

[2] P. S. Epstein, Phys. Rev. **41**, 91 (1932).

[3] J. C. McLennan, A. C. Burton, A. Pitt and J. O. Wilhelm, Phil. Mag. **12**, 707 (1931); Proc. Roy. Soc. London **A136**, 52 (1932); J. C. McLennan, Trans. Roy. Soc. Canada **25** III, 191 (1931); Proc. Roy. Inst. Great Brit. **27** III, 446 (1932).

[4] K. Försterling, Ann. d. Physik **72**, 30 (1923).

[5] All equations in the present paper are written in Gauss' units.

$$b=\frac{-2\Delta e^{-\eta}\sin\eta}{1+\Delta^2e^{-2\eta}-2\Delta e^{-\eta}\cos\eta}$$

and

$$\Delta=\frac{(\sigma_2/\mu_2)^{\frac{1}{2}}-(\sigma_3/\mu_3)^{\frac{1}{2}}}{(\sigma_2/\mu_2)^{\frac{1}{2}}+(\sigma_3/\mu_3)^{\frac{1}{2}}};\quad \eta=\frac{4\pi}{c_0}l(\mu_2\sigma_2\nu)^{\frac{1}{2}}.$$

Here σ_3 and μ_3 denote respectively the static conductivity and the permeability of the wire, σ_2 and μ_2 the same quantities for the shell, i.e., the surface layer in our case. (σ_1 and μ_1 were used by Försterling for the surrounding medium which is air in our case) l denotes the thickness of the layer and c_0 the velocity of light.

If now we treat η as small and develop $a+b$ and $a-b$ in powers of η introducing the quantity $q=(\sigma_2\mu_3/\sigma_3\mu_2)^{\frac{1}{2}}$, we obtain

$$\begin{aligned}a-b=&\,q-(1/2)q(q^2-1)\eta^2\\&+(1/6)(q^2-1)(3q^2-1)\eta^3\\&-(1/12)q(q^2-1)(3q^2-2)\eta^4\\&+(1/360)q(q^2-1)(45q^4-60q^2+17)\eta^6\\&-(1/2520)(q^2-1)(315q^6-525q^4\\&\qquad+231q^2-17)\eta^7+0\cdot\eta^8\cdots,\end{aligned}\tag{2}$$

$$\begin{aligned}a+b=&\,q-(q^2-1)\eta+(1/2)q(q^2-1)\eta^2\\&+(1/12)q(q^2-1)(3q^2-2)\eta^4\\&+(1/60)(q^2-1)(15q^4-15q^2+2)\eta^5\\&-(1/360)q(q^2-1)(45q^4-60q^2+17)\eta^6\\&\qquad+0\cdot\eta^7\cdots.\end{aligned}$$

If the properties of the surface layer are the same as those of the core, in other words, if we are dealing with a uniform wire, q assumes the value 1 and Eqs. (1), as we have to expect, reduce to the Rayleigh formulas

$$R'=\frac{1}{c_0r}\left(\frac{\mu_3}{\sigma_3}\nu\right)^{\frac{1}{2}};\quad \nu L_i=\frac{c_0}{2\pi r}\left(\frac{\mu_3}{\sigma_3}\nu\right)^{\frac{1}{2}}.\tag{3}$$

We are led to the same formulas even in the case of a very thin surface layer provided the frequency is not too high, since the expansions of $a\pm b$ can be cut off at the first term q, especially if we consider ferromagnetic conductors.

Due to the fact that the expansion for $a-b$ shows no linear term in η, in contradistinction to $a+b$, the inner self-induction of the wire will be much sooner affected by the frequency because of the presence of a surface layer, than the resistance. This is just the circumstance used in the above-mentioned work of Wien for his explanation of the discrepancy in the values of μ computed on the one hand from the self-induction and, on the other hand from the ohmic resistance.

II. Frequency Dependence of Superconductivity

In case the core of the wire is superconductive but the surface layer shows usual conductivity, q becomes equal to zero, making the terms of order less than three vanish in the expansion for $a-b$. Setting the permeability equal to 1 we find for the ohmic resistance per unit of length

$$R_s'=\frac{1}{c_0r}\left(\frac{\nu}{\sigma_2}\right)^{\frac{1}{2}}\frac{\eta^3}{6}\left[1-\frac{17}{420}\eta^4-\frac{1}{504}\eta^6\cdots\right],\tag{4}$$

where now $\eta=4\pi l(\sigma_2\nu)^{\frac{1}{2}}/c_0$. Neglecting higher orders we may write therefore[6]

$$R_s'=\frac{32}{3}\frac{\pi^3}{c_0^4}\frac{l^3}{r}\sigma_2\nu^2.\tag{5}$$

If we now introduce the resistance R_0' of the wire at the temperature 0°C, using the simple Rayleigh formula $R_0'=(\nu/\sigma_0)^{\frac{1}{2}}/c_0r$, we have for the ratio R_s'/R_0' of the resistances for the same frequency ν (σ_0 = conductivity at 0°)

$$\frac{R_s'}{R_0'}=\frac{32}{3}\frac{\pi^3}{c_0^3}l^3\sigma_2\sigma_0^{\frac{1}{2}}\nu^{\frac{1}{2}}.\tag{6}$$

The use of the Rayleigh formula for R_0' is justified since it is reasonable to assume in the case of ordinary conductivity a thickness l of the layer which is smaller than about 10^{-6} cm corresponding to a depth in which the entire crystal structure is already established. If so, by formulas (1) and (2) no influence of the layer will occur up to a frequency sensibly higher than 10^{10} sec.$^{-1}$. It may be noticed that (6) shows no dependence of the ratio R_s'/R_0' on the radius of the wire in agreement with the experimental results of McLennan on tin, investigated for different radii.

We must now state something about the conductivity σ_2 of the surface layer at temperatures sufficiently low for the core to be superconduc-

[6] For the inner self-induction we would obtain $L_i=2l/r$.

tive. We will assume that the conductivity σ_2 is the same as the conductivity of the core would be had no superconductivity occurred and write in a convenient form

$$\sigma_2 = R_0\sigma_0/R, \tag{7}$$

where R_0/R means the ratio of the resistances for direct current, R_0 being the resistance at the temperature of 0°C, R the resistance at the temperature at which the wire usually exhibits superconductivity; but now under the condition this superconductivity does not occur. Over the whole temperature range of superconductivity this ratio R_0/R is practically constant, since there is practically no change in R. The fact that the superconducting state is destroyed by a sufficiently high magnetic field would allow us to determine very accurate values of R_0/R,[7] but sufficiently accurate values can be easily estimated by using ordinary measurements of the conductivity at low temperatures without any applied magnetic field. Our statement about the conductivity σ_2 of the surface layer already implies that this layer would probably be entirely different from those surface layers commonly adopted in the theory of crystal structure.

Substituting (7) in Eq. (6) we obtain finally for the ratio of the high frequency resistances

$$\frac{R_s'}{R_0'} = \frac{32}{3}\frac{\pi^3}{c_0^3} l^3 \frac{R_0}{R}\sigma_0^{\frac{1}{2}}\nu^{\frac{1}{2}} = a l^3 \nu^{\frac{1}{2}}, \tag{8}$$

where a represents a constant factor characterizing the metal used. Using the values $5.04\cdot10^{-5}$ $7.7\cdot10^{-5}$ and $5.7\cdot10^{-5}$ e.m.u. for the conductivities σ_0 of the three superconductive metals, lead, tin and tantalum respectively and the corresponding values $9.6\cdot10^{-4}$, $7.9\cdot10^{-4}$ and 720.10^{-4} for the ratio R/R_0,[8] we find for the constant factor a:

$$a = 0.155 \text{ for lead} \qquad a = 0.283 \text{ for tin}$$
$$a = 0.002 \text{ for tantalum.}$$

Eq. (8) shows that the ratio R_s'/R_0' depends on the third power of the thickness of the surface layer, whereas the frequency enters to the 3/2 power.

In order to understand the rôle played by the surface layer in the phenomenon of the frequency dependence of superconductivity, we have to establish some connection with the experiments of McLennan and his coworkers. First of all they find that the temperature at which the high frequency resistance begins to vanish ("starting point") is a little lower than the transition temperature for direct current, and this difference seems to be larger for higher frequencies. The experimental values of R_s'/R_0' at the starting point are about 0.07 for lead, 0.095 for tin and 0.24 for tantalum. If we now make the existence of a non-superconductive layer responsible for the fact that the resistance has not already vanished although the temperature is lower than the ordinary transition point, we can ask for the thickness l that this layer must have by substituting these values for R_s'/R_0' into the formula (8). Since the resulting values of l are only of approximate significance, we set for simplicity R_s'/R_0' equal to 0.1 for lead and tin, 0.2 for tantalum. We give the resulting values of l in Table I; together with those values of l which would result from using the value $R_s'/R_0' = 0.01$; this value represents about the limit of experimental information in the method used by the above-mentioned authors. These letter values of l may be brought in some way into connection with the "vanishing point," namely the temperature low enough, the high frequency resistance seems also to have vanished completely. In the case of tin, where measurements have been performed for different frequency we also give the corresponding values of l separately. We do not conceal that some values of l (indicated by brackets) correspond to values of η so large that terms of higher order in the expan-

TABLE I.

Substance	Transition point for d.c. (°A)	Frequency ν	*Starting Values* Temp. (°A)	Corresponding value of l (cm)	*Vanishing Values* Temp. (°A)	Corresponding value of l (cm)
Lead	7.26	$1.10\cdot10^7$	<7.0	$(2.5)\cdot10^{-4}$	—	$1.2\cdot10^{-4}$
Tin	3.71	$0.208\cdot10^7$	3.72	(5) "	3.66	1.2 "
	(starting value 3.77)	1.10 "	3.66	(2.1) "	3.61	1.0 "
		1.61 "	3.65	(1.7) "	3.59	0.8_2 "
Tantalum	4.34	1.14 "	4.22	14. "	4.13	5 "

[7] W. Meissner, Ann. d. Physik **13**, 641 (1932). Resistance of lead in a magnetic field below the transition temperature.

[8] Value for lead, W. Meissner;[7] values for tin and tantalum, W. Meissner, Phys. Zeits. **26**, 689 (1925); McLennan, Proc. Roy. Inst. Great Brit. **27**, III, 449 (1932).

sion for $a-b$ should be taken into account, but we do not believe that this would effect noticeably our subsequent discussion.

At first glance the thickness of the surface layer seems to be very large, moreover this thickness appears to depend on the temperature. This latter effect we would explain perhaps by assuming that at a lower temperature more parts of the outer regions of the wire join the core in passing over into the superconducting state. From formula (8) we get smaller values of l for higher frequencies, thus requiring lower transition temperatures for higher frequencies, as the experiments on tin really seem to indicate. In this connection we notice that the "starting" value of l at the frequency $1.61\cdot 10^7$ lies fairly close to the "vanishing" value of l at the frequency $0.208\cdot 10^7$, as we might expect since the corresponding values of the temperature are the same. Our whole treatment of the problem does not permit a too detailed verification (for example, our calculations are made for a straight wire, whereas the experiments were performed with a coiled wire); moreover, the results of the experiments are hardly definite, and little attention was paid to the quality of the surfaces of the wires. Therefore we only can say it is possible in principle to explain the phenomenon of the frequency dependence of superconductivity by the existence of a surface layer, although the required thickness of these layers are very large; at the end of the paper we shall see some reason for such a thick layer.

III. Frequency Dependence of Ferromagnetism

In a similar way we assume that in the case of ferromagnetism the core of the wire will always show its full ferromagnetic properties (μ_3), but that the surface layer never exhibits such properties. The electric conductivity of the surface layer we assume to be the same as that of the coil, so that we can set

$$\mu_2=1;\quad \sigma_2=\sigma_3=\sigma$$

and consequently

$$q=\mu_3^{\frac{1}{2}};\quad \eta=4\pi l(\sigma\nu)^{\frac{1}{2}}/c_0.$$

If for simplicity we neglect 1 in the presence of $q^2=\mu_3$, which is certainly justified in the case of iron, we have for the expansions of $a\pm b$

$$\begin{aligned} a-b&=q\left[1-\frac{q^2}{2}\eta^2+\frac{q^3}{2}\eta^3-\frac{q^4}{4}\eta^4+\frac{q^6}{8}\eta^6\cdots\right]\\ a+b&=q\left[1-q\eta+\frac{q^2}{2}\eta^2+\frac{q^4}{4}\eta^4+\frac{q^5}{4}\eta^5-\frac{q^6}{8}\eta^6\cdots\right]. \end{aligned} \tag{9}$$

Substituting these expansions into (1) we find for the high frequency resistance R' and the inner self-induction L_i of the ferromagnetic wire:

$$\begin{aligned} R'&=\frac{1}{c_0 r}\left(\frac{\mu_3}{\sigma}\nu\right)^{\frac{1}{2}}\left[1-\frac{q^2}{2}\eta^2+\frac{q^3}{2}\eta^3\cdots\right],\\ \nu L_i&=\frac{c_0}{2\pi r}\left(\frac{\mu_3}{\sigma}\nu\right)^{\frac{1}{2}}\left[1-q\eta+\frac{q^2}{2}\eta^2\cdots\right]. \end{aligned} \tag{10}$$

If now we denote by μ_r and μ_s the permeability of the wire computed, as is customary, by the ordinary Rayleigh formulas from the high frequency resistance and the inductance respectively, we have

$$R'=\frac{1}{c_0 r}\left(\frac{\mu_r}{\sigma}\nu\right)^{\frac{1}{2}}\quad\text{and}\quad \nu L_i=\frac{c_0}{2\pi r}\left(\frac{\mu_s}{\sigma}\nu\right)^{\frac{1}{2}}, \tag{11}$$

combining (10) and (11) we finally obtain the following equations expressing μ_r and μ_s in terms of μ_3,

$$\begin{aligned} \left(\frac{\mu_r}{\mu_3}\right)^{\frac{1}{2}}&=1-\frac{q^2}{2}\eta^2+\frac{q^3}{2}\eta^3\cdots\\ \left(\frac{\mu_s}{\mu_3}\right)^{\frac{1}{2}}&=1-q\eta+\frac{q^2}{2}\eta^2\cdots. \end{aligned} \tag{12}$$

In the case of iron we shall write $\eta=0.126\, l\nu^{\frac{1}{2}}$, introducing the value of conductivity $\sigma_0=1.0\cdot 10^{-4}$ e.m.u. for pure iron. In order to compare our formulas (12) with the experimental results for high frequency, some uncertainty arises as to the value to be taken for the permeability μ_3 of the core. It is reasonable to use the static initial value of μ although this value depends highly on the kind of iron used.

Very recently Hoag and Jones[9] have published measurements of the permeability μ_s of iron for very high frequency ($\lambda=64$ cm and lower). In

[9] G. Barton Hoag and Haydn Jones, Phys. Rev. **42**, 571 (1932).

their paper they illustrate (Fig. 1) the experimental work done in the last few years on the frequency dependence of the permeability of iron in the region from several hundreds of meters down to a few centimeters. Even if we overlook those results which show some peculiar behavior, there is no good agreement among the different observers; we may only say that the results seem to indicate that at a wave-length of the order of 1 meter, the diminution of the permeabilities μ_s and μ_r occurs with increasing frequency, and that μ_s starts to diminish earlier than μ_r in accordance with (12).

The value $\mu_s = 30$ given by Hoag and Jones for a wave-length of about 60 cm is already too small for practical use in the expansion formula (12). If we use Michels[1] value $\mu_s = 59.3$ for $\lambda = 350$ cm and use, as Wien did in his explanation of the phenomenon, the value 75.5 for μ_3, we are led to the value $l = 1.2 \cdot 10^{-5}$ cm for the thickness of the surface layer, with the corresponding value $\mu_r = 74.3$, whereas Michels finds $\mu_r = 73$. Applying this value for l to the case of the wave-length $\lambda = 64$ cm we obtain from (12) $\mu_s = 42$, a value which is, as we have to expect, higher than that observed by Hoag and Jones. We intend to discuss the whole phenomenon in more detail in a forthcoming paper dealing with measurements of the permeability of iron at very high frequencies, and conclude here with the statement that our explanation of the diminution of μ_s and μ_r, in the region $\lambda = 1$ meter, leads to a thickness of the surface layer of the ferromagnetic wire of the order of 10^{-5} cm.

IV. Some Remarks about the Surface Layer

The interpretation of ferromagnetism by means of the theory of quanta seems to lead to the conception of a block structure of the ferromagnetic crystals particularly in the paper of Epstein. In the case of a cubical block the edge of the elementary cube would be of the order of 10^{-6} or 10^{-5} cm (roughly in accord with the thickness of the surface layer found above for a ferromagnetic wire). If this is so, and if on account of the skin effect the electric and magnetic field lines are so closely gathered at the surface of the wire that the thickness of their range is comparable with the size of the elementary block we might conceivably expect phenomena as above described, or, perhaps better interpreted, the ferromagnetic wire possesses a surface layer which never can show ferromagnetic properties. This also gives a principle reason for the negative character of the Hagen-Ruben's experiments on the reflecting power of ferromagnetic mirrors in the far infrared, which show no typical difference between ferromagnetic and nonferromagnetic substances. In the case of superconductors we may suppose that the circumstances at the surface are in some way similar; pointing to an explanation of the frequency dependence of superconductivity discussed above.[10]

If we state that the existence of a block structure may be responsible for the appearance of a nonsuperconductive or ferromagnetic shell this may be understood in about the following way. The saturated electrically or magnetically polarized blocks which lie in the immediate neighborhood of the surface of the wire can produce surface charges which may react on these blocks by their depolarizing field in such a way that the preliminary conditions for superconductivity or ferromagnetism are disturbed and hence the wire would be represented in first approximation by a superconductive or ferromagnetic core surrounded by a surface layer which can exhibit neither superconductive nor ferromagnetic properties. The thickness of these surface layers may be conceivably of the order of one or several block edges.

The influence of the magnetic field due to the current has been neglected completely in our analysis. This is permissible, as we only want to see in a general way if the frequency dependence of superconductivity could be explained by the existence of a nonsuperconductive shell, and because the present experimental data do not allow a too refined treatment. Very recently Silsbee, Scott, Brickwedde and Cook[11] published their preliminary experimental results regarding the transition temperatures corresponding to various definite values of the current and of the frequency (0.2 up to 1.2×10^6). Whereas for large

[10] For quantum theoretical interpretation of superconductivity, see R. de Kronig, Zeits. f. Physik **78**, 744 (1932); **80**, 203 (1933).

[11] F. B. Silsbee, R. B. Scott, F. G. Brickwedde and T. W. Cook, Bull. Am. Phys. Soc. **8**, No. 2 (1933); paper 54.

values of the currents the results can be explained on the basis of the skin effect and the variation of the transition point with the magnetic field due to the current, for low values of the currents the measurements indicate the existence of a small difference in the transition points for direct and for high frequency currents. This difference is indeed to be expected on the basis of our model. Further results by the above-mentioned authors probably will clarify the situation.

It may be mentioned here that Breit[12] computed the penetration of a magnetic disturbance into the interior of a superconductive homogeneous wire assuming the resistivity to be only a function of the temperature and of the magnetic field. He found that a wire already should show superconductivity when the current only flows in a sheet of the thickness of atomic distances. This result is not contradictory to our considerations, since it refers translated into terms of our model, only to the mechanism of superconductivity within the superconductive core.

Zwicky,[13] in a series of papers, mostly concerning structure sensitive properties of crystals, suggests the idea of a secondary crystal structure with a corresponding lattice constant of the order of magnitude of about fifty to a thousand atomic distances. According to his model of the crystal both ferromagnetism and superconductivity are cooperative effects of all the atoms or molecules within the elementary cell of the secondary crystal structure; this interpretation is in some accord with the ideas involved in the above-mentioned theory of ferromagnetism. It also may be of some interest to notice that in the particular cases of iron, tin and lead the lattice constants suggested by Zwicky are of the same order of magnitude as those we find for the thickness of the surface layer in the explanation of the frequency effects, the lattice constant of iron being also about 1/10 of those of the two other metals.

If we treat the problem of frequency dependence of ferromagnetism and superconductivity as a further consequence of the skin effect, the wire possessing a surface layer with no ferromagnetic or superconductive properties, and if there are fundamental reasons for the presence of such a layer, then we should expect corresponding phenomena for very thin layers (foils) investigated in static magnetic and electric fields. No little research work has been done in this field during the last years;[14] but at present neither the ferromagnetic nor the superconductive properties of such layers are quite clear. However, the fact seems to stand out, that the difficulties in these investigations arise when we approach thicknesses of layers of the order of magnitude of those discussed above.

The whole treatment of the frequency dependence of ferromagnetism and superconductivity is nothing more than an attempt to explain these phenomena without being forced to assume a change in physical characteristics, such as permeability, which should occur at a relatively low frequency of about 10^7 or 10^8 sec.$^{-1}$.

[12] G. Breit, Proc. Amsterdam Academy **26**, 529 (1923).

[13] F. Zwicky, Phys. Rev. **43**, 270 (1933), where all other references are given.

[14] For the case of superconductivity of very thin layers see: G. T. Silzov, and H. Kamerlingh Onnes, Comm. Leiden 16ª, 180ª, 1925. For the ferromagnetic analogue: L. R. Ingersoll and S. S. de Vinney, Phys. Rev. **26**, 86 (1925); L. R. Ingersoll and T. D. Hanawalt, Phys. Rev. **34**, 972 (1925) and others.

LETTERS TO THE EDITOR

Prompt publication of brief reports of important discoveries in physics may be secured by addressing them to this department. Closing dates for this department are, for the first issue of the month, the twentieth of the preceding month; for the second issue, the fifth of the month. The Board of Editors does not hold itself responsible for the opinions expressed by the correspondents.

On the Theory of Real Crystals

In a letter with the title *The Plasticity of Rocksalt and Its Dependence upon Water*[1] in connection with a communication of Barnes,[2] the experimental possibilities for further examining this effect in rocksalt crystals were discussed. In addition I mentioned that, for explanation, the secondary structure of crystals, postulated by Zwicky, need not be considered, because the existence of a secondary structure in rocksalt at present has no theoretical or experimental support. Zwicky[3] has attempted to defend his theory, although in connection with the effect of water on the plasticity of rocksalt—the actual subject of my letter—he gives no positive relevant arguments.

Zwicky has not denied the absence of *experimental* proofs for the reality of a secondary structure of rocksalt; on this fact agreement seems to be established. On the other hand he rejects the theoretical paper of Orowan[4] cited by me, referring to his German publication which has now appeared.[5] It seems not necessary to discuss this point further, *since Zwicky in his own paper states explicitly, that a proof of a secondary structure of crystals in the mathematical sense does not exist and is hardly possible.*[6] This frank statement in his German publication (March 16, 1933) is very satisfactory for elucidation of things, as in the letter to *The Physical Review* (April 10, 1933),[7] Zwicky does not say anything about it, rather denoting it as a particular superiority, that his theory gives a number of quantitative predictions of the structure-sensitive properties of crystals. Nevertheless according to Zwicky's own judgment above mentioned, these predictions are *theoretically wholly unfounded*—as also previously indicated in my letter.

As there is no possibility for a *theoretical* proof of the existence of a secondary structure, the question arises whether the *experimental* facts, mentioned by Zwicky in favor of this conception, are suitable to offer a conclusive proof. Unfortunately macroscopic crystals are systems including always a considerable number of foreign atoms, by which a reliable extrapolation to the pure crystal is prevented. The significance of this lies in the fact, that secondary planes of pure crystals would never be visible. Thus microscopic facts of various metallic crystals till now explained as secondary planes must be realized by assistance of effects of contamination or plastification. For instance Straumanis has admitted expressly this possibility for his results on zinc crystals, consulted by Zwicky in favor of his theory. Very questionable are also the etching and evaporation observations mentioned by Zwicky; his explanation is by no means the only one.

If it should be experimentally demonstrated that, in the crystals referred to, real regularities exist, their existence *in all other crystals* could never be proved. It is quite possible that here only properties of *certain groups of substances* can be in question, as the structure-sensitive properties examined for these substances (e.g., magnetism) does *not* exist for other crystals at all.

Therefore our own experiments have been undertaken principally on structure-sensitive properties *common to all crystallized matter* as cohesion, plasticity or self-diffusion of crystals. Zwicky has criticized some statements on imperfections of crystals, cohesion and plasticity, which he ascribes to me, but which in that form are not due to me and for which no citations are given. It is a confusion of cohesion and plasticity, when Zwicky asserts that contrary to the "imperfection" theory on increasing the number of imperfection an augmentation of cohesion has been established by experiment. By elimination of the plasticity by help of low temperature the cohesion is in fact *reduced* by chemical or mechanical imperfections, as we have recently demonstrated.[8] As erroneous is the statement of an independency of temperature of the gliding strength in the neighborhood of the melting point. There is no general law of this kind. As far as I see, here can be considered only experiments by Georgieff and Schmid on bismuth crystals.[9] But these measurements were not performed at the elastic limit, but on crystals already stretched plastically to some

[1] A. Smekal, Phys. Rev. **43**, 366 (1933).
[2] R. B. Barnes, Phys. Rev. **43**, 82 (1933).
[3] F. Zwicky, Phys. Rev. **43**, 765 (1933).
[4] E. Orowan, Zeits. f. Physik **79**, 573 (1932).
[5] F. Zwicky, Helv. Phys. Acta **6**, 210 (1933).
[6] F. Zwicky, reference 5, p. 213.
[7] F. Zwicky, Phys. Rev. **43**, 765 (1933).
[8] W. Burgsmüller, Zeits. f. Physik **80**, 199 (1933); **83**, 317 (1933); K. Steiner and W. Burgsmüller, Zeits. f. Physik **83**, 321 (1933); A. Smekal, Zeits. f. Physik **83**, 313 (1933); Phys. Zeits. **34** (1933).
[9] M. Georgieff and E. Schmid, Zeits. f. Physik **36**, 759 (1926).

0.3 percent, which in the neighborhood of the melting point even during the drawing experiment could have intensive recrystallization.

According to Zwicky's theory of secondary structure the low macroscopic gliding strength of the crystals would correspond to the real molecular stresses along that pair of secondary planes operating as gliding plane. In his German publication Zwicky gives a calculation of these stresses for the rocksalt lattice.[10] According to the "imperfection" theory these molecular stresses should be at the elastic limit about 1000 times higher, corresponding to the stresses calculated by the theory of the ideal crystal lattice. Thus, here is given the possibility of an experimental decision between both theories. As we have shown by experiments, the actual molecular stresses are in fact already at the elastic limit much higher than the macroscopic shearing strength and of the order of those following the ideal lattice theory.[11]

ADOLF G. SMEKAL

Institut für theoretische Physik
der Universität Halle,
June 28, 1933.

[10] F. Zwicky, reference 5, p. 212.

[11] A. Smekal, Phys. Zeits. **34** (1933); report at the Gauvereins-meeting of the Deutsche Physikalische Gesellschaft in Freiberg, June 10, 1933.

Band Spectra Measurement of Mass

The masses of the elements may be measured by three general methods: (1) the mass-spectrograph gives a method in which the motion of an ion is calculated in the presence of an electric or magnetic field or both, and from this the mass deduced; (2) a value for the mass of an element may be derived from artificial disentigration experiments provided the masses and energies of the other constituents of the reaction are known and (3) band spectra furnish a method from which the ratio of the masses of an isotope may be determined.

For the case of Li^7 the values of the masses given by methods (1) and (2) are in excellent agreement when we use the reaction $Li^7+p\rightarrow 2\alpha$. The agreement is not quite as satisfactory for $Li^6+H^2\rightarrow 2\alpha$.[1] The ratio of the masses of the lithium isotopes from band spectra is in disagreement with the ratio from Costa's and Bainbridge's mass-spectrograph data and that from method (2).[2]

In the case of Be the first two methods do not agree when we use the reaction $Be^9+\alpha\rightarrow C^{12}+n$ to calculate the mass of Be as neutrons of too high an energy are occasionally observed.[3]

For the case of boron, methods (1) and (3) agree very closely, whereas the mass obtained by the second method from the reaction $B^{11}+p\rightarrow 3\alpha$ are lower.[4]

The discrepancies between the masses determined by the mass-spectrograph and the masses computed from artificial disintegration experiments may arise from the production of γ-rays or from one of the nuclei entering into the reaction being in an excited state with long mean life. The excitation might arise from a previous collision.

With these data in mind we have examined the band spectrum theory on which these mass ratios are determined to see whether these discrepancies are of a fundamental nature or not.

Kronig[5] has shown that the effective mass M that appears in the relationship MR^2 should be replaced by

$$MR^2+(m/2)[\xi_1^2+2\zeta_1^2+\Sigma_r(\xi_r^2+\eta_r^2+2\zeta_r^2)]$$
$$M=M_1M_2/M_1+M_2.$$

m = electronic mass and ξ_1, etc., the electronic coordinates. This substitution will change the observed moment of inertia I by as much as 1 part in 10^{-4}. For the molecule H^2Cl^{35} where 4/5 of an electron has been taken to be associated with the H^2 atom, this will reduce the ratio factor by 8 parts in 10^{-5}.

There is one other effect which may play a rôle and that is the change in the effective radius of the nucleus as the mass of the isotope is changed. The electronic isotope effect in band spectra has been observed by Jenkins and McKellar[4] for BO and they find the surprisingly large value of 0.33 cm^{-1}. For the H_2^2 molecule, the discussion may be conveniently divided into two different calculations. If we suppose that each electron is associated with a definite nucleus, as in the method of Heitler and London, then we have the perturbation arising from the electrons being at the position of its own nucleus—the probability of this event is to a first approximation measured by $\psi^2(0)$—and the perturbation arising from the electrons being at the position of the other nucleus—the probability of this latter event is to a first approximation given by $\psi^2(R)$. For the H_2^2 molecule this change is negligible. For the H^2Cl^{35} molecule, preliminary calculations indicate that ρ may be changed by as much as 1 part in 10^{-5} by this perturbation. If we use these values for the contribution of these two perturbations we find a value of the mass of H^2 of 2.01360 with the same limits of error as those reported by Hardy, Barker and Dennison.[6] This is in good agreement with

[1] Cockroft and Walton, Proc. Roy. Soc. **A137**, 229 (1932); Lewis, Livingston and Lawrence, Phys. Rev. **44**, 56 (1933).

[2] Bainbridge, Phys. Rev. **44**, 56 (1933); Jenkins and McKellar, Phys. Rev. **44**, 325A (1933).

[3] Bainbridge, Phys. Rev. **43**, 367 (1933); Kurie, Phys. Rev. **43**, 771 (1933).

[4] Cockroft, Phys. Rev. **44**, 314A (1933); Kirchner, Naturwiss., June 23, 1933; Aston, Proc. Roy. Soc. **A115**, 487 (1927); Jenkins and McKellar, Phys. Rev. **42**, 464 (1932); Oliphant and Lord Rutherford, Proc. Roy. Soc. **A141**, 259 (1933).

[5] Kronig, Zeits. f. Physik **46**, 814 (1928); **50**, 347 (1928).

[6] Hardy, Barker and Dennison, Phys. Rev. **42**, 279 (1932).

Bainbridge's value.[7] The electron distribution used in the calculation of the mean values of ξ_i^2, etc., was taken from the x-ray determination of the distribution of the electron density of the Cl negative ion.[8]

From a study of the analysis of the CuF band system as given by Ritschl,[9] a value for the ratio of the mass of Cu^{63} to that of Cu^{65} has been derived. The value is such that if we take for the value of Cu^{63}, $63-x$, then the value of the mass of Cu^{65} is $65-x$ where x is the same in both results to one part in 10^{-4}. These values fit in with our ideas that the addition of two neutrons to Cu^{63} to form Cu^{65} should change the mass by 2.000.

ARTHUR BRAMLEY

Bartol Research Foundation of
The Franklin Institute,
Swarthmore, Pennsylvania,
July 14, 1933.

[7] Bainbridge, Phys. Rev. **44**, 57 (1933).
[8] Wollan, Rev. Mod. Phys. **4**, 205 (1932).
[9] Ritschl, Zeits. f. Physik **42**, 172 (1927).

Failure to Detect the Radioactivity of Beryllium with the Wilson Cloud Chamber

In an attempt to detect the radioactivity of beryllium, suggested by the high mass found for Be^9 by Bainbridge[1] and reported to exist by Langer and Raitt,[2] the writers have taken 4800 stereoscopic pairs of photographs with a large Wilson cloud chamber, the piston of which was partially covered by 120 sq. cm of very pure Be, as a fine powder and also as finely crystalline plates. To increase the range of any α-particles emitted, the chamber was filled with helium or hydrogen, gases of the lowest stopping powers, at a pressure of two-thirds of an atmosphere, which increased the range over that in standard air by a factor of about 8 for helium and about 6 for hydrogen. At great intervals, some photographs showed α-ray tracks undoubtedly due to contamination of the chamber, since these tracks originated in the walls of the chamber and not in the Be. The best set of 1600 pairs of photographs contained only 4 such tracks.

By the Bragg-Kleeman rule, the atomic stopping power of Be atoms for α-particles is 0.75 that of O atoms, so that the reported α-particles from Be, of 1 cm range, would penetrate 5.1μ of Be. The roughness of the Be layer in the chamber gave, for α-ray emission, a surface several times the area covered. For the reported half-life of 10^{14} years, this surface should have emitted about 5 α-particles per second, or one on every other photograph, if 0.1 sec. is estimated as the period at the bottom of each expansion during which α-particles that enter the chamber will form cloud-tracks. In the one set of photographs already cited, the 4 tracks due largely, if not entirely, to contamination form only one-half percent of such a number, and in general, less than one-thousandth of such a number of tracks not attributable to contamination of the chamber, was found. As a result, the half-life of Be appears to exceed 10^{17} years if it emits α-particles of 1 cm range.

Lord Rayleigh's[3] observation that the oldest beryls cannot be old enough to have collected the helium they contain solely on the basis of radioactive decay of Be if the half-life is 10^{14} years, is still more in point if the half-life is so much greater.

Based on the probability that neutrons would be emitted in the radioactive disintegration of Be^9, since He^5 is not found to accumulate[4] in beryl, so that decay of Be^9 would result ultimately in the production of two α-particles and one neutron, irrespective of the actual steps involved in the disintegration, a second, less promising attempt to detect the radioactivity of Be was made. The cloud-chamber was surrounded by 200 pounds of beryl and one-half pound of pure Be, so distributed that, disregarding absorption of neutrons by the beryl and scattering of neutrons into the chamber by surrounding matter, a half-life for Be of 10^{14} years would have given about 200 neutrons through the chamber in the tenth of a second during which resulting recoil tracks and disintegration events would have been detected. To increase the length of such tracks, helium, hydrogen or a 4 : 1 hydrogen-nitrogen mixture filled the chamber. If these neutrons were as effective as those of Feather[5] in the production of recoil tracks, then his estimate of the number of neutrons passing through his chamber at the time of the expansion and the frequency with which he obtained recoil tracks, gives about 10 as the number of recoil tracks which could have been expected in the 1300 pairs of photographs taken in the experiment with beryl. The few long α-tracks found in these photographs occurred as frequently as in a blank run of 300 pairs taken with the beryl far removed, and can be ascribed to contamination of the chamber. No definite evidence was thus found for the emission of neutrons arising directly from the radioactive disintegration of Be^9 or from the bombardment of neighboring Be nuclei by α-particles emitted in this disintegration.

If Be^9 disintegrates into two α-particles and one neutron, the masses at present used for these particles indicate that 4.2×10^6 e.v. of energy is available for the disintegration. Since, however, 1.0067 may be somewhat higher than the true mass of the neutron, it may be assumed that the energy is equal to or greater than 4.2×10^6 e.v. If the total disintegration occurs in one step, neutrons of moderately high velocity could be produced provided the γ-rays do not use up too much of this energy, and it would be possible to detect such neutrons by the recoil atoms produced.

In conclusion, the recent work of Evans and Henderson[6] and of Lord Rayleigh[3] and the investigations here reported cast considerable doubt upon the existence of any detectable radioactivity of Be^9.

DAVID M. GANS
WILLIAM D. HARKINS
HENRY W. NEWSON

George Herbert Jones Laboratory,
University of Chicago,
July 18, 1933.

[1] K. T. Bainbridge, Phys. Rev. **43**, 367 (1933).
[2] R. M. Langer and R. W. Raitt, Phys. Rev. **43**, 585 (1933).
[3] Lord Rayleigh, Nature **131**, 724 (1933).
[4] J. T. Tate and P. T. Smith, Phys. Rev. **43**, 672 (1933).
[5] N. Feather, Proc. Roy. Soc. **A136**, 709 (1932).
[6] R. D. Evans and M. C. Henderson, Phys. Rev. **44**, 59 (1933).

Measurements on the Effect of Light on Spurious Contact Potentials and "Trapped" Electrons

Changes in contact potential between a thoriated filament (operating at 1325°K) and a nickel collector can easily be measured by observing the thermionic current received on the collector as a function of the retarding potential. Shifts in the contact potential of such a nickel collector which depend on the time and on the previous history have been reported.[1] The surface model used to explain those results depended on the assumption that the potential barrier is of the "hill-valley" type shown in Fig. 13.[2] In detail it is assumed that on the nickel there is an adsorbed gas layer and on this is a layer of thorium atoms which have been evaporated from the filament during the process of activation. After long periods of time the surface attains the same state within 0.02 volt or less, independent of past history. This we will call the "normal" state. After a current of 2×10^{-6} is allowed to flow to the collector with an accelerating potential of 8.0 volts for ten seconds, the surface becomes 0.1 volt or greater *negative* with respect to the normal state but returns along exponential decay curves toward the normal state about 0.03 volt in 300 seconds. Many hours are required for complete recovery. The hypothesis has been made that the electrons are "trapped" in the valley of the potential barrier. It is at once obvious that if such were the case it should be possible to remove these trapped electrons photoelectrically. *Experiment* shows that the contact potential of this surface can be changed very appreciably by exposure to light and the normal state can be realized much more quickly than in the absence of light.

After a current of 20×10^{-6} amp. is allowed to flow to the collector with an accelerating potential of 100 volts for ten seconds, the surface becomes 0.1 volt or greater *positive* with respect to the normal state and again tends to return to the normal if left alone, but the time required is many hours. A supply of 8-volt electrons from the filament restores the potential very quickly however. It is also possible to accelerate the return to the normal condition by supplying the electrons photoelectrically from the nickel itself. That is, light again accelerates the return to the normal causing the surface potential to become *negative* with the time at a more rapid rate than is observed in the absence of light. Thus it seems as though the 100-volt electrons produced some "secondary" electrons by "ionizing" some of the atoms of the surface layer. About one ionized atom per thousand is all that would be required to produce the observed shift in contact potential. The electron currents from the filament to the collector at accelerating potentials of 8.0 volts or more were entirely reproducible and independent of the changes taking place at the collector surface which indicates that none of the changes observed can be attributed to changes in the surface of the emitting filament.

WAYNE B. NOTTINGHAM

Department of Physics,
Massachusetts Institute of Technology,
July 19, 1933.

[1] W. B. Nottingham, Phys. Rev. **39**, 183 (1932).
[2] W. B. Nottingham, Phys. Rev. **41**, 793 (1932).

The Effect of Grinding and Etching on a Pair of Split Calcite Crystals

We have recently been making a search for a pair of calcite crystals suitable for making observations with a two-crystal x-ray spectrometer in the wave-length range 0.1–0.2 Angstrom. On account of the small Bragg angle it was necessary to have crystals at least 3.5 inches long. One pair (our No. 3), which had been split by the method used by Bergen Davis—saw-cut parallel to cleavage plane by milling machine—gave sufficiently narrow rocking curves in the (1, −1) position at 0.4A. At 0.2A, however, not only were the rocking curves much wider, but they were unsymmetrical,—and they varied, in both width and symmetry, from point to point along the face of the crystals, as was ascertained by limiting the beam by suitably disposed slits so that only a small part of the cleavage face was used. However, all these curves, taken from various parts of the crystal face, showed a maximum at very nearly the same angle, showing that the imperfections at 0.2A were not due to warping of the crystal planes, or other similar causes.

It occurred to us that this unsatisfactory behavior at 0.2A might arise from the fact that in spite of the care with which the crystal was split there was a series of steps on the cleavage face, and that therefore to the x-ray beam incident at the small Bragg angle, the crystal might present a surface made up largely of such steps rather than a series of reflecting *planes;* whereas the steps would be relatively less prominent at larger Bragg angles.

Accordingly, we ground the cleaved surface of each crystal to a plane (less than 10″ out of parallelism with the crystal planes); polished lightly with rouge; and then etched (for a few seconds) with an 0.7 normal solution of HCl, after the manner described by Manning.[1] The result of this first treatment was a slight increase in the width of the rocking-curve at 0.4A in comparison with the curves for the cleaved surfaces. But at 0.2A not only was the rocking curve narrower than before grinding and etching, but, more important from an experimental standpoint, it was constant as to shape, width and position for different parts of the crystal surface.

Since the removal of the large amount of material from the crystal face on first grinding might have caused considerable breakage of the surface planes, it was thought that a second very light grinding, with subsequent careful etching, might produce still narrower rocking curves. This conjecture was confirmed, as is shown by the data in Table I.

[1] Manning, Phys. Rev. **43**, 1050 (1933).

TABLE I. *Rocking curve widths in seconds (full width at half maximum) before and after grinding and etching.*

Wave-length	0.4A	0.2A	0.15A	0.2A
Position	1, −1	1, −1	1, −1	2, −2
Width before polishing and etching	4.6±0.2″	variable 7 to 14″		3.1″
Width after first polishing and etching	6.4±0.2″	constant 5.7±0.2″	4.5″	3.4″
Width after second polishing and etching	3.6″	2.7″	2.9″	1.65″

It is to be noted from Table I that the widths of the rocking curves decrease more or less regularly below 0.4A, contrary to the data shown by Allison,[2] whose results may perhaps be explained by the above "step effect."

It is recommended, therefore, that calcite crystals, for use on x-ray spectrometers at wave-lengths in the region 0.1–0.2A should be ground, polished and etched, unless the cleavage surfaces be exceptionally good. Such treatment produces crystals with very nearly homogeneous faces and with rocking curves as narrow as any reported for the best cleaved surfaces.

It is not improbable that, with these treated crystals a progressive change of rocking-curve width with time will be observed. We shall report on this point later.

F. K. RICHTMYER
S. W. BARNES
K. V. MANNING

Cornell University,
July 24, 1933.

[2] Allison, Phys. Rev. **41**, 1 (1932).

Proceedings of the American Physical Society

MINUTES OF THE CHICAGO MEETING, JUNE 19–24, 1933

THE 186th regular meeting of the American Physical Society (perhaps the most important scientific session in its history to date) was held in Chicago, June 19–24, 1933 as a joint meeting with Section B of the American Association for the Advancement of Science in connection with "A Century of Progress Exposition." The presiding officers were Paul D. Foote, President of the Society, Arthur H. Compton, Vice-President, Niels Bohr, E. C. Crittenden, C. J. Davisson, Vice-President of Section B of the American Association for the Advancement of Science, Enrico Fermi, W. D. Harkins, K. Lark-Horovitz, F. Wheeler Loomis, L. W. McKeehan, and J. C. Slater.

The scientific program began on Monday morning at Eckhart and Ryerson Laboratories of the University of Chicago with three parallel sessions of contributed papers followed by three sessions in the afternoon. The remainder of the week was taken up with symposia which differed from the customary sessions in that they were joint sessions with other scientific societies and sections of the A.A.A.S., namely Section A and the American Mathematical Society, Section B and the American Meteorological Society, Section C (Chemistry), the American Astronomical Society, and the American Section of the International Union of Pure and Applied Physics. The attendance at some sessions ran as high as six hundred and fifty. The sessions also had heightened interest and value because of the presence of the distinguished foreign guests who had been officially invited by the American Association for the Advancement of Science. These guests were F. W. Aston of Cambridge, England, J. Bjerknes of Bergen, Norway, Niels Bohr of Copenhagen, J. D. Cockroft of Cambridge, England, Lipót Fejér of Budapest, Enrico Fermi of Rome and Tullio Levi-Civita of Rome.

The following public addresses were delivered at the Exposition Grounds:

Atmospheric Soundings: Methods and Results. J. BJERKNES, *Geophysical Institute, Bergen, Norway.*

Theory of Hyperfine Structures. ENRICO FERMI, *University of Rome.*

Space and Time in Contemporary Physics. NIELS BOHR, *University of Copenhagen.*

The Physical Society dinner with one hundred and ten guests was held in the Congress Hotel on Wednesday evening at six-fifteen o'clock. After dinner the Society attended the public program held in the beautiful auditorium in Thorne Hall on the campus of the Northwestern University Medical Center. This program was under the auspices of Sections B and C of the A.A.A.S. with Niels Bohr presiding:

1. The Story of Isotopes. F. W. ASTON, *University of Cambridge, England.*

2. New Light on Nuclear Physics. R. A. MILLIKAN, *California Institute of Technology.*

In addition to the complete program of the American Meteorological Society, the Bulletin of the American Physical Society carried the following symposia:

A. APPLICATION OF QUANTUM MECHANICS IN CHEMISTRY

Tuesday Morning, June 20, 9:30 A.M., International House; Joint Session, American Physical Society, Section B and Section C.

1. Electron Energies in Atoms and Molecules. J. C. SLATER, *Massachusetts Institute of Technology.*

2. Quantum Mechanics of Condensed Ring Systems, Free Radicals and Other Complex Molecules. LINUS PAULING, *California Institute of Technology.*

3. Quantum Mechanics and Chemical Reactions. HENRY EYRING, *Princeton University.*

4. Band Spectra and Molecular Structure. R. S. MULLIKEN, *University of Chicago.*

B.

Tuesday Afternoon, 1:45 P.M., Mandel Hall; Section A with Section B as guests.

1. Some Mathematical Aspects of the New Mechanics. TULLIO LEVI-CIVITA, *University of Rome.*

2. Quantum Mechanics and Asymptotic Series. G. D. BIRKHOFF, *Harvard University.*

C. ISOTOPES

Wednesday Morning, June 21, 9:30 A.M.; International House; Joint Session of Section C with Section B and the American Physical Society.

1. Neutrons and Isotopes. W. D. HARKINS, *University of Chicago.*

2. Some Measurements of the Relative Abundance of Isotopes. F. W. ASTON, *University of Cambridge, England.*

3. The Masses of Isotopes and the Disintegration of Atoms. K. T. BAINBRIDGE, *Bartol Research Foundation.*

4. Isotopic Fractionation of Water. E. W. WASHBURN, *Bureau of Standards.*

5. A Diffusion Method of Separation of Isotopes. HAROLD C. UREY, *Columbia University.*

6. The Magneto-Optic Method in the Study of Isotopes. FRED ALLISON, *Alabama Polytechnic Institute.*

D.

Wednesday Morning, June 21, 9:30 A.M.; Mandel Hall; American Mathematical Society and Section A.

1. The Infinite Sequences Arising in the Theories of Harmonic Analysis, of Interpolation and of Mechanical Quadratures. LIPÓT FEJÉR, *University of Budapest.*

2. On the Use of Cesàro Means in Determining Criteria for Fourier's Constants. C. N. MOORE, *University of Cincinnati.*

3. Certain Problems of Closest Approximation. DUNHAM JACKSON, *University of Minnesota.*

E. THE MEASUREMENT OF GEOLOGIC TIME

Wednesday Afternoon, 2:00 P.M.; Hall of Science, Fair Grounds. Joint Session of Section E (Geology) with Sections B and C and the American Physical Society.

1. General Survey of the Problem. ALFRED C. LANE, *Tufts College, Medford, Mass.*

2. Working Formulae for the Age of a Radioactive Mineral. A. F. KOVARIK, *Yale University.*

3. The Significance of the Isotopes of Uranium and Lead. C. S. PIGGOT, *Geophysical Laboratory, Washington, D. C.*

4. The Actinium Series of Radioactive Elements and the Measurement of Geologic Time. A. V. GROSSE, *University of Chicago.*

5. Variation in Concentration of Radioactive Elements in Nature and Regularities of Their Increase. I. KURBATOV, *3205 Wenonah Ave., Berwyn, Ill.*

6. The "Helium Method." A New Outlook. W. D. URRY, *Massachusetts Institute of Technology.*

7. Pb/U Ratio of Pitchblende from Great Bear Lake, Canada, and Its Probable Age. J. P. MARBLE, *U. S. Geological Survey, Washington, D. C.*

8. Thorianite from Eastern Pennsylvania. R. C. WELLS, *U. S. Geological Survey, Washington, D. C.*

9. Post-Glacial Time Calculations from Recent Geothermal Gradient Measurements in the Calumet Copper Mines. W. O. HOTCHKISS, *Michigan College of Mines and Technology,* AND L. R. INGERSOLL, *University of Wisconsin.*

10. The Radium Content of the Travertine Deposits of Mammouth Hot Springs, Yellowstone Park, as an Index of Their Age. HERMAN SCHLUNDT, *University of Missouri.*

F. SPECTROSCOPY AND ASTRONOMY

Thursday Morning, June 22, 9:30 A.M.; International House; Joint Session with the American Astronomical Society.

1. Astrophysics and the Ionization Theory. W. S. ADAMS, *Mount Wilson Observatory.*

2. Technique of Stellar Spectrophotometry and Intensities of Some Stellar Absorption Lines. THEODORE DUNHAM, JR., *Mount Wilson Observatory.*

3. Atomic *Configurations* in Spectroscopy. A. G. SHENSTONE, *Princeton University.*

4. Matter in Inter-Stellar Space. OTTO STRUVE, *Yerkes Observatory.*

G. NUCLEAR DISINTEGRATION

Friday Morning, June 23, 9:30 A.M.; International House.

1. Recent Work on Nuclear Disintegration at The University of California. E. O. LAWRENCE, *University of California.*

2. The Disintegration of Light Elements by High Velocity Protons. J. D. COCKROFT, *University of Cambridge, England.*

3. Disintegration Experiments on Elements of Medium Atomic Number. M. A. TUVE, *Department of Terrestrial Magnetism, Washington, D. C.*

4. Disintegration of Nuclei by Neutrons. W. D. HARKINS, *University of Chicago.*

5. Discussion by Niels Bohr.

H.

Saturday Morning, June 24, 9:30 A.M.; Mandel Hall; American Section of the International Union of Pure and Applied Physics with foreign guests; presided over by E. C. Crittenden of the Bureau of Standards.

1. The Broader Aspects of the International S.U.N. Committee's Activities. SIR RICHARD GLAZEBROOK, *Chairman of the International S.U.N. Committee (read by R. A. Millikan).*

2. Magnetic Units. HENRI ABRAHAM, *Professor of Physics at The Sorbonne, and General Secretary of the I.U.P.A.P. (read by A. E. Kennelly).*

3. Mathematical Considerations Underlying the Most Desirable System of Physical Units, Especially Electromagnetic Units. LEIGH PAGE, *Yale University.*

4. A Definitive System of Units. GEORGE A. CAMPBELL, *Research Engineer, American Telephone and Telegraph Company.*

5. The Establishment and Maintenance of the Electrical Units. HARVEY L. CURTIS, *Physicist, U. S. Bureau of Standards.*

6. Possible Extensions of the Existing International Series of Electric Units (ohm, volt, ampere, coulomb, farad, henry, joule, watt) into a Complete Absolute System. A. E. KENNELLY, *Professor Emeritus of Electrical Engineering, Harvard University.*

Meeting of the Council. At the meeting of the Council held on June 22, 1933 two candidates were transferred from membership to fellowship and twenty-four were elected to membership. *Transferred from Membership to Fellowship:* Joseph G. Brown and W. Edwards Deming. *Elected to Membership:* Tsunesaburo Asada, Melvin L. Barlow, Edward S. Bettis, Ware Cattell, Norman S. Grace, Edward H. Green, Beno Gutenberg, Nis Hansen, Jr., Tatuo Hayasi, Eisaburo Honde, Ralph C. Hosterman, B. Jennings, Hikotaro Kakeshita, Osamu Minakawa, George A. Morton, Sotohiko Nishida, Tokiharu Okaya, Masao Sawada, Matsuhei Tamura, Alexander Wolf, Hidetsugu Yagi, Hikoji Yamada, Gale Young, and Hideki Yukawa.

The Secretary reported the death of two members, J. Lawrence Dunham and A. S. Galajikian.

There were eighty contributed papers on the regular scientific program of the Society. Numbers 1, 2, 3, 8, 14, 15, 22, 40, 41, 42, 47, 48, 49, 52, 63, 71, 75, 76, and 80 were read by title. The abstracts of these papers are given in the following pages. An *Author Index* will be found at the end.

W. L. SEVERINGHAUS, *Secretary*

ABSTRACTS

1. Efficiency of Chemiluminescence Accompanying Oxidation of Grignard Compounds. CLARENCE DELMAR THOMAS, *Missouri School of Mines (Rolla), and* R. T. DUFFORD, *University of Missouri (Columbia).*—The chemiluminescence which accompanies the reaction of certain Grignard reagents with oxygen has been studied quantitatively. The input energy, assumed equal to the heat of oxidation, was determined for sixteen compounds, by special calorimetric methods adapted to use with such highly reactive substances. The amounts of material used were found by titration. The luminous output was measured with a specially-built sphere photometer; the curves of mean spherical candlepower against time were integrated to find the total energy radiated. On the basis of 620 lumens per watt, the efficiencies can be computed for the luminescence. The values obtained range from about 10^{-7} to 2.6×10^{-5} percent, the highest values being given by p-ClC_6H_4MgBr. (See also the accompanying abstract by Asling and Dufford.)

2. Efficiency of Chemiluminescence Accompanying the Wedekind Reaction. WALTER LOUIS ASLING, *Missouri Wesleyan College (Warrenton), and* R. T. DUFFORD, *University of Missouri.*—The chemiluminescence accompanying the reaction of certain Grignard reagents with chloropicrin has been studied quantitatively. The input energy, assumed equal to the heat of reaction, was measured for eleven compounds, by using specially adapted calorimetric methods. The luminous output was measured with a specially built sphere photometer, the methods used being similar to those of Thomas and Dufford (see accompanying abstract). The efficiencies measured range from 4.4×10^{-8} percent to 10^{-9} percent. The significance of these values with regard to the possible origin of the luminescence is discussed.

3. New Observations on the Photovoltaic Effect. R. T. DUFFORD, *University of Missouri.*—The behavior of a number of types of photovoltaic cell, especially cells containing Grignard solutions, is studied and compared with that of other types of cells. The need for extension of current theories of electrode potentials in order to explain the phenomena is pointed out, and a possible direction along which such extension might be made is suggested.

4. Electrical Characteristics of Barrier-Layer Photo-Cells. PAUL R. GLEASON, *Colgate University.*—The resistance of barrier-layer photo-cells has been determined over a wide range of illumination and for currents both in the same and the opposite direction to the photocurrents. The bridge circuit used had to be compensated for the voltaic effects of the cells. The general shape of the curves agrees in the one case with those for photoconducting selenium cells and with the curves for contact rectifiers in the case of the variation with the current through the cell. The results for the Photronic cell are not in agreement with those of Romain (Rev. Sci. Inst. **4**, 83 (1933)). He gave a linear relation for the variation of the conductivity with illumination and also with leakage current. One cuprous oxide cell made in this laboratory exhibited unusual characteristics. The current output was at least one-tenth that usually obtained for cuprous oxide cells (Vorderwand) in spite of the fact that the cell shows practically no rectification for currents comparable with the photocurrents. Waibel and Schottky (Phys. Zeits. **33**, 583 (1932)) stated that such cells yield about 0.0001 the current of the rectifying cells. For higher values of the current, this cell is unusual in giving a rectified current in the same direction as the photocurrent.

5. The Photoelectric Properties of Magnesium Layers. G. DÉJARDIN AND R. SCHWÉGLER, *University of Lyons.*—The photoelectric sensitivity of magnesium has been carefully studied, by using a mercury arc and a hydrogen tube giving an intense continuous emission in the ultraviolet. The energy emerging from the monochromator was measured by a Moll thermopile or, for greater convenience, was deduced from the response of a calibrated potassium cell, sensitized by coating the window with a fluorescent mixture of sodium salicylate and dextrine. Between 3400 and 2300A, the effective sensitivity of this cell is accurately proportional to λ. The spectral distribution curve is nearly the same for mirrors obtained on glass by evaporation of pure magnesium in highly exhausted bulbs, and for the layers deposited on nickel by sputtering in argon. The sensitivity has no maximum between 2100A and the threshold, which occurs at 3400A. Near 2537A, the mean value of the yield is 10^{-4} amp. watt. The long wave limit is usually shifted above 4000A for layers produced in poor vacuum, but the yield never rises to the exceedingly large value indicated by De Laszlo. Bright mirrors obtained by evaporation of a magnesium and barium alloy have their threshold above 5000A and the spectral curve shows a singularity about 3400A. In combination with appropriate filters, a MgBa cell is suitable for measuring the erythemal output of quartz mercury lamps.

6. Effect of Temperature on the Energy Distribution of Photoelectrons. W. W. ROEHR AND L. A. DUBRIDGE, *Washington University, St. Louis, Mo.*—An extended experimental test has been carried out of the theory of energy distribution recently developed by DuBridge (Phys. Rev. **43**, 727 (1933)). Photoelectrons were released by monochromatic light from an outgassed filament of Mo placed at the center of a large collecting sphere connected to an FP54 amplifier. Photocurrent measurements at filament temperatures up to 1000°K were made possible by heating the filament with the interrupted current furnished by a special Thyratron circuit. The results obtained are in complete quantitative agreement with the theory and show: (1) The "temperature tails" to the current-voltage curves are appreciable at room temperature and become rapidly more pronounced at higher temperatures. (2) For a *clean* surface at room temperature the most probable energy is about 0.75 of the (extrapolated) maximum and shifts to lower values for high temperatures. (3) The observed curves show an excellent fit to the theoretical curves for the whole range of temperatures and wave-lengths examined. (4) From the shifts required to fit the observed curves the maximum energy at 0°K can be determined, and the values so obtained for a series of different wavelengths at any fixed temperature fit closely the Einstein equation.

7. Progress Report on the Electrostatic High Voltage Generator at Round Hill. L. C. VAN ATTA, E. W. SAMSON* AND R. J. VAN DE GRAAFF, *Massachusetts Institute of Technology.*—Preliminary trials have been made with one of the two units comprising the electrostatic high voltage generator at Round Hill (Phys. Rev. **43**, 149 (1933)). A current of 0.75 milliampere was delivered to the sphere by a single experimental paper belt three feet wide running self-exciting at 5600 feet per minute. A current of 2 milliamperes is expected in the second unit with a charging assembly now under construction consisting essentially of two belts each four feet wide. Details of the charging mechanism will be given, together with the results of voltage measurements to be made on the completion of the second charging assembly. Sufficient voltage and power for nuclear research are now assured, and the construction of a vacuum tube of the type previously described (Phys. Rev. **43**, 158 (1933)) has been started.

* National Research Fellow.

8. The Exponential Law of Radioactive Disintegration. ARTHUR E. RUARK, *University of Pittsburgh.*—The radioactive decay law $N = N_0 e^{-\lambda t}$ is based on the assumption that the probability w for an atom to disintegrate in unit time is constant. The question arises, if the exponential law is accurately followed, can we conclude that w is independent of the age of the atom? It might happen that atoms of different ages have different decay probabilities; and w might depend on age in such a way that exponential decay curves result. Wolfke has shown, however, that w cannot depend on the age of the atom. To generalize this, suppose the members A, B, etc., of a series to have decay probabilities w_A, w_B, etc. Then we can demonstrate the theorem, if all members decay exponentially; and if each w is at most a function of the age of the atom, the ages of its ancestors and the ages of its descendants; then the w's are constant. Therefore, the assumption of constant probability of disintegration in unit time, which is the basis of all theories of disintegration, is necessary as well as sufficient.

9. The Disintegration of the Elements by Swiftly Moving Protons. M. STANLEY LIVINGSTON, MALCOLM C. HENDERSON AND ERNEST O. LAWRENCE, *University of California.*—Using our apparatus for the multiple acceleration of ions to high speed we have bombarded various elements with protons ranging in energy from 600,000 to 1,600,000 volts and in every instance have obtained evidence of disintegration. Li yields alpha-particles of 8.5 and 9.1 cm range when bombarded by protons of 600,000 and 1,400,000 volts respectively. The difference in range corresponds to the difference of proton energies and proves that the process involves capture of the proton. Be yields 3.3 cm alpha-particles and a few with ranges as great as 6.1 cm. The low energy group have an excitation threshold of 900,000 volts. NaCl yields alpha-particles with ranges up to 3.4 cm when bombarded by 1,100,000 volt-protons. A few 2.7 cm alpha-particles were observed from both Al and Mg (commercial purity) and still fewer 2.2 cm alpha-particles from NH_4NO_3 when bombarded by 750,000 volt-protons. There is a possibility at the present time that some of the observations are due to impurities. This possibility we are investigating.

10. Three Types of Nuclear Disintegration of Calcium Fluoride by Bombarding Protons of Very Great Energy.

ERNEST O. LAWRENCE AND M. STANLEY LIVINGSTON, *University of California.*—Calcium fluoride when bombarded by swiftly moving protons yields alpha-particles of three distinct ranges. Protons of energies between 600,000 and 950,000 volts produce alpha-particles of 2.8 cm range. Between 950,000 and 1,350,000 volts the protons produce both 2.8 cm and 5.6 cm alpha-particles; while from 1,350,000 volts to 1,600,000 volts an additional alpha-particle group of 6.8 cm range is excited. The thresholds for excitation of these alpha-particle groups are sharp and the yield in each case rapidly increases linearly with increase of the range of the protons above the threshold value. For example, the yield of 6.8 cm alpha-particles increases tenfold for protons between 1,400,000 and 1,600,000 volts.

11. The Disintegration of Nuclei by Swiftly Moving Ions of the Heavy Isotope of Hydrogen. GILBERT N. LEWIS, M. STANLEY LIVINGSTON AND ERNEST O. LAWRENCE, *University of California.*—Using a sample of hydrogen containing fifty percent of the heavy isotope, H^2, we have produced 2,000,000 volt H^2H^1 ions. These ions striking any target immediately yield 660,000 volt-protons and 1,330,000 volt H^2 nuclei which we call deutons. Eight targets were used and in every case disintegration with emission of alpha-particles was observed. LiF yields large numbers of alpha-particles of two ranges, 8.2 cm and 14.8 cm. The latter, corresponding to an energy of 12,600,000 volts, are the highest speed alpha-particles yet observed either from natural or artificial disintegration. NH_4NO_3 gives many alpha-particles with range 6.8 cm which are almost certainly due to N. This element is of especial interest because it typifies elements of nuclear type $4n+2$. Al, Be and Mg, all of only commercial purity, give alpha-particles of 6.8 cm, 3.3 cm, and both 3.3 and 6.8 cm, respectively. NaCl, CaF_2 and B_2O_3 gave 2.8, 3.8 and 4.4 cm alphas respectively. In these three cases the results may be due to the proton alone. With Li the disintegration was obtained with deuton energies as low as 300,000 volts. With N and Be definite disintegration thresholds were observed, both at 600,000 volts, while with Al no disintegration was observed below 1,100,000 volts.

12. Production of Neutral Rays of Several Hundred Ion-Volt-Equivalent, the Absolute Measurement of Their Intensity, and the Ionizing Function of Argon Rays in Argon. OTTO BEECK, *California Institute of Technology.*—Earlier experimental investigations and theoretical considerations suggested that the possibility of ionizing any atom by any stable atom or ion of equal energy is largest if the atom is struck by its own atom. A method has been worked out to produce a strong monochromatic beam of atomic rays up to several hundred ion-volt-equivalent and to measure its absolute intensity by a thermo-method. Thus having laid the ground for a large variety of investigations, first the ionizing function of A° in A was investigated between 350 and 650 ion-volt-equivalent. The quantitative values were found about 4 times as high as in the collision of K^+ and A at similar energies.

13. On Neutrons from a Beryllium-Radon Source. J. R. DUNNING AND G. B. PEGRAM, *Columbia University.*—Further studies of Be-radon neutrons have been made by using the linear amplifier-oscillograph-Thyratron detector system as described previously (Phys. Rev. **43**, 497 (1933)) in a large room and with a thin-walled ionization chamber, both to minimize effects of scattered neutrons. Absorption curves have been obtained for C, Al, Pb, Cu, and paraffin up to 21 cm thickness, and single points for 4 cm thickness of a number of other elements, with the residual scattering reduced to about 1 percent. Since absorption is largely scattering, the form of the curves is a function of the type and distribution of material, and must be interpreted in terms of angle scattering functions and multiple scattering of the neutrons. These measurements are in general agreement with the theory developed by Professor I. Rabi treating scattering as an elastic sphere collision between neutron and nucleus on a wave mechanics basis, with a radius for the neutron of the order of 1.3×10^{-13} cm. Further scattering measurements have been made for C, Al, Cu, Sn, and Pb, at angles between 45° and 135°. When a beam of neutrons was sent through a magnetic field of 10,000 gauss, 15 cm in length, no measurable deflection was observed, indicating that the neutron does not have the properties of a free magnetic pole of any large multiple of unit strength. The angle distribution of neutron emission has been studied using a source in which the beryllium was bombarded with alpha-particles from one direction only. Approximately twice as many neutrons are recorded in the forward direction as in the backward direction, after being filtered through either 5 or 8 cm of lead.

14. Probable Errors of the Parameters in an Empirical Formula. W. EDWARDS DEMING, *Bureau of Chemistry and Soils, Washington, D. C.*—In the situation where only one coordinate of each point is subject to errors of observation, and where there are no rigorous relations between the parameters, systematic procedures are well known for computing the probable errors of the parameters evaluated by the method of least squares. For much of the work in physics the situation just described is not general enough, because oftentimes more than one coordinate of each point is subject to error, and the parameters may not all be independent. A methodical process is now given for solving and checking the results to obtain the probable errors of the parameters in the general case. The squares of the probable errors in the parameters $a, b, \cdots, p$ turn out to be

$$t_a^2 = t^2\{A_1 - A_1(A'F_a^{n+1} + A''F_a^{n+2}) - A_2(A'F_b^{n+1} + A''F_b^{n+2}) - \cdots - A_p(A'F_p^{n+1} + A''F_p^{n+2})\}$$

$$t_b^2 = t^2\{B_2 - B_1(B'F_a^{n+1} + B''F_a^{n+2}) - B_2(B'F_b^{n+1} + B''F_b^{n+2}) - \cdots - B_p(B'F_p^{n+1} + B''F_p^{n+2})\}$$

etc., wherein $A_1, A_2, \cdots, A_p, A', A''$ are the values of $a-a_0, b-b_0, \cdots, p-p_0, \lambda_{n+1}, \lambda_{n+2}$ that are obtained by replacing the constant column of Eqs. (13) in the general solution (Phil. Mag. **11**, 146 (1931)) by 1, 0, 0, ···, 0;

$B_1, B_2, \cdots, B_p, B', B''$ are obtained by replacing the constant column by 0, 1, 0, $\cdots$, 0; etc. t is the probable error of an observation of unit weight.

15. A Fundamental Connection Between Hamiltonian Dynamics and Wave Mechanics. CORNELIUS LANCZOS, *Purdue University.*—Field equations which are deduced from a variational principle can be considered in the function space to represent the dynamical problem of a moving mass point. The variational principle is the "Hamiltonian principle" of this dynamics. The Lagrangian equations of motion are equivalent to the given system of field equations. Introducing instead of Lagrange's dynamics, Hamilton's dynamics the canonical equations of motion and canonical transformations are obtained: they are equations of first order while the number of variables is doubled. The possibility of canonical transformations can be used for prescribing special requirements that the Hamiltonian function shall satisfy. We require that the canonical equations of motion shall form a *self-adjoint* system of differential equations. The 4 field equations of the vector potential may then be written as 2 complex equations of second order. The coordinated canonical equations of motion in the Hamiltonian dynamics of the function space result in a system of 4 complex equations of first order: they are Dirac's equation of a free electron.

16. A Canonical Coordinate System in Riemannian Geometry. EDWARD L. AKELEY, *Purdue University.*—Let $(\lambda_1 \cdots \lambda_n)$ be the characteristic values of λ associated with the pencil of tensors $G_{\mu\nu} - \lambda g_{\mu\nu}$, where $g_{\mu\nu}$ is the Riemannian metric tensor, and $G_{\mu\nu}$ its contracted Riemann-Christoffel tensor. If $\partial(\lambda_1 \cdots \lambda_n)/\partial(x_1 \cdots x_n) \neq 0$, the λ's form a canonical coordinate system. If $g_{\mu\nu} dx_\mu dx_\nu = \bar{g}_{\mu\nu} d\lambda_\mu d\lambda_\nu$, the $g_{\mu\nu}$ form a set of invariants which completely characterize the geometry. For these geometries, in addition to the parallelism of Levi-Civita, there exist definable types of integrable distant parallelism. Furthermore, certain Euclidean geometries can be invariantively associated with such a geometry. For $n = 2$ no geometries of this type exist. For $n > 2$ it is shown that they do exist, and some of their properties, in particular, in the neighborhood of the origin, have been studied.

17. On E. A. Milne's Theory of World Structure. H. P. ROBERTSON, *Princeton University.*—The theory of world structure recently proposed by E. A. Milne (Zeits. f. Astrophys. **6**, 1–95 (1933)) is found to rest on a postulate which is equivalent to that on which the theory of relativistic cosmology is based, thus disposing of his most fundamental objections to the latter theory. From one standpoint Milne's theory may be considered as the kinematical preliminary to the dynamical problem which is completely solved, in accordance with the general relativity theory of gravitation, by the so-called expanding universe theory; from another, consistent with that on which Milne's prediction of the linear velocity-distance relationship is obtained, it is interpretable as a special case of the alternative theory in which the influence of matter on the structure of the universe is considered negligible. The gravitational extension of Milne's solution, considered from this latter point of view, leads to an expanding universe which differs inappreciably from it unless the density of all matter in the universe exceeds Hubble's lower limit of 5×10^{-31} g/cm^3 by at least a hundred-fold.

18. Binding Forces in the Alkali Metals According to the Free Electron Theory. O. K. RICE, *Harvard University.*—Although there have been a considerable number of attempts to work out in some detail the nature of the cohesive forces in the alkali metals, it has seemed worth while to see how far one could go with the simplest possible hypothesis, according to which the metal consists of singly charged positive ions imbedded in a sea of free electrons. Frenkel first showed that the fact that the electrons in the metal obey the Fermi statistics, results in an effective repulsive force which will be balanced by attractive electrical forces; but, as he pointed out, the finite size of the ions prevents this being more than a qualitative picture, and he suggested taking this into account by including repulsive forces between electrons and ions. In the present work, I have introduced an intrinsic ionic volume, into which the electrons are supposed to be unable to penetrate, this simply being subtracted from the atomic volume in the Fermi expression for the kinetic energy of the electrons. For the attractive potential an expression involving a Madelung constant of a size about equal to those occurring in cases of uniunivalent crystals, and the same for all the alkali metals, is used. One can then calculate the energy of the metals from the experimental value of the atomic volume, getting excellent agreement with experiment. The method is not so successful in calculating the compressibilities; but, aside from the fact that the compressibilities at absolute zero may only be inferred from measurements around room temperature, it appears that a relatively small correction to the Fermi energy expression can give the correct compressibility without greatly upsetting the calculation of the energy. The latter is, then, to be considered as significant.

19. Distribution of Conduction Electrons in d.c. Currents. ERNST WEBER, *Polytechnic Institute of Brooklyn, Brooklyn, New York.*—A new series of experiments is described (Phys. Rev. **43**, 781A (1933)) in which magnetic fields perpendicular to a large conductor carrying direct current of several hundred amperes are used. These experiments bear out the fact that the current distribution in the conductor depends upon the length over which the magnetic field is applied. Different arrangements are used to explore the current distribution over the entire conductor and to measure simultaneously the temperature distribution. It is intended to investigate this new effect of low magnetic fields upon large currents also for materials other than copper.

20. Magnetic Force and the Law of Action and Reaction. FORREST F. CLEVELAND, *University of Kentucky.* (*Introduced by F. W. Warburton.*)—The classical expression, $\mathbf{df} = i(\mathbf{ds} \times \mathbf{H})$ where $\mathbf{dH} = i(\mathbf{ds}' \times \mathbf{r})/cr^3$, for the force on a

current element in a magnetic field predicts that the force exerted on one side of a rectangular circuit by the other three sides *is not equal and opposite* to the force reaction on the three sides. Experimental evidence is presented to show that these forces *are* equal and opposite and hence that the classical expression is invalid for this partial circuit. Ampere's expression for the force between current elements,

$$\mathbf{d}^2\mathbf{f} = -\frac{ii'}{c^2r^2}\mathbf{r}\left[2(\mathbf{ds}'\cdot\mathbf{ds}) - \frac{3}{r^2}(\mathbf{ds}'\cdot\mathbf{r})(\mathbf{ds}\cdot\mathbf{r})\right]$$

when applied to this circuit predicts that the law of action and reaction should hold, thus offering, apparently, greater promise for calculations involving partial circuits than the classical force equation.

21. Electric Waves, Derived from Weber's Energy Equation. F. W. WARBURTON, *University of Kentucky.*—An auxiliary vector **G**, defined as equal, both in magnitude and direction, to the magnetic force per unit length on a current, corresponds, when using Ampere's law of force between current elements, to the classical magnetic field **H**. Weber's energy equation is applied to a system of two moving electrons and two positive charges, a source, $-e'(v')$ and $+e'$, and an absorber, $-e(v)$ and $+e$. **G** and the electric field **E** may be found from the space and time rates of change of the mutual energy. Div **G** contains the factor $2(\mathbf{v}\times\mathbf{r})\cdot(\mathbf{v}'\times\mathbf{r})-(\mathbf{v}\cdot\mathbf{r})(\mathbf{v}'\cdot\mathbf{r})$, while $\partial E/c\partial t$ contains $(\mathbf{v}\times\mathbf{r})\cdot(\mathbf{v}'\times\mathbf{r})-2(\mathbf{v}\cdot\mathbf{r})(\mathbf{v}'\cdot\mathbf{r})$, and their difference yields

$$\nabla^2 A = \frac{\mu\epsilon}{c^2}\frac{\partial^2 A}{\partial t^2} - \frac{\mu\epsilon v \sin^2\theta}{c^2 r\cos\theta}\frac{\partial A}{\partial t} - \frac{\mu\epsilon' v'\cos\beta}{cr^3\cos\theta}$$

where A is the vector potential, directed along r, and β, θ are the angles between v and v', v and r. This wave is homogeneous in the region between the source and the absorber ($\cos\beta=0$), but on reaching the absorber it represents the variation in mutual potential energy of source and absorber, governing the transfer of energy to the latter. The interpretation is that a change in energy of the source is propagated with velocity $c/(\mu\epsilon)^{\frac{1}{2}}$ and may be absorbed by the first electron ($\cos\beta+0$) which it reaches.

22. Reflection of a Spherical Light-Wave from a Moving Plane Mirror. N. GALLI-SHOHAT, *Helen Schaeffer Huff Memorial Research Fellow, Bryn Mawr.*—When a spherical wave meets a moving plane mirror, the locus of the points in space where individual rays meet the mirror is a concave or convex surface according to whether the mirror is approaching or receding. From this surface reflection occurs as if it were a *fixed mirror*. This can be shown by applying Huyghens principle (as it was done before for a plane wave by Hicks, Righi, Hedrick). A sufficiently small part of the spherical wave can be considered as a plane wave. We can construct for such an elementary wave a fixed mirror (in the above sense). We find that such a mirror is turned relative to the actual one by

$$\angle\alpha = |(v_N/c)\sin\varphi + (v_N^2/c^2)\sin 2\varphi + \cdots|;$$

hence, the reflected ray rotates by 2α (v_N-perpendicular component of v to the mirror, φ angle of incidence). We further show that in the first order the reflected wave is a spherical wave, its center being the virtual image of the source of light. Furthermore, due to the motion, object and image distances p_0, q_0, equal for the plane mirror, change to $p_0(1\pm v_N/c)$ and $q_0(1\mp v_N/c)$ from which the focal length of the fixed mirror can be found. In the second order individual rays appear as coming from different points of the axis, and the virtual image is thus distorted.

23. The Reflection of Plane Wave Pulses from Plane Parallel Plates. MORRIS MUSKAT, *Gulf Research Laboratory, Pittsburgh, Pa.*—A wave theory analysis has been developed for the reflection of wave pulses from plates, which heretofore has been treated by the methods of geometrical optics. The general theorem is proved that if the reflection coefficient for a harmonic wave system is exactly periodic in the frequency of the waves, the reflections from the plate due to an incident pulse will consist of a series of wave trains of exactly the same form as the incident pulse. This theorem may be applied to electromagnetic waves polarized in and normal to the plane of incidence, longitudinal waves in fluid media, and transverse waves polarized normal to the plane of incidence in general elastic media. For problems involving more than two interfaces or for waves in general elastic media in which both longitudinal and transverse waves are excited, the reflection coefficients possess terms of several periodicities which are, in general, incommensurable with each other. By expansion into series consisting of terms of a single periodicity, each term will again give wave pulses which are undistorted with respect to the incident pulse. The resultant reflected wave systems, however, will show an apparent distortion due to the overlapping of the separate pulses.

24. The Structure of Rubber as Shown by the Time Lag of Fibering. W. E. SINGER, J. D. LONG AND W. P. DAVEY, *The Pennsylvania State College.*—The authors have found by x-ray methods that there is a time lag between the time when rubber is stretched and the time when a fiber structure is produced. Rubber must be of such a nature and such a structure as to account for the following characteristics: (1) A more or less critical temperature limit for the time lag of fibering. (2) A time lag of fibering unaffected by stretching the rubber above this critical temperature and then cooling rapidly. (3) A higher percentage stretch required to develop the fibrous structure after mechanical working and aging. (4) A relaxation time of less than 0.5 second. (5) A time lag of fibering independent of the length of time the rubber is held stretched, at least between 2 and 5 seconds. (6) A shorter time lag of fibering with a slow rate of stretching. (7) The enormous extensibility of rubber. All this mass of data is consistent with the picture that rubber consists of a tangle of spiral (or zigzag) shaped molecules whose ends are rather firmly anchored, but whose lengths can be temporarily untangled by the application of an external force.

25. Elastic Constants of Zinc. ALVIN W. HANSON, *University of Iowa. (Introduced by E. P. T. Tyndall.)*—The elastic constants of zinc have been determined by static torsion and bending experiments. The bending experiments were performed on single crystals of 0°, 45°, and 90° orientation; the torsion experiments on crystals of 0°, 70°, and 90°. From these measurements three constants are directly determined and certain combinations among the constants are obtained from which the remaining two constants may be computed. The crystals used in the bending experiments were of square cross section, about 7 mm on a side. Those used in the torsion experiments were of circular cross section, approximately 6 mm in diameter. The crystals were grown in a horizontal electric furnace under conditions which would insure the least possible strain. Strained crystals were found to give variable results.

26. Hooke's Law and Crystal Structure. A. E. CASWELL, *Oregon State College, Corvallis, Oregon.*—Cohesion between atoms and molecules in solids and liquids is usually assumed to be due to electrostatic or magnetic attractions and the derived force equations contain as one factor some inverse power of the distance between centers of force, that is, of the spacing. Unquestionably these forces play an important part in cohesion but fail to account for Hooke's law of elasticity according to which the force of restitution is directly proportional to the change in the spacing, either in extension or compression. It is shown that if in a crystal or other solid the atoms are arranged so that in various directions there are rows of electron orbits with the orbits in each row perpendicular to the direction of the row, relatively close together and with the electrons revolving in the same direction, so each row resembles a miniature solenoid, Hooke's law follows. When the spacing is increased until a row of orbits fails to behave as a solenoid Hooke's law no longer holds and the substance has passed its elastic limit. In diamagnetic substances each row of orbits is matched by an equivalent row or rows in which the electrons revolve in the opposite direction.

27. Crystallization of Polymorphous Substances I. K. LARK-HOROVITZ AND S. E. MADIGAN, *Purdue University.*—The stability of a compound in a polymorphous system is determined by the thermodynamic potential of the pure compound and the interaction between the compound and the support on which the crystallization takes place. The cubic form of ZnS—zincblende—has been evaporated in vacuo at temperatures well below the transition point $\alpha-\beta$ZnS and deposited on various surfaces held at 20°C. The deposit formed was cubic on all surfaces with a cubic lattice (copper, aluminum, diamond, etc.) and on amorphous surfaces (glass, fused quartz). It also remained cubic on pure zinc and mica or crystalline quartz. On zinc oxide a mixture of the hexagonal modification—wurtzite—with an abundance of cubic modification has been formed. The deposit of ZnS on hexagonal cadmium sulphide is almost purely hexagonal—wurtzite. ZnS has been deposited simultaneously on hexagonal cadmium sulphide and on copper surrounding the cadmium sulphide. The deposit was hexagonal on cadmium sulphide and cubic on the copper. Wurtzite when evaporated in vacuo is deposited on cubic surfaces cubic—as zincblende—but remains wurtzite if deposited on hexagonal ZnS.

28. A Resistance Function for Dense Fluids. LOUIS THOMPSON, *Naval Proving Ground, Dahlgren, Va.*—Experiments conducted with projectiles in unstable motion through short water ranges have led to the result that the order of retardation can be predicted by means of the air resistance function, provided that a coefficient for unstable flight in air is introduced. Because of the inherent instability of the motion, large variations occur in the path of the water runs of the projectile from round to round and quite irregular changes of course in the same run. The retardation data are subject to large variations and the rough approximation afforded by the resistance function is probably as satisfactory as any to be had as far as the prediction of performance in any specific case is concerned. The resistance is $R=(\rho/\rho_0)i(V,\theta)V^2L^2\bar{F}$, where $\bar{F}\equiv F(V/V_S, VL\rho/\mu)$ for air, taking mean value for velocities of similar range of V/V_S, ρ density water, ρ_0 density air, $i(V,\theta)$ factor, average value determined from range or retardation data for unstable flight in air. L diameter of projectile, θ angular deviation of the axis.

29. Fluidities of Thixotropic Gels: Bentonite Suspensions. H. A. AMBROSE AND A. G. LOOMIS, *Mellon Institute of Industrial Research and Gulf Research Laboratory, Pittsburgh. (Introduced by Paul D. Foote.)*—Flow measurements on bentonite suspensions, showing both the property of thixotropy, and of fluidity variable with shearing stress, were performed in capillary tubes, brass pipes, and a rotary consistometer of special design. The latter instrument was used to show that the structure of such gels must be broken down or built up until an equilibrium state of flow is attained to obtain reproducible measurements. No slippage at the walls was found in non-plug flow. Turbulent flow of bentonite suspensions was investigated in one-half and one inch pipes. It is shown that these materials behave as any viscous liquid, in the turbulent region, and that the volume of flow at any pressure gradient may be assumed to be the same as for water, without great error. The importance of obtaining equilibrium flow conditions for fluidity measurements is stressed.

30. A New Visco-Conductimeter. C. L. BABCOCK AND J. V. HOFFACKER, *Purdue University. (Introduced by K. Lark-Horovitz.)*—Two platinum cylinders having diameters of 1 inch and 1/4 inch are arranged concentrically and the interspace is filled with the liquid under investigation. With a special gear train the rotating speed of the outer cylinder can be varied from 3.48 radians per second to $3.48\times10^{-8.74}$ radians per second. The torque on the inner cylinder due to the viscosity of the liquid is counterbalanced by using a specially constructed balance so that the torque can be read off directly as weight of a rider times lever arm (null method). The platinum cylinders

serve also as electrodes and in this way resistance and viscosity are measured simultaneously. Polarization effects are avoided by using 500 cycle alternating current for the conductivity measurements. The instrument has been used for ordinary liquids at room temperature and for silicate glasses up to 1400°C and its results agree with results obtained by other methods.

31. Viscosity and Conductivity of Molten Glasses. K. LARK-HOROVITZ AND C. L. BABCOCK, *Purdue University.*—With the instrument described above, the conductivity and viscosity of different molten glasses has been investigated as a function of temperature up to 1400°C by taking measurements about 50°C apart. It has been shown that in no case is there a sudden break in the viscosity or conductivity curves as functions of temperature; neither one can be represented as a simple exponential of $1/T$. Resistivity and viscosity are not simply proportional but can be represented in most cases over the whole temperature range from softening point (e.g., 700°C for H.E. soda lime, 750°C for 702 EJ) up to about 1400°C by a formula $\eta = A\rho^B$. In this equation A and B change from glass to glass: therefore, the process of conductivity and viscosity cannot be based on the same principle, but the experiments point to the fact that while viscosity is determined by aggregations in the glass and their change with temperature, conductivity takes place in the true liquid interstices.

32. The Beat Note-Combinational Tone Controversy. HERBERT HAZEL AND R. R. RAMSEY, *Indiana University.*—The Helmholtz-Koenig controversy, participated in by Lord Rayleigh, Preyer, Bosanquet, Waetzmann, Edser, Rucker, and others, is settled on the basis of the conditions for modulation. Experimental study of the conditions necessary for modulation shows that combinational tones or sideband frequencies are produced whenever a product term of the two parent frequencies is involved, regardless of whether linear or nonlinear response characteristics are used. Two periodic disturbances added in a linear medium do not cause response in a resonant circuit tuned either to a frequency equal to the difference between the two added frequencies or to a frequency equal to their sum. Experimental results using a linear wave-meter circuit as the analyzer were obtained with electromagnetic waves in the audiofrequency band and in the radiofrequency band. An electro-acoustical wave meter, designed for response to sound waves between 500 and 5000 cycles per second, was used in the study of the addition of sound waves. Modulation of currents produced by an a.c. generator can be secured by varying the field strength of the generator. The process has been generally explained as one requiring a nonlinear magnetization curve. Using air-core coils we have found that modulation in the linear circuit occurs due to the product $(H_0+H \sin \omega_1 t) \sin \omega_2 t$.

33. Tone Analysis and Physical Characteristics of Violins. T. H. STEVENS AND R. B. ABBOTT, *Purdue University.*—A direct recording cathode-ray oscillograph has been used in conjunction with a condenser microphone and suitable amplifier to obtain steady state records of violin sound waves. The curves have been analyzed to twelve components, and studies made of factors characterizing violins of widely different tone quality; also, ways in which the tone quality of an instrument may be varied. Many resonance frequencies have been found, corresponding to natural vibration periods of the air cavity or of parts of the body. The distribution of energy among the components of the emitted wave is found to vary widely among various instruments, and gives a means of distinguishing between good and poor instruments as well as between "brilliant" and "dark" tones. Good carrying power is associated with considerable amplitudes in high order components. The effect of speed, pressure and position of the bow on the string has been given especial study. It is found that, within certain limits, increasing the pressure, or bowing nearer the bridge, cause relatively more of the radiated energy to be carried by lower order components. Extremely undesirable tones, described as squeaking or scraping, are found to be nonperiodic.

34. Some Frequencies of Multiple Resonators. RUTH O. JENKINS AND R. B. ABBOTT, *Purdue University.*—Frequencies at which a driving force was made to operate in order to locate resonance frequencies of a driven acoustical system were investigated in several cases. Electrical circuit analogies were the bases of mathematical investigations and specially designed vibration meters and stethoscopes were used to indicate resonance points. Sirens, tuning forks and closed organ pipes produced sound pressure for the driving force. In the case of two Helmholz resonators coupled in parallel, the wattless acoustical current was equated to zero giving an eighth degree equation with frequency as variable. $aw^8+bw^6-cw^4+dw^2-ew^0=0$. Two equal real and six imaginary roots satisfied the equation. The two real ones were found experimentally to exist as the equation required. A violin body can be considered as an air system coupled with two diaphragms, namely, the top and bottom. The air system is composed of two air resonators coupled in parallel. The diaphragms were made inoperative by packing the violin in sand. Four air cavity resonance points were located near 256, 512, 768, and 1024 cyc./sec. By using the same violin with top and bottom free to vibrate, the same resonance points were indicated by a vibration meter applied to back and front. Other violins gave similar results.

35. Study of a New Water Jet with Stroboscope and Camera. JOHN J. HOPFIELD, *Basic Science Division, A Century of Progress.*—Two small water jets that impinge at nearly a right angle form a leaf-shaped film jet with streamers tangential to its edges. In ordinary light both the streamers and the leaf-shaped film show stationary periodicity; the former doubtless due to the pulsation of the regularly spaced droplets that form them, and the latter to a series of fixed waves on its surface. The jet emits a high frequency note which can be changed by varying the spacing of the nozzles or the pressure of the water. Stroboscopic examination of the jet shows that ripples travel over the leaf-shaped film in the direction of

flow, and impart to it a corded structure. The streamers are found to be made up of equally spaced droplets formed with the frequency of the ripples. Photographs of the jet taken with a rapidly moving film give much interesting data. Because of its relative simplicity a straight jet also was studied in an attempt to correlate the wave motion with the constants of the liquid. When the above double nozzle is used with a flame, a high frequency note is emitted.

36. On the Calculation of the Permeability of the Cell Surface to Oxygen. N. RASHEVSKY, *Westinghouse Research Laboratories, East Pittsburgh, Pennsylvania.*—An attempt is made to calculate the permeability of the cell surface to oxygen from oxygen pressure—oxygen consumption curves at low oxygen pressures. A mathematical study of such curves has been made by R. W. Gerard under the assumption that the only limiting factor for the penetration of oxygen into the cell is the coefficient of diffusion D. There is, however, another factor, the permeability h of the cell surface. The introduction of the latter into consideration means mathematically a different boundary condition for the diffusion equation. This leads to a different expression for the oxygen pressure—oxygen consumption curve and a good agreement with Gerard's data for fertilized Arbacia eggs is obtained with $D=7\times10^{-7}$ cm^2 min.$^{-1}$ and $h=4.2\times10^{-4}$ cm min.$^{-1}$. For some other cells no such agreement can be found. The meaning of this is discussed.

37. Sources of Positive Ions: Thermionic Properties of the System Li_2O, Al_2O_3, SiO_2. E. J. JONES AND S. B. HENDRICKS, *Bureau of Chemistry and Soils, Washington, D. C.*—It is known (J. L. Hundley, Phys. Rev. **30**, 864 (1927)) that some compounds of Li_2O, Al_2O_3, and/or SiO_2 are satisfactory as thermionic sources of positive ions. We have used an arbitrary mixture $3Li_2O.1Al_2O_3.3SiO_2$ corresponding to a known compound and have found it to give constant emission of large currents (4×10^{-4} amp./cm^2) for long periods of time (40 hours). A similar material containing potassium was satisfactory as a source of potassium ions. The various compounds of Li_2O, SiO_2 and Al_2O_3 (see R. Ballo and E. Dittler, Zeits. f. anorg. Chem. **76**, 39 (1912) for an approximate equilibrium diagram) were prepared as homogeneous crystals and their thermionic properties were tested and found to be far superior to that mentioned above. The compounds were examined optically and by x-ray diffraction before and after prolonged use as thermionic sources in order to find the nature of the lattice changes accompanying the emission of positive ions.

38. An Effect of Space-Charge in Probe Analysis of a Plasma. R. H. SLOANE, *Queen's University, Belfast and* K. G. EMELEUS, *University of Michigan.*—By the use of a collector with mutually insulated sections to which different potentials could be applied, it has been shown, by using a low voltage arc in argon, that under the special conditions of short collector and small electron concentration the positive ion sheath which forms on insulating surfaces near a collector in a plasma may lead to serious misinterpretation of the characteristics of the collector. The collector characteristics obtained have been analyzed in the conventional way for Maxwellian distributions, and by a newer method in which no initial assumption is made concerning the energy distribution other than that it is isotropic. The double differentiation of the characteristic in the second method is facilitated by making use of the identity $y^{-1}(d^2y/dx^2)=d^2\ln y/dx^2+(d\ln y/dx)^2$. The effect is twofold, first, a general diminution in the apparent concentration of electrons in the plasma, and, second, an apparent preferential suppression of the slowest electrons. Under most working conditions, these are probably inconsiderable at low pressure, but perhaps important at a pressure of a few mm and higher.

39. The Faraday Dark Space. K. G. EMELEUS AND O. S. DUFFENDACK, *University of Michigan.*—The plasma diffusion theory of the negative glow and Faraday dark space gives no account of the optical structures observed. This is a preliminary report on new work on the Faraday dark space, mainly experimental. In helium further probe evidence is adduced to show that the region considered is a plasma. Tentative explanations are given of the failure of He_2 bands to appear in the negative glow, whilst they do appear in the Faraday dark space. It is found that with a trace of neon an almost isolated cap of neon light appears in the middle of the Faraday dark space, the He_2 bands being unaffected, whilst with a trace of nitrogen, nitrogen arc lines and negative bands replace He_2 bands. The resonances involved in the dissociation and excitation of the nitrogen are not clear, and are being further studied. The whole is consistent with there being an important contribution of metastable atoms to phenomena in the Faraday dark space, and it is suggested the phenomena there actually observed are those otherwise inferred from the experiments of Langmuir, Kenty and others on effects of impurities on propagation of resonance radiation through gases.

40. Self-Focussing Electron Streams. WILLARD H. BENNETT, *Ohio State University.*—In cylindrically symmetric streams of electrons containing positive space charge just sufficient to neutralize the static charge of electrons, the mutual magnetic attraction of electrons gives a system whose parts act under an inverse square law of force. It can be shown that such a system is stable, and when the current exceeds a certain calculable value, the stream is self-focussing. Subject to certain restrictions with respect to initial stream conditions, collisions, and currents, the theory is applicable to several types of streams of charged particles and is necessary for an understanding of streams in high potential tubes.

41. Vibrating Velocity Selectors for Atomic Rays. J. TYKOCINSKI TYKOCINER, *University of Illinois.*—Two types of velocity selectors have been constructed on the basis of the theory published in 1927 (J. Opt. Soc. Am. **14**, 423 (1927)). In the first type each of the two vibrating parts consists of an aluminum plate 6×6 mm provided with a slit 3×0.03 mm and held in a magnetic field by

two bronze ribbons and eccentric rollers. By adjusting the latter the slits of the vibrating systems may be aligned. The natural frequency of the slit system is 750 per sec. Its range of velocity selection is from 50 to 150 m/sec. For larger velocities (300 to 900 m/sec.) serves the second type of selector in which the mass of the vibrating system has been considerably reduced by eliminating the aluminum plate. Two vibrating Duraluminum ribbons separated by a gap 0.02 mm define the width of the slit for the atomic rays. The natural frequency of the vibrating system has been thus increased to 7000 per sec. A thermionic oscillator combined with an amplifier supplies the driving alternating current adjustable from 3000 to 10,000 cycles per sec. At a frequency of 8750 a current of 0.08 amp. produces an amplitude of vibration equivalent to three times the width of the slit. The effect of the magnetic field, temperature and pressure on the amplitude of the slit has been investigated.

42. Application of a Vibrating Velocity Selector for the Determination of the Magnetic Moment of Hydrogen. JACOB KUNZ, *University of Illinois.*—Referring to the vibrating selector (see preceding abstract) preparations are nearly completed for a precise determination of the moment of H. The atoms produced by a high frequency ring discharge pass through two Pyrex slits, then through the two slits of the selector and then through the non-homogeneous magnetic field and strike the molybdenum target. A most unusual difficulty has been overcome arising from the necessity of aligning four slits and the edge of pole pieces. Two of the slits being 0.02 mm wide produced diffraction of a beam of light so that the usual optical method of alignment failed. The method finally adopted consists in the use of three transit telescopes, two of which are centered on the slits and the third is focussed on the slits by means of a right-angle prism.

43. Rate of Vaporization of Molybdenum in Vacuo. LAWRENCE NORRIS AND A. G. WORTHING, *University of Pittsburgh.*—The changes in weight of various long filaments of molybdenum electrically heated in vacuo to various incandescent temperatures have been the basis of this study. In all cases two nearly identical filaments were mounted in a single bulb. Both filaments were heated to 2150°K by the same current during a 20 minute aging period. Thereafter only one of the two filaments was operated at the desired temperature until completion of the vaporizing period. To avoid the cooling effects of the supports, only central portions of the filaments were used in determining weight losses. Contrary to what might normally be expected, but in agreement with what one of the authors had found for tungsten, operation at constant current resulted very closely in constant temperature. When plotted the results are represented very closely for the temperature range $1600°K < T < 2400°K$, by an empirical equation of the form $\log m = A + B/T + C/T^2$. When m, the rate of vaporization, is expressed in g/cm² sec., and T in °K, A, B and C have values 7.57, -33.25×10^3, and 5.50×10^6. The values reported here for m are greater than those reported by Jones, Langmuir and Mackay by a factor of about 2.5 at 2400°K and of about 11.5 at 1600°K.

44. A New Method of Studying the Electrical Properties of Monomolecular Films on Liquids. H. G. YAMINS AND W. A. ZISMAN, *Harvard University.*—A new method is described for measuring the potential jump, dV, in passing through a monomolecular film floating upon any liquid. It has been found possible to measure dV by a null method to 0.001 volt in a few minutes of manipulation of a very simple apparatus. Obvious improvements in the amplifier employed will no doubt make it possible to measure dV to 0.00001 volt. Determinations of dV on films of oleic acid, palmitic acid, tricaprylin, trimyristin and trilaurin showed excellent agreement with the work of Guyot who used a much less satisfactory method due to Righi. The applications to the study of the polar moments and structure of organic molecules are pointed out. In particular the recent work of Fosbinder and Lessig on the study of protein structure and enzyme reactions is briefly discussed.

45. Single Electrode Potentials and the e.m.f. of a Cell. E. HUTCHISSON AND A. L. ROBINSON, *University of Pittsburgh.*—The e.m.f. of a cell has been obtained by summing the potential differences at the metal-liquid and metal-metal interfaces (electrolyte at unit activity) calculated by applying a Born-Haber-Fajans' cycle. If ΔF_S, ΔF_I, ΔF_H and ΔF_ϕ represent the free energies of sublimation, ionization, hydration and electron emission, the e.m.f. of a Cu-Zn displacement cell becomes:

$$2(\text{e.m.f.}) = (\Delta F_S^{Zn} + \Delta F_I^{Zn} + \Delta F_H^{Zn^{++}} - 2\Delta F_\phi^{Zn}) - (\Delta F_S^{Cu} + \Delta F_I^{Cu} + \Delta F_H^{Cu^{++}} - 2\Delta F_\phi^{Cu}) + 2(\Delta F_\phi^{Zn} - \Delta F_\phi^{Cu}).$$

Although ΔF_ϕ enters into the single electrode p.d. it cancels out in the total e.m.f. Since the work functions are not accurately known, the single electrode p.d. (but not the calculated e.m.f.) have large uncertainties. It

Metal and ion	Single electrode-electrolyte p.d. (volts)	E.m.f. of a (metal)-(hydrogen on Pt) cell	
		Calculated (volts)	Experimental (volts)
Li, Li^+	$+0.9 \pm 0.4$	+2.95	+2.96
K, K^+	$+0.3 \pm 0.2$	+2.85	+2.92
Na, Na^+	$+0.4 \pm 0.3$	+2.71	+2.71
Zn, Zn^{++}	-0.35 ± 0.2	+0.77	+0.76
Pb, Pb^{++}	-0.6 ± 0.3	+0.14	+0.12
Cu, Cu^{++}	-0.45 ± 0.1	−0.33	−0.34
Ag, Ag^+	$-0.55 + 0.01$	−0.76	−0.80

will be noted that the difference between the single electrode p.d. for Cu and Zn is only about 0.1 volt while the e.m.f. of such a cell is 1.1 volts, indicating that the metal-metal contact p.d. is almost equal to the e.m.f. Since the e.m.f. of a cell is usually known very accurately, the cycle may be reversed and the more uncertain quantities calculated.

46. The Use of Triode Vacuum Tube Rectifiers to Supply Constant Voltage. L. A. RICHARDS, *Cornell University.*—Fluctuations in the a.c. power supply usually make it impossible to obtain constant d.c. voltage from a rectifier-filter circuit. If triode power amplifier tubes are substituted for the usual half wave rectifiers it has been found that a fairly steady d.c. output, E_{dc}, can be obtained by having changes in the a.c. line voltage, E_{ac}, automatically change the negative bias, E_g, of the triode grids. Several grid control circuits have given good results. The following data taken with triodes in the conventional full

I Type 50 Tube 8.9 m.a. load		II Type 50 Tube 29.7 m.a. load		III Type 10 Tube 5 m.a. load		IV Type 10 Tube 8.7 m.a. load	
E_{ac}	E_{dc}	E_{ac}	E_{dc}	E_{ac}	E_{dc}	E_{ac}	E_{dc}
104.2	535.4	105.5	431.8	106.3	1000.4	112.5	521.0
111.	534.7	110.	433.3	108.2	1000.4	116.3	523.0
117.	534.6	115.	433.2	110.2	1000.2	119.	523.2
121.	534.9	119.7	433.2	112.2	1000.6	125.	523.5
126.	535.8	125.2	432.9	114.4	1000.7	129.5	523.5
				115.9	1000.3	136.	525.0
				118.5	999.0		

wave battery eliminator circuit indicate the degree of regulation which may be attained. Another type of control circuit with a combination of a.c. and d.c. on the grids of the triode rectifiers gave the results shown by the fourth set of data. It seems likely that further refinements in the design and adjustment of the grid control circuits can give more precise regulation. It is evident that by use of suitable tubes steady d.c. at much higher voltage may be produced.

47. The Emissivity of a Non-Black Body. L. T. DEVORE, *The Pennsylvania State College.*—All bodies found in nature differ from the accepted black body, as defined by Kirchoff, by virtue of the fact that their indices of refraction differ from unity. An expression is derived to show the functional relation between the emissivity, wave-length, and temperature for a non-black body.

$$\epsilon_{(\lambda,T)} = [A^2 + B_0(C^{-1}\rho^{E/KT} + 1)^{-1}\lambda^2/(\lambda^2 - \lambda^2_m)]^{3/2}.$$

Assuming the existence of a single absorption band the emissivity at constant temperature takes the form,

$$\epsilon_{(\lambda)} = [A^2 + M\lambda^2/(\lambda^2 - \lambda^2_m)]^{3/2}.$$

A^2, M and λ_m of this equation have been determined for tungsten by taking three experimentally determined points from Hulburt's data. By using the values of the constants obtained in this manner to solve for the emissivities corresponding with other wave-lengths, the formula has been verified by the almost perfect agreement shown between the calculated and experimentally determined values of the emissivities.

48. A Tungsten Filament Lamp as a Standard Source for Radiation Measurements. L. T. DEVORE AND R. F. BAKER, *The Pennsylvania State College.*—A tungsten filament lamp with a quartz window has been designed to fulfill the following requirements: (1) A continuous spectrum, (2) A constant energy distribution, (3) Reproducible characteristics, (4) Measurable intensities throughout the spectral region, (5) Uniform emitting surface. The lamp has been constructed without cement seals in such a manner as to facilitate the replacement of filaments. Filament temperatures as high as 3400°K have been attained without destroying the filament. The calibration of the lamp consists in two essential details: (1) Temperature-current calibration, (2) Spectral emissive power-temperature calibration.

49. A New Method for Amplifying and Recording Small e.m.f's. H. E. MORGAN, L. T. DEVORE AND R. F. BAKER, *The Pennsylvania State College.*—The potential difference to be measured is applied to a sensitive galvanometer. The fluctuations of the galvanometer mirror cause a beam of light to play across the cathode of a photoelectric cell. As the angular displacement of the galvanometer mirror increases the light flux falling on the photoelectric cell cathode increases and the output of the photoelectric cell increases. The current from the photoelectric cell is recorded by means of a microampere recorder and the whole instrument is calibrated against a series of known potential differences.

50. Standard Wave-Lengths in the Copper Spectrum in the Region 80A to 650A. F. S. COOPER AND P. GERALD KRUGER, *University of Illinois.*—The copper spectrum has been photographed with a 21 ft. grating at 87° angle of incidence in the region 80A to 650A. Several hundred lines in Cu VI, VII, VIII and IX, have been observed. A strong line about every Angstrom has been chosen as a standard and its wave-length calculated by expanding the grating equation $n\lambda = e(\sin\theta - \sin\phi)$ as a power series about some chosen line. The coefficients are calculated from known wave-lengths. Al lines measured by Söderqvist and Edlén (Zeits. f. Physik **69**, 356 (1931)) in several orders and an unpublished list of oxygen lines which have been standardized by Edlén have served as primary standards. The spectra of Co, Ni, Cu and Zn have been photographed in this region and a partial analysis of these spectra has been made.

51. Multiplets of O III, O IV, and O V in the Region 100A to 650A. P. GERALD KRUGER AND W. E. SHOUPP, *University of Illinois.*—The oxygen spectra have been photographed with a twenty-one foot grating at 87° angle of incidence in the region 100A to 650A. Several groups of lines have been found each of which extended over about one-half of an Angstrom on the plate. From these groups the following transitions in the oxygen spectra have been identified.

O III	$2s^2 2p^2\,{}^3P_{0,1,2} - 2s^2 2p 3s\,{}^3P^0_{0,1,2}$
	$2s^2 2p^2\,{}^3P_{0,1,2} - 2s^2 2p 3d\,{}^3D^0_{1,2,3}$
	$2s^2 2p^2\,{}^3P_{0,1,2} - 2s^2 2p 3d\,{}^3P^0_{0,1,2}$
O IV	$2s 2p^2\,{}^4P_{1/2,3/2,5/2} - 2s 2p 3d\,{}^4D^0_{1/2,3/2,5/2,7/2}$
	$2s 2p^2\,{}^4P_{1/2,3/2,5/2} - 2s 2p 3d\,{}^4P^0_{1/2,3/2,5/2}$
O V	$2s 2p\,{}^3P^0_{2,1,0} - 2s 3s\,{}^3S_1$

The $\Delta\nu$ separations of lines in other multiplets, which have been observed previously, have been remeasured with the result that the oxygen term values are more accurately known than before.

52. Spectrum of Cb IV. R. J. LANG, *University of Alberta*.—The spectrum of columbium has been photographed from 2500 to 250A in the vacuum spark and from 2500 to 1250A in the spark in nitrogen. It has thus been possible fairly well to separate the lines of Cb IV and Cb III. In Cb IV besides the known triplet terms $(4d5s)^3D$ and $(4d5p)^3F^3D$, the further triplet terms have been located: the deepest term $(4d^2)^3F$ and $(4d^2)^3P$ $(4d5p)^3P$ $(5s5p)^3P$ and part of the second members of some of the deeper terms. The singlet term $(4d5p)^1P$ is also located. The spectrum of Cb III consisting of doublet and quartet combinations is very rich in lines throughout the ultraviolet and this is in the process of analysis.

53. The Fine Structure of $H_\alpha{}^2$. R. C. WILLIAMS AND R. C. GIBBS, *Cornell University*.—While attempting to investigate the fine structure of the $H_\alpha{}^2$ line of hydrogen from gas containing a moderately concentrated amount of the heavier hydrogen isotope, we had the good fortune to obtain from Professor G. N. Lewis of the University of California a small supply of water containing approximately equal amounts of the two isotopes. By fairly prolonged discharge through the water vapor in a suitably cooled Wood tube it was found possible to accumulate sufficient hydrogen gas in the tube so that a discharge could be maintained without difficulty when those portions of the tube from which the discharge was to be photographed were immersed in liquid air. By using a three mm etalon spacing in connection with a three prism Zeiss spectrograph, interferometer patterns were photographed with the H^2 "doublets" spaced about half way between those of successive orders of H^1. With type IV C Eastman plates, microphotometer curves remarkably free from plate grain were obtained, thus enabling with the aid of appropriate intensity marks, the conversion of these curves to true relative intensity values. The patterns of H^2 are markedly sharper than those of H^1 and accordingly reveal a smaller half line width. The component separations and their relative intensities as revealed by an analysis of the intensity curves are substantially in agreement with recent theory and the $\Delta\lambda$ found between corresponding components in $H_\alpha{}^1$ and $H_\alpha{}^2$ confirm those reported by Urey, Brickwedde and Murphy.

54. Hyperfine Structure and Nuclear Spin of Tantalum. NORMAN S. GRACE, *Commonwealth Fund Fellow, and* EDWIN MCMILLAN, *National Research Fellow, at the University of California*.—The hyperfine structures of some tantalum arc lines have been resolved, using a Schüler tube source and a Fabry-Perot etalon crossed with a prism spectrograph. Almost all the lines in the spectrum have structure. λ5997 is clearly resolved into eight components, degrading toward the violet, with a total separation of 0.782 cm^{-1}. The presence of eight components indicates that either I or J has the value 7/2, and application of the interval rule shows that the other is of the order of 17/2. Seven other structures have been analyzed, and they can all be explained in terms of $I=7/2$, not in terms of $I=17/2$. This fixes the nuclear spin of tantalum at 7/2. The possibility of using hyperfine structures as a means of determining J-values of levels where these are not known, as is the case with tantalum, is shown.

55. Second Order Zeeman Effect in the Arc Spectrum of Mercury. J. B. GREEN AND R. A. LORING, *Ohio State University*.—Professor Condon has suggested in correspondence with us, that the displacement of the parallel component of Hg I λ5790 $^1P_1-{}^1D_2$, which should show no Paschen-Back effect, might be accounted for by the second order perturbation caused by the closeness of the $^3D_1$ and $^1D_2$ levels. The $^1D_2$ level itself must be considered as partially a triplet level, for L–S coupling has completely broken down. This is clearly shown by measurements of the g-values of $^1D_2$ and $^3D_2$ which are 1.02 and 1.09, respectively, instead of 1.00 and 1.17, showing not only a distortion of the g-values, but a breakdown of the Pauli g-sum rule. Preliminary measurements of the displacement of the parallel component in fields varying from 20,000 to 40,000 gauss seem to indicate, however, that the effect is not purely quadratic as would be expected; for the smaller field strengths the shift (to the red always) is proportional to the square of the field, while for larger fields it seems to be more nearly proportional to the first power, indicating that the true character of the relation is probably a combination of the two.

56. Stellar Stark Line He λ4470. J. S. FOSTER AND A. V. DOUGLAS, *McGill University*.—At Victoria we have taken 3-prism spectra of γ Pegasi and three other B stars showing Stark effects. From the contours of the line He λ4471 we have constructed, in each case, the theoretical Stark line λ4470 $(2p'-4f)$ which should accompany it. Struve has observed in many B stars a rather strong line at 4470 which he has identified as $2p-4f$. The calculations show, however, that the true Stark line should be relatively weak, with an appreciable displacement toward the violet from zero field position. On many of our plates the theoretical $2p-4f$ is identified with a well-defined portion of the heavy complex line which otherwise remains unknown.

57. Isotope Shift in Neon. J. H. BARTLETT, JR. AND J. J. GIBBONS, *University of Illinois*.—The theory of isotopic displacement due to the motion of the nucleus (see Hughes and Eckart, Phys. Rev. **36**, 694 (1930)) has been extended to atoms with any number of electrons, and applied to the transitions $2p^53s-2p^53p$ in neon. With the Hartree method, single electron wave functions have been obtained. The theory gives a shift in singlet states of 0.022 cm^{-1} more than that in triplet states, as against approximately 0.018 cm^{-1} measured by Nagooka and Mishima (Scientific Papers, Tokyo Institute, **13**, 306 (1930)).

58. Redetermination of the Mass Ratio of the Lithium Isotopes from the Band Spectrum. F. A. JENKINS AND ANDREW MCKELLAR, *University of California*.—Using new

spectrograms of the $^1\Pi \leftarrow ^1\Sigma$ bands of Li_2 from the second order of the 21-foot grating, accurate wave-length data have been obtained for the (0,0), (0,1) and (0,2) bands from both the isotopic molecules, Li^7Li^7 and Li^6Li^7. From these data, the vibrational and rotational constants for the $^1\Sigma$ state have been computed by least squares, and values of the mass-coefficient ρ $(=(\mu/\mu')^{\frac{1}{2}})$ obtained which are considerably more accurate than those previously found from the $^1\Pi$ state. The best value of ρ, obtained as the quotient ω_e'/ω_e is 1.04141 ± 0.00008. This corresponds to a mass ratio $Li^7/Li^6 = 2\rho^2 - 1 = 1.1690 \pm 0.0003$. The mass-spectrograph data of Costa give a ratio of 1.1663, with an estimated limit of error not exceeding 0.0007. Our new result is still higher than the value 1.1678 ± 0.0008 obtained from the $^1\Pi$ state. Small corrections, due to possible higher terms in the vibrational energy, modification of the formulae in quantum mechanics, etc., have been examined, and their effects shown to be negligible. From the ratio $B_e'''/B_e'' = \rho^2$, we find $\rho = 1.0422 \pm 0.0007$, in satisfactory agreement with the results from the vibrational constants. Experiments on the disintegration of Li^7 by protons give accurately the mass of Li^7 as 7.015, and using this we find the mass of Li^6 to be 6.001.

59. Nuclear Moment of Na, and Polarization of Resonance Radiation. N. P. HEYDENBURG AND A. ELLETT, *State University of Iowa.*—The zero field polarization of Na *D* resonance radiation, 16.5 percent agrees with that calculated for a nuclear moment of 1 (16.6 percent), whereas Rabi (Stern, Gerlach) and Urey (Bands) find $I = 3/2$ for which the polarization is 15.4 percent. The zero field polarization of the λ3303 doublet is found to be 19.2 percent (Heydenburg) too high for either $I = 1$ or 3/2. The value of 15.4 percent for $I = 3/2$ is computed on the assumption of uniform intensity distribution in the source and perfectly sharp stationary states. Correcting for intensity distribution raises the polarization (0.2) to 0.6 percent. Breit (private communication) has worked out the effect of finite breadth of stationary states. By calculating intensities in the Paschen-Back effect of hyperfine multiplets for $I = 3/2$ and fitting observations (Larrick, *D* lines; Heydenburg, λ3303) we find $A(4^2P_{3/2}) = 1.93 \times 10^{-4}$ cm^{-1}, $A(3^2P_{3/2}) = 7.7 \times 10^{-4}$ cm^{-1}. With $\tau(4^2P_{3/2}) = 3.7 \times 10^{-8}$; $(3^2P_{3/2}) = 1.6 \times 10^{-8}$, the corrections for finite breadth of states and distribution in source give $P(D_1 + D_2) = 16.5$ percent, $P(\lambda 3303) = 18.8$ percent. Experimentally the ratio $A(3^2P_{3/2})/A(4^2P_{3/2})$ is found to be 4 while Goudsmit's theoretical equations give 3.3 for this ratio, and 0.035 cm^{-1} as the separation in $3^2S_{\frac{1}{2}}$ when calculated from the *A* values of $^2P_{3/2}$, compared with Schüler's 0.06 cm^{-1}. τ values were calculated from Prokofjew's theoretical *f* values.

60. Rotational Structure of the Raman Band (0000) → (020±2) in Linear Symmetrical Molecules YX_2. J. RUD NIELSEN, *Institute of Theoretical Physics, University of Copenhagen.*—A. Langseth and the writer (Zeits. f. physik. Chemie **B19**, 427 (1932)) observed six very faint lines in the Raman spectrum of CO_2 and interpreted them tentatively as maxima of rotational branches. The lines 1325 and 1344 cm^{-1} were ascribed to transitions from the normal state to the level $V_1 = 0$, $V_2 = 2$, $V_3 = 0$, $l = \pm 2$. Because of the apparent absence of a *Q*-branch, doubt was expressed as to the correctness of this interpretation. In order to clear up this point, the intensities of the individual rotational lines associated with the transition (0000) → (020±2) have been calculated. The calculation, which is based upon Placzek's polarizability theory, follows a method similar to that employed by Rademacher and Reiche (Zeits. f. Physik **41**, 453 (1927)) and leads to results agreeing with the more general formulas recently obtained by Placzek and Teller (Zeits. f. Physik **81**, 209 (1933)) by a formally different method. It turns out that a *Q*-branch should be present. Hence, the doubt as to the interpretation of the lines has not been removed, and further experimental evidence is desirable.

61. Raman Spectra of Some Linear Triatomic Molecules. A. LANGSETH AND J. RUD NIELSEN, *University of Copenhagen.*—A detailed study has been made of the Raman spectra of N_2O, CO_2, liquid CS_2, and the ions SCN^- and N_3^- in aqueous solution. All spectra have been photographed with high dispersion, and, with the help of a spectrograph of lower dispersion, the depolarizations of the main lines have been determined for all molecules except N_2O. For CO_2 and CS_2 the relative intensities were also measured. The results obtained, which are discussed in the light of the theories of Fermi, Dennison and Placzek, support the conclusion that these molecules are of linear structure.

62. A New Monochromatic Filter. W. H. AUGHEY AND W. D. LANSING, *Experimental Station, E. I. duPont de Nemours and Company.*—In the course of ultra-centrifugal investigations, a need was felt for monochromatic blue (4358A) radiation from a Hg arc. No available dry filter was found to transmit the blue without contamination from the violet (4047A) line. It was discovered that an alkaline solution of β-methyl esculetin (Vliet, Organic Syntheses, **IV**, 45-6 (1925)) would transmit the blue line and absorb the violet completely. Dry filters were made by bathing fixed and washed photographic plates in a 0.5 percent water solution of the dye with sufficient sodium hydroxide to neutralize one of the hydroxyls in the dye. After drying, completed filters were made by cementing two plates with the gelatine sides together. With ordinary photographic plates, the only radiation from a quartz mercury arc transmitted in sufficient intensity to affect the plate is the 4358A line. This filter, it must be pointed out, is only a photographic monochromat, and cannot be used for visual work.

63. X-Ray Investigations at High Pressures. WILLI M. COHN, *Berkeley, California.*—X-ray investigations have been carried out with a Bridgman bomb. The substance to be investigated is inserted into the bomb, and the pressure applied. A monochromatic x-ray beam passes through the following parts in the bomb: slit, beryllium window, slit, sample, window of amorphous material (Bakelite, glass). The film is arranged outside of the bomb. Hydrostatic pressures have been obtained up to 3000 atmospheres so

far. Some results of the experiments are discussed showing changes of modifications taking place in the crystals investigated.

64. The Crystal Lattice of Ammonium Persulphate, $(NH_4)_2S_2O_8$, and the Structure of the Persulphate Group. R. C. L. MOONEY AND W. H. ZACHARIASEN, *University of Chicago.*—The crystal lattice of the isomorphous ammonium and caesium persulphates was determined accurately and uniquely in order to obtain exact data on the structure of the persulphate group. The symmetry is monoclinic and the space group is $P2_1/n$ (C_{2h}^5). The unit cell contains four molecules. All atoms are lying in general positions, so that the lattice is characterized by 18 degrees of freedom. The cell size and parameter values for the ammonium compound are: $a=7.80$A $b=7.98$A $c=6.12$A $\beta=95°9'$. The per-

	$2\pi x$	$2\pi y$	$2\pi z$		$2\pi x$	$2\pi y$	$2\pi z$
NH_4	52°	45°	90°	O_{II}	10°	75°	250°
S	49°	126°	260°	O_{III}	75°	145°	340°
O_I	15°	180°	215°	O_{IV}	105°	120°	210°

sulphate group may be pictured as two SO_4 groups linked together by a bond across a center of symmetry between two oxygen atoms. Each sulphur atom is tetrahedrally surrounded by four oxygen atoms at a distance of 1.50A. The distance between two oxygen atoms connected by the valence bond is 1.31A. The angle between the two bonds of these oxygen atoms is 128°. The structure of the group may be interpreted in terms of electron pair bonds by writing the formula as $(O_3^{-1}S^{+2}OOS^{+2}O_3^{-1})^{-2}$. Ammonium is surrounded by 12 oxygen atoms at an average distance of 3.15A. The atomic arrangement explains the observed birefringence.

65. The Crystal Structure of Boric Acid. W. H. ZACHARIASEN, *University of Chicago.*—The crystal lattice of boric acid, H_3BO_3, was determined in order to get information about the hydrogen bond. Boric acid crystals are triclinic holohedral with the following dimensions of the unit cell: $a=7.04$A $b=7.04$A $c=6.56$A $\alpha=92°30'$ $\beta=101°10'$ $\gamma=120°$. This cell contains four molecules and there are thus 42 degrees of freedom in the structure. The positions of boron and oxygen atoms were fixed by intensity considerations and may be described as follows:

	$2\pi x$	$2\pi y$	$2\pi z$		$2\pi x$	$2\pi y$	$2\pi z$
B_I	235°	155°	90°	O_{III}	275°	235°	90°
B_{II}	115°	275°	90°	O_{IV}	75°	195°	90°
O_I	155°	115°	90°	O_V	75°	315°	90°
O_{II}	275°	115°	90°	O_{VI}	195°	315°	90°

The hydrogen positions were determined by considerations of interatomic distances. Conveniently the structure may be described as a pile of identical and strictly two-dimensional lattices. The vertical distance between successive layers is 3.18A, so that the forces linking the layers together are extremely weak. The atomic arrangement within each layer is of hexagonal symmetry. The building blocks of the two-dimensional lattice are triangular BO_3-groups (B—O =1.35A) and collinear O—H—O groups (O—O =2.71A). Each oxygen atom is linked to one boron and two hydrogen atoms. The layers are piled together in such a manner that the oxygen atoms of one layer are lying almost exactly above or below boron and hydrogen atoms of the two neighboring layers. The atomic arrangement accounts for the properties of the crystals.

66. The Crystal Structure of Sodium Thio-Antimonate. CHING-YEUNG HUI, *Cornell University.*—Sodium thio-antimonate ($Na_3SbS_4\cdot 9H_2O$), an optically active cubic crystal, was investigated by x-rays. Laue, oscillation and powder photographs were made. There are four molecules to the unit cell, the length of which is 11.835A. The density calculated from the x-ray data is 1.927 as compared with 1.864 given by C. Soret as the best value (Archiv. de Sci. Physiques et Naturelles **16**, 468 (1886)). The space group is $P2_13$ (T^4). There are four optically active cubic crystals known to the author. Each of these has now been shown to belong to $P2_13$.

67. Crystal Structure of Potassium Uranyl Acetate. I. FANKUCHEN, *Cornell University.*—Potassium uranyl acetate has been reported as tetragonal, axial ratio = 1.2831. A study has been made with powder, rotation, oscillation and Laue methods. These indicate that it is dimorphous, both forms being tetragonal. For one, $a=14.38$, $c=25.80$. This corresponds to an axial ratio of 1.27, checking the reported value. For the other, $a=13.99$, $c=27.70$. Its axial ratio, 1.40, lies in the range of values of the axial ratios of the remainder of the uranyl acetates reported as isomorphous with the potassium uranyl acetate. Both unit cells have approximately the same volume and contain 16 molecules. Both are body centered. The space group is probably $I4_12$ (D_4^{10}). In both forms the uranium atoms are approximately in a face centered lattice of 1/4 the height of the actual unit cell. This is more nearly the case in the second form.

68. X-Rays Produced by Fast Mercury Ions. WESLEY M. COATES AND ERNEST O. LAWRENCE, *University of California.*—A study has been made of the production of x-rays by mercury ions having energies up to 2.4×10^6 electron-volts. The ions were obtained by the method of Sloan and Lawrence (Phys. Rev. **38**, 2021 (1931)). The following targets were used: lithium, boron, carbon, oxygen, aluminum, sulfur, nickel, copper, molybdenum, silver, tin and lead. The radiation first becomes measurable when the ions have energies of about one million electron-volts and the intensity increases rapidly as the energy of the ions increases. For all of the elements lighter than copper the wave-length of the radiation is characteristic of the target. The elements heavier than copper give the mercury M radiation in increasing abundance as the atomic number increases. The intensity of the radiation excited in molybdenum by the mercury ions is about ten times as great as that excited in

the same target by 3800 volt-electrons. The efficiency of the process is such that at least one out of every 2000 mercury ions having an energy of 2.4×10^6 electron-volts succeeds in producing a 2400 volt quantum from a silver target.

69. Scattering of X-Rays from Powdered Crystals at Low Temperatures. FORD PENNELL AND G. E. M. JAUNCEY, *Washington University, St. Louis, Missouri.*—We have recently shown (Phys. Rev. **43**, 505 (1933)) that Jauncey's theory of the diffuse scattering from crystals together with the theory of the intensity of the Debye-Scherrer circles gives the intensity of the x-rays scattered by a powdered crystal over a wide range of values of $(\sin \frac{1}{2}\phi)/\lambda$ into an ionization chamber window. We have now determined the ratio of the intensity of x-rays scattered from the powdered crystal at 103°K to that from the crystal at 295°K for each of several scattering angles between 12° and 36°. For KCl the ratios varied from 0.965 to 0.995 with a probable error of about 0.012. For NaF the ratios varied from 0.960 to 1.015 with a probable error of about 0.010. The ratios are thus nearly unity but show a tendency, more marked in the case of KCl, to be less than unity by the order of one percent. This may indicate a slight decrease of the true atom form factor at low temperatures, a possibility suggested by Jauncey (Phys. Rev. **42**, 453 (1932)).

70. Sensitiveness of Photographic Films to X-Rays at Low Temperatures. G. E. M. JAUNCEY AND H. W. RICHARDSON, *Washington University, St. Louis, Missouri.*—Dewar found that the sensitiveness of a photographic film to light is considerably reduced when the film is at liquid air temperature. Likewise it is known that the sensitiveness to x-rays is reduced at this temperature. We have made a quantitative study of the sensitiveness to x-rays of different parts of the same film which were at different temperatures. The amount of blackening of a film was determined by means of a microphotometer. The exposure times necessary to produce equal blackening at temperatures of 103°, 203° and 293°K, respectively, were determined. From these the rates of blackening for a given intensity of x-rays were found to be proportional to 0.32, 0.49 and 1.00 at the respective temperatures. On plotting against temperature and drawing a monotonic curve, it seems that the rate at 0°K is 0.17 or about one-sixth of the rate of blackening at room temperature. The x-ray tube was operated at 55 kv peak and the rays passed through 1.065 cm of aluminum. The effective wave-length as measured by absorption was 0.33A.

71. The Magnitudes of the *L* Absorption Discontinuities of Thallium. C. G. PATTEN, *University of California.* (*Introduced by R. B. Brode.*)—Uniform evaporated films of thallium were used in obtaining values for the magnitudes of the *L* absorption discontinuities and the variations of the absorption coefficients with wave-lengths. The thallium was of such a thickness as to absorb over 50 percent of the radiation at the maximum values. The thallium film was coated with a very thin film of aluminum to prevent oxidation. The ionization currents were measured with a (FP_{54} Pliotron) vacuum tube amplifier and an accuracy of one percent is claimed. By considering the scattering as negligible the magnitudes of the discontinuities are

$$\delta_{L_I} = 1.149, \quad \delta_{L_{II}} = 1.409, \quad \delta_{L_{III}} = 2.529, \quad \delta_L = 4.093.$$

Values of c, the exponent of λ in the equation $\mu = A\lambda^c$, have been obtained. The results are in good agreement with values obtained for gold by Uber and Patten, Phys. Rev. **42**, 229 (1932).

72. The Laws of Absorption for Soft X-Rays. ELMER DERSHEM, *University of Chicago.*—The absorption of the unresolved $L\alpha_{12}$ lines of copper ($\lambda = 13.37$A) and iron ($\lambda = 17.67$A) in nitrogen, oxygen and carbon dioxide has been investigated by a photographic method previously described by Dershem and Schein, Phys. Rev. **37**, 1238 (1931). Improvements in apparatus and technique have made it possible to measure the x-ray absorption coefficients of a gas in this wave-length region with a probable error for a single observation not greater than 1.5 percent. The results so far obtained show that for wave-lengths shorter than that of the *K* limit the absorption coefficients vary approximately as the 2.35 power of the wave-length and the 4.36 power of the atomic number of the absorber. For hard x-rays these values are known to be very closely 3 and 4, respectively. The present results are in good agreement with those of other investigators who have used moderately soft x-rays and found that the exponent of λ decreases steadily with increase in λ while the exponent of Z increases slightly with increase of wave-length.

73. Wave-Lengths of Certain *M* Series Lines by the Ruled Grating. E. G. PURDOM AND J. M. CORK, *University of Michigan.*—By using the experimental procedure described by one of us (Phys. Rev. **35**, 1456 (1930)), (Phys. Rev. **42**, 743 (1932)), measurements have been extended to include the *M* series emission spectra for the heavy elements. This method makes use of multiple positive orders and allows the correct determination of the wave-lengths even should uncertainties exist in the position of the direct or reflected beam or in the angle of incidence. With the exception of rhenium (75), at least five good plates have been obtained and the wave-lengths determined for the elements from hafnium (72) through bismuth (83), thorium (90) and uranium (92). The wave-lengths are found to be consistently greater than the corresponding results obtained by means of the crystal method. Moseley diagrams for the various lines are smooth curves.

74. Experimental Study of the Rocking Curves of the Mn $K\alpha$ Lines from Pure Mn and from Several Mn Alloys. LYMAN G. PARRATT, *University of Chicago.*—With a double-crystal vacuum spectrometer rocking curves of the Mn $K\alpha$ lines from pure Mn and from several alloy targets have been recorded. The widths at half maximum intensity vary with the combination of elements and with their relative concentrations in the target. Targets of Mn–Ni show an approximately linear increase in the width of $K\alpha_1$ with relative increase of nickel, reaching at 50–50 molecular concentration a maximum width 23.3 percent greater than the width from pure Mn, then an approximately linear decrease with

the same slope as before. The eutectoid mixture of Mn–Cu also shows increased width; an alloy of Mn–Fe (50–50) yields little or no increase; Mn–Cr (50–50) gives a decrease of some 5 percent. A layer of oxide on the surface of the pure Mn target increases the width as much as 18.7 percent. Changes in the width of α_2 follow closely those of α_1. All the rocking curves are asymmetrical and their shapes vary with the type of target used. The relative intensity of α_1 to α_2 (if taken as the ratio of areas under the resolved or component rocking curves) remains 2 to 1 irrespective of the composition of the target.

75. A Method to Supplement Dimensional Analysis. ARTHUR E. RUARK, *University of Pittsburgh.*—Attempts to apply dimensional analysis often yield misleading results because of failure to include all the independent variables, and dimensional constants. The technique of dimensional analysis contains no prescription for discovering and eliminating such errors. Often, to avoid these difficulties, dimensional analysis may be replaced by another procedure. This consists in writing down the differential equations and boundary conditions of the problem, or of some problem of the same type characterized by simpler geometrical and kinematic conditions. The variables can always be replaced by dimensionless ones. The dimensionless variables and dimensional constants which appear in these equations are identical with those occurring in the final integrated form of our physical equations. The dependent variables can be written out as power (or Fourier) series involving the independent ones, and study of their form is often helpful. Physical dimensions, natural periods, etc., cannot well be overlooked. Defects in our knowledge, preventing complete formulation of the problem, are brought out clearly by this procedure. When one is unable to write out approximate differential equations and boundary conditions, it is hard to see how a dimensional analysis could succeed, except by chance.

76. A Photographic Recording Photoelectric Densitometer. L. T. DEVORE, *The Pennsylvania State College.*—Difficulties encountered by previous workers in designing a direct reading photoelectric densitometer have been largely overcome in the design of this instrument. The cell employed is a P. J. 23 gas-filled, central anode tube operated at a low anode potential. A d.c. amplifier has been developed and methods evolved for calibrating this amplifier and keeping its characteristics constant under operating conditions. A simple photographic recorder has been developed. The instrument is capable of duplicating results with great precision.

77. The Specific Isotope Effect in the Lead Spectrum. BERYL H. DICKINSON, *Ryerson Physical Laboratory, University of Chicago.*—An approximate calculation of the specific isotope effect proposed by Hughes and Eckart (Phys. Rev. **36**, 694 (1930)) has been made for the separation of Pb(206) and Pb(208) levels in four different configurations of the lead atom. For these calculations a wave function consisting of an 82-order determinant was used after Slater's method. Assuming that all electrons move in a common field the magnitude of the specific isotope displacement may be shown to be:

$$\Delta W = -(1/2M)\,\Sigma_{(a,\,b)}\{|P_x(a,\,b)|^2 + |P_y(a,\,b)|^2 + |P_z(a,\,b)|^2\},$$

in which M is the nuclear mass. The P's are summed over all pairs of electrons in the atom:

$$P_x(a,\,b) = (h/2\pi i)\int \psi^*(a)(\partial\psi(b)/\partial x)d\tau.$$

By assigning a nuclear charge $70 < Z < 80$ it is found that the calculated specific isotope displacements are in agreement with those observed by Schuler and Jones (Zeits. f. Physik **75**, 565 (1932)) and by Kopfermann (Zeits. f. Physik **75**, 363 (1932)).

78. Photoelectric Measurement of the Shapes of Solar Absorption Lines. THEODORE DUNHAM, JR., *Mount Wilson Observatory.*—Since photography as an intermediate step in spectrophotometry introduces several undesirable complications, a microphotometer operating directly in the solar spectrum has been developed. Light passes through a moveable slit in the focal plane of a 30-foot Littrow spectrograph and into a photoelectric cell connected to the grid of an FP-54 Pliotron, with a shunt of 6.6×10^{11} ohms. Improved stability has been obtained by placing the photoelectric cell and Pliotron in an evacuated container, in accordance with the experience of Hafstad (Phys. Rev. **40**, 1044 (1932)) and Whitford (Astrophys. J. **76**, 213 (1932)). The lead from the cell runs directly to the grid without the use of insulators. Commercial rheostats and potentiometers have also been eliminated. The Pliotron is operated from a single battery across a manganin wire potential divider which also supplies the balancing current for the galvanometer. Fluctuations due to variations in battery voltage are less than those arising in the grid circuit from shot-effect and from the photoelectric cell. A 6-inch plane grating has been used in the second order. The first and second slits are each 18 mm long and 0.03 mm wide (0.03A). Under these conditions a potassium hydride cell produces 5×10^{-14} amperes in the continuous background of the spectrum at λ5000, corresponding to a galvanometer deflection of 1000 mm, and a single measurement of the intensity at any point on the contour of a line is in error by less than 1 percent.

79. Investigation on Mitogenetic Radiation by Means of a Photoelectric Counter Tube. EGON LORENZ, *Harvard Medical School.* (*Introduced by Otto Oldenberg.*)—A Geiger-counter tube for ultraviolet radiation was constructed by evaporating the photoelectric material (spectroscopically pure Cd or Zn) upon the wall of a quartz tube having a window of 6 to 7 cm². The absolute calibration of this tube was such that radiation having an intensity of approximately 10 quanta per cm² per second between 3000 and 2000A could be detected. Numerous samples of various biological materials were placed upon the window of the counter tube. In all cases the number of counts was the same (within the statistical error) with and without

biological material. Energy considerations show that mitogenetic radiation, if it exists, must have an intensity of approximately 100 quanta per second in order to produce the reported biological effects. Since this counter tube can detect 1/10 of this amount of energy and since negative results were obtained, the existence of mitogenetic radiation could not be confirmed.

80. The Variation in Sensitivity of the Photronic Cell with X-Ray Wave-Lengths. PAUL R. GLEASON, *Colgate University.*—The characteristics of the Weston Photronic Cell and the Tungsram Type S cell under exposure to x-rays, as recently reported (Phys. Rev. **43**, 775 (1933)), have been studied further and the results extended. The cells responded when exposed to the full radiation of a 600 kv tube, although absorption measurements indicated that no radiation of wave-length shorter than about 0.045A contributed materially to the output. The time lag under these conditions was about two minutes. The earlier results for longer wave-lengths indicated peculiarities in the spectral response curve. Those data were obtained with full radiation under little or no filtration. More valid results were expected with monochromatic radiation. This was approximated to by the method of "end-radiation." Results of this test indicated a discontinuity in the sensitivity curve near the K absorption limit of lead. These results do not agree with those of Scharf and Weinbaum (Zeits. f. Physik **80**, 465 (1933)). It is probable that some of the lead placed on the front of the cell as a metallic transparent electrode has combined or mixed with the selenium, and that the absorption of x-rays associated with the photoelectric action takes place in this layer. If the cell responds equally for equal energy absorption in this layer, it is expected that a thin filter, largely of lead, placed over the cell will make the response of the cell equal for equal incident energy regardless of wave-length.

81. Stress Concentration at a Circular Hole in a Plate in Monaxial Tension. S. C. HOLLISTER AND G. J. SCHOESSOW, *Purdue University.* (*Introduced by K. Lark-Horovitz.*)—Mathematical solutions of the stress at a circular hole in an infinitely wide plate in tension have been given by Kirsch, Howland (Phil. Trans. [A] **229**, 49 (1929)) and others, giving a tangential tensile stress at a margin of the hole of three times the average stress on the net section. Engineers are frequently faced with problems involving ratio of width of plate to hole diameter (W/d) of small values. Partial solutions have been offered for such cases but such solutions are not in agreement with each other. An investigation by photoelastic analysis was undertaken to establish stress concentration factors for such cases. It was found that the factor of 3 held when W/d equals 8 or more; and that for ratios of W/d from 1.5 to 8, the stress concentration factor may be expressed by the equation: $3.0-1.6(8-W/d)^{3.6}/1100$, this stress concentration being expressed as a ratio of tensile stress at the edge of the hole to the average tensile stress on the net section.

AUTHOR INDEX TO ABSTRACTS OF THE CHICAGO MEETING

Abbott, R. B.—see Jenkins
—— see Stevens
Akeley, Edward L.—No. 16
Ambrose, H. A. and A. G. Loomis—No. 29
Asling, Walter Louis and R. T. Dufford—No. 2
Aughey, W. H. and W. D. Lansing—No. 62

Babcock, C. L.—see Lark-Horovitz
—— **and J. V. Hoffacker**—No. 30
Baker, R. F.—see DeVore
—— see Morgan
Bartlett, J. H., Jr., and J. J. Gibbons—No. 57
Beeck, Otto—No. 12
Bennett, Willard H.—No. 40

Caswell, A. E.—No. 26
Cleveland, Forrest F.—No. 20
Coates, Wesley M. and Ernest O. Lawrence—No. 68
Cohn, Willi M.—No. 63
Cooper, F. S. and P. Gerald Kruger—No. 50
Cork, J. M.—see Purdom

Davey, W. P.—see Singer
Déjardin, G. and R. Schwégler—No. 5
Deming, W. Edwards—No. 14
Dershem, Elmer—No. 72
DeVore, L. T.—Nos. 47, 76
—— see Morgan
—— **and R. F. Baker**—No. 48
Dickinson, Beryl H.—No. 77
Douglas, A. V.—see Foster
DuBridge, L. A.—see Roehr
Duffendack, O. S.—see Emeleus
Dufford, R. T.—No. 3
—— see Asling
—— see Thomas
Dunham, Theodore, Jr.—No. 78
Dunning, J. R. and G. B. Pegram—No. 13

Ellett, A.—see Heydenburg
Emeleus, K. G.—see Sloane
—— **and O. S. Duffendack**—No. 39

Fankuchen, I.—No. 67
Foster, J. S. and A. V. Douglas—No. 56

Galli-Shohat, N.—No. 22
Gibbons, J. J.—see Bartlett
Gibbs, R. C.—see Williams
Gleason, Paul R.—Nos. 4, 80
Grace, Norman S. and Edwin McMillan—No. 54
Green, J. B. and R. A. Loring—No. 55

Hanson, Alvin W.—No. 25
Hazel, Herbert and R. R. Ramsey—No. 32
Henderson, Malcolm—see Livingston
Hendricks, S. B.—see Jones
Heydenburg, N. P. and A. Ellett—No. 59
Hoffacker, J. V.—see Babcock
Hollister, S. C. and G. J. Schoessow—No. 81
Hopfield, John J.—No. 35
Hui, Ching-Yeung—No. 66
Hutchisson, E. and A. L. Robinson—No. 45

Jauncey, G. E. M.—see Pennell
—— **and H. W. Richardson**—No. 70
Jenkins, F. A. and Andrew McKellar—No. 58
Jenkins, Ruth O. and R. B. Abbott—No. 34
Jones, E. J. and S. B. Hendricks—No. 37

Kruger, P. Gerald—see Cooper
—— **and W. E. Shoupp**—No. 51
Kunz, Jacob—No. 42

Lanczos, Cornelius—No. 15
Lang, R. J.—No. 52
Langseth, A. and J. Rud Nielsen—No. 61
Lansing, W. D.—see Aughey
Lark-Horovitz, K. and C. L. Babcock—No. 31
—— **and S. E. Madigan**—No. 27
Lawrence, Ernest O.—see Coates
—— see Lewis
—— see Livingston
—— **and M. Stanley Livingston**—No. 10
Lewis, Gilbert N., M. Stanley Livingston and Ernest O. Lawrence—No. 11
Livingston, M. Stanley—see Lawrence
—— see Lewis
—— **Malcolm C. Henderson and Ernest O. Lawrence**—No. 9
Long, J. D.—see Singer
Loomis, A. G.—see Ambrose
Lorenz, Egon—No. 79
Loring, R. A.—see Green

Madigan, S. E.—see Lark-Horovitz
McKellar, Andrew—see Jenkins
McMillan, Edwin—see Grace
Mooney, R. C. L. and W. H. Zachariasen—No. 64
Morgan, H. E., L. T. DeVore and R. F. Baker—No. 49
Muskat, Morris—No. 23

Nielsen, J. Rud—No. 60
—— see Langseth
Norris, Lawrence and A. G. Worthing—No. 43

Parratt, Lyman G.—No. 74
Patten, C. G.—No. 71
Pegram, G. B.—see Dunning
Pennell, Ford and G. E. M. Jauncey—No. 69
Purdom, E. G. and J. M. Cork—No. 73

Ramsey, R. R.—see Hazel
Rashevsky, N.—No. 36
Rice, O. K.—No. 18
Richards, L. A.—No. 46
Richardson, H. W.—see Jauncey
Robertson, H. P.—No. 17
Robinson, A. L.—see Hutchisson
Roehr, W. W. and L. A. DuBridge—No. 6
Ruark, Arthur E.—Nos. 8, 75

Samson, E. W.—see Van Atta
Schoessow, G. J.—see Hollister
Schwégler, R.—see Déjardin
Shoupp, W. E.—see Kruger
Singer, W. E., J. D. Long and W. P. Davey—No. 24
Sloane, R. H. and K. G. Emeleus—No. 38
Stevens, T. H. and R. B. Abbott—No. 33

Thomas, Clarence Delmar and R. T. Dufford—No. 1
Thompson, Louis—No. 28
Tykociner, J. Tykocinski—No. 41

Van Atta, L. C., E. W. Samson and R. J. Van de Graaff—No. 7.
Van de Graaff, R. J.—see Van Atta

Warburton, F. W.—No. 21
Weber, Ernst—No. 19
Williams, R. C. and R. C. Gibbs—No. 53
Worthing, A. G.—see Norris

Yamins, H. G. and W. A. Zisman—No. 44

Zachariasen, W. H.—No. 65
——see Mooney
Zisman, W. A.—see Yamins